

# **The changing chromatome as a driver of disease: A panoramic view from different methodologies**

Isabel Espejo<sup>1</sup>, Luciano Di Croce,<sup>1,2,3</sup> and Sergi Aranda<sup>1</sup>

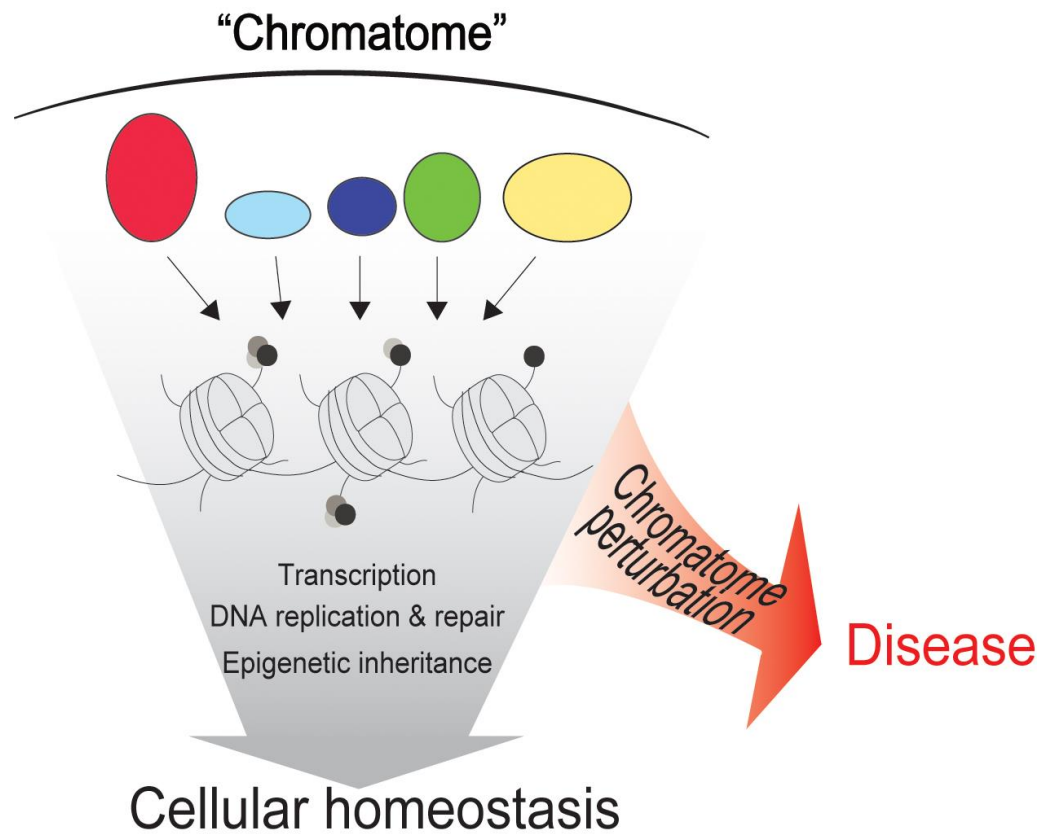
1. Centre for Genomic Regulation (CRG), Barcelona Institute of Science and Technology, Dr. Aiguader 88, Barcelona 08003, Spain
2. Universitat Pompeu Fabra (UPF), Barcelona, Spain
3. ICREA, Pg. Lluís Companys 23, Barcelona 08010, Spain

\*Corresponding authors:

Luciano Di Croce (Luciano.DiCroce@crg.eu)

Sergi Aranda (sergi.aranda@crg.eu)

## GRAPHICAL ABSTRACT



Chromatin-bound proteins regulate gene expression, replicate and repair DNA, and transmit epigenetic information. Several human diseases are highly influenced by alterations in the chromatin-bound proteome. Thus, biochemical approaches for the systematic characterization of the chromatome could contribute to identifying new regulators of cellular functionality, including those that are relevant to human disorders.

## SUMMARY

Chromatin-bound proteins underlie several fundamental cellular functions, such as control of gene expression and the faithful transmission of genetic and epigenetic information. Components of the chromatin proteome (the “chromatome”) are essential in human life, and mutations in chromatin-bound proteins are frequently drivers of human diseases, such as cancer. Proteomic characterization of chromatin and *de novo* identification of chromatin interactors could thus reveal important and perhaps unexpected players implicated in human physiology and disease. Recently, intensive research efforts have focused on developing strategies to characterize the chromatome composition. In this review, we provide an overview of the dynamic composition of the chromatome, highlight the importance of its alterations as a driving force in human disease (and particularly in cancer), and discuss the different approaches to systematically characterize the chromatin-bound proteome in a global manner.

## 1 INTRODUCTION

2 Chromatin is the macromolecular complex formed by DNA together with physically-  
3 associated proteins and non-coding RNAs. At a functional level, the chromatin-bound  
4 proteome (the so-called “chromatome”) includes numerous different proteins that  
5 regulate the tridimensional structure of chromatin fibers within the nucleus as well as  
6 correct gene transcription, timely replication of the chromatin, and genomic integrity.  
7 [1,2,3] The chromatome comprises very diverse proteins with distinct functional  
8 interacting domains, enzymatic activities, isoforms, and/or post-translational  
9 modifications (PTMs). [4,5] The spatial distribution of proteins present on chromatin is  
10 also very distinct, and some proteins are highly abundant and cover large chromatin  
11 regions (e.g. telomeres, centromeres), whereas others are discretely distributed within  
12 a few nucleotides. [6] Furthermore, the temporal residency of chromatin proteins can  
13 vary remarkably, ranging from a few milliseconds for transcription factors (TF) to  
14 several hours for stable histone proteins. [7,8] Perturbations in chromatome composition,  
15 protein distribution across the genome, and chromatin interaction dynamics are directly  
16 responsible for several human diseases, including cancer. [2,9,10,11]

17 The levels of messenger RNAs (mRNAs) are poor predictors of protein levels; [12,13]  
18 [14,15] and do not reflect functional changes affecting protein–chromatin interactions.  
19 Thus, experimental chromatome profiling is likely to outperform transcriptome  
20 determination on predicting chromatin functionality and organization. [16,17]

## 22 THE CHROMATIN PROTEOME IS HIGHLY DYNAMIC

23 The core nucleosome histones are the most abundant eukaryotic nuclear proteins,  
24 with ~8,500–17,000 copies per Mb of genome. [6] Nucleosomes are the functional unit  
25 of the chromatin and comprise two of each of the core histones H2A, H2B, H3, and  
26 H4, which wrap up ~147 bp of DNA. [18,19] Histones are basic (rich in lysine and  
27 arginine) and neutralize the negative charge of DNA. Finally, the linker histone H1  
28 binds the DNA at the entry and exit of the nucleosomes, thereby increasing their  
29 stability and topological organization. [20]

30 The chromatin topology fluctuates across the genome, from the densely arranged  
31 constitutive and facultative heterochromatin to the low nucleosome–occupied  
32 euchromatin. [21,22] The stable constitutive heterochromatin generally associates with  
33 preservation of genome integrity and accurate chromosome segregation. In contrast,  
34 the dynamic interchange between facultative heterochromatin and euchromatin  
35 appears essential for regulating the access of the DNA replication, repair, and

transcription machineries to genomic regulatory regions. [23,24,25] These genomic regulatory regions mainly comprise promoters, enhancers, and insulators. In humans, these genomic regions harbor the 90% of the DNA sequences recognized by over 1600 predicted TFs, [26,27] which mostly occurs through the DNA-binding domains of C2HZ2 zinc fingers ( $n = 747$  proteins, in humans) and homeodomains ( $n = 196$ ). [27] TFs primary recruit transcriptional regulators to control the cell-specific gene expression programs. [28 ,29] For instance, the so-called pluripotent TFs (POU5F1, SOX2, and NANOG) work together to recruit the RNA polymerase complex to the promoters of pluripotent genes, and transcriptional repressive regulator **SETDB1**, to lineage-specific regions, thus sustaining embryonic stem cell self-renewal. [30] Although most TFs bind exclusively at accessible chromatin, several pioneer TFs can directly bind the nucleosome surface and induce sequence-specific chromatin topology changes [31] by recruiting ATP-dependent chromatin remodeling complexes (CRCs), [32] histone- or DNA-modifying enzymes, and/or architectural proteins, thereby converting a “*closed*” chromatin region into an “*open*” (and accessible) region.

The human ATP-dependent CRCs comprises around 100 different proteins classified into four major complex subfamilies: switch/sucrose non-fermentable (SWI/SNF), chromodomain helicase DNA-binding (CHD), imitation switch (ISWI), and inositol-requiring 80 (INO80). [33,34] The four complexes break the histone–DNA interactions using ATP, thereby regulating nucleosome distribution and density across the genome, as well as their predisposition to chemical modifications. [34,35,36,37] Chemical PTMs in nucleosomal histones provide additional regulatory information for the recruitment of other **chromatin-bound** proteins. [5,8,38,39,40] In humans, over 100 histone ‘writer’ enzymes, and 50 ‘eraser’ enzymes, have been identified [41] as responsible to introducing or releasing more than 400 different histone PTMs. [42] Methylation and acetylation of lysines at the N-terminal tails of H3 and H4 are the most abundant and functionally described PTMs, and phosphorylation and ubiquitination are also well-characterized. [43,44,45] The different histone PTMs can recruit histone readers that contain specific histone PTM recognition domains, thus facilitating changes in chromatin topology and genome functionality. [46] For instance, histone lysine acetylation disrupts the histone–DNA electrostatic interactions and mediates the recruitment of one or several of the YEAST- ( $n = 4$ ) and bromodomain- ( $n = 46$ ) containing proteins [39] on active promoters and enhancers. [47] In contrast, histone lysine methylation does not alter the overall charge of chromatin and has a heterogeneous functionality, through the recruitment of histone readers that contain

72 Tudor ( $n = 41$ ), PWWP ( $n = 24$ ), PHD ( $n = 99$ ), WDR ( $n = 361$ ), or chromodomains  
73 ( $n = 29$ ).<sup>[5]</sup>

74 DNA chemical modifications can also influence protein interactions with chromatin. In  
75 particular, cytosine methylation in CpG dinucleotides is recognized by methyl-binding  
76 proteins with methyl-CpG-binding domains (MBD) ( $n = 11$ ), C2H2 zinc finger domains  
77 ( $n = 8$ ), or SET- and RING finger-associated domains (SRA) ( $n = 2$ ),<sup>[48]</sup> to mediate  
78 transcription, DNA repair, and genome stability.<sup>[48,49,50]</sup>

79 Finally, different structural proteins contribute to the spatial rearrangements of the  
80 chromatin. The CCCTC-binding factor (CTCF) and the protein complex cohesin  
81 contribute to the formation of genomic loops. At the megabase scale, these genomic  
82 interacting loops separate self-interacting domains, the so-called topologically  
83 associated domains (TADs), which can group together several functional units formed  
84 by several kilobases of DNA, known as “insulated neighborhoods”.<sup>[51,52]</sup> Overall,  
85 chromatin display a notable heterogenic and dynamic proteome composition that  
86 regulates all DNA-based processes.

## 87 88 **CHROMATOME ALTERATIONS IN HUMAN DISEASE**

89 Several pieces of evidence indicate that misregulation of chromatome integrity can  
90 profoundly influence human diseases (Figure 2).

91 Within protein coding regions, analysis of exome sequencing data from 60,706 normal  
92 individuals identified loss-of-function (LoF) intolerant genes ( $n = 3\,230$ ) with a lower  
93 mutation rate than expected.<sup>[53]</sup> Notably, almost 1/3 ( $n = 903$ ) of the LoF intolerant  
94 genes encode for **chromatin-bound** proteins (Supplementary Table 1), which suggests  
95 that their LoF might confer reproductive or survival disadvantages to carriers.  
96 Accordingly, inherited mutations in several of these proteins are causative of multiple  
97 developmental deficiencies and intellectual disabilities, including mutations in any of  
98 the six SWI/SNF subunit genes (*SMARCB1*, *SMARCA4*, *SMARCA2*, *SMARCE1*,  
99 *ARID1A*, and *ARID1B*), which compromise the transcriptional regulation of several  
100 neurodevelopmental genes and correlate with high penetrance of Coffin–Siris  
101 syndrome.<sup>[54]</sup>

102 Changes in the DNA sequences responsible for protein recruitment can also disrupt  
103 the function of chromatin-bound proteins. Nearly 90% of all phenotype-associated  
104 mutations identified by genome-wide association studies (GWAS) are located in non-  
105 coding DNA sequences.<sup>[55,56,57]</sup> Generally, these mutations associate with open  
106 chromatin regions, suggesting that they are located within regulatory DNA elements,  
107 such as promoters, enhancers, silencers, splicing branchpoints, and TAD borders.

108 [26,58,59,60] For instance, GWAS identified a strong risk variant associated with sporadic  
109 cases of Parkinson's disease (PD). This genomic variant localizes within a  
110 transcriptional enhancer that regulates the expression of the  $\alpha$ -synuclein (*SNCA*), a  
111 key gene associated with PD. At a functional level, the high-risk single-nucleotide  
112 polymorphism (SNP) variant disrupts the sequence-specific binding of EMX2 and  
113 NKX6-1 transcriptional repressors, thus increasing *SNCA* expression in neurons to  
114 pathological levels. [61]

115 The spontaneous acquisition of somatic mutations in chromatin-bound proteins is also  
116 associated to human pathogenesis, and in particular, to cancer. [9,28,29,62] Intensive  
117 exome sequencing of thousands of cancer genomes across of multiple cancer types,  
118 together with the development of computational algorithms, have enabled cancer  
119 driver mutations in specific genes to be identified. [63,64,65,66] Notably, about 50% of the  
120 commonly identified cancer driver genes ( $n = 120$ , from [63,64,65,66]) encode chromatin-  
121 bound proteins ( $n = 62$ ), strongly underscoring the impact of chromatin deregulation  
122 as a primary event establishing cancer malignancy. For instance, *TP53* is the most  
123 commonly mutated gene across the Pan-Cancer collection ( $> 3\ 000$  tumors from 12  
124 major cancer types) and is mutated in about 42% of the samples. [67] Histone writer  
125 and eraser enzymes are among the most mutated category of genes, comprising 13  
126 enzymes ranging from 0.8% (*EZH2*) to 6.6% (*MLL3*) of mutational frequency over the  
127 12 Pan-Cancer types. [67] Strikingly, mutations affecting the methyl transferase of the  
128 Polycomb repressive complex 2 (*PRC2*), *EZH2* (which methylates lysine 27 of histone  
129 H3, giving H3K27me<sub>2/3</sub>), [18] is often one of the few genetic abnormalities in cancer  
130 genomes with a low mutation burden. Thus, LoF mutations at *EZH2* are present in  
131 almost 2% of patients with acute myeloid leukemia (AML), which harbors the lowest  
132 mutation frequency of adult cancers (0.28 mutation per megabase). [67,68]

133 The recent identification of mutations in histone genes in pediatric cancers, which also  
134 usually have a low mutation burden, has reinforced the hypothesis that misregulation  
135 of chromatin is a central mechanism in cancer development. In particular, the mutation  
136 of the lysine residue 27 of histone H3 to methionine (H3K27M) is found in up to 80%  
137 of children with diffuse intrinsic pontine gliomas (DIPG), an aggressive pediatric high-  
138 grade gliomas. [69,70] Even though H3K27M represents less than 20% of histone H3 in  
139 DIPG cells, it induces a large misregulation of chromatin by directly compromising the  
140 activity of *EZH2*. Accordingly, H3K27M induces: a widespread decrease of H3K27me<sub>3</sub>  
141 and H3K27me<sub>2</sub>, which are essential histones PTMs for chromatin compaction and  
142 transcriptional silencing; an increase in H3K27ac, H3K4me<sub>3</sub>, and H3K36me<sub>2</sub>; and  
143 reduced DNA levels of 5-methylcytosine (5mC). [71,72,73,74,75] Genome-wide occupancy

144 studies by CHIP-seq and biochemical analyses indicate the existence of heterotypic  
145 H3K27M-K27ac in DIPG cells that colocalizes with bromodomain proteins on actively  
146 transcribed genes, where PRC2 is excluded. <sup>[76]</sup> Remarkably, analysis of the chromatin  
147 reorganization of DIPGs has provided the foundation for two promising therapeutic  
148 strategies against DIPG, of using either bromodomain and the extraterminal domain  
149 (BET) protein or EZH2 inhibitors. <sup>[76,77]</sup> These suggest that misregulation of histone  
150 modifiers, and in general, of chromatin-bound proteins, results in the acquisition of  
151 aberrant chromatin organization that can be exploited as vulnerabilities to target  
152 tumoral cells. Thus, the identification of changes in the chromatin composition can  
153 open new therapeutic approaches in several human diseases.

### 154 **TECHNICAL CHALLENGES OF CHROMATOME CHARACTERIZATION**

155 The proteomic characterization of the chromatin (chromatome) is a challenging endeavor  
156 due to (i) the difficulty of cleanly separating chromatin material from other cellular  
157 organelles, which can result in the presence of contaminants, (ii) the physicochemical  
158 heterogeneity of different chromatin regions, which require a balanced stringency of  
159 purification, and (iii) the mechanic sensitivity of heterochromatin to external forces, which  
160 can perturb the physiological chromatin composition during purification.

161 During interphase (the period between two cell divisions), chromatin is a water-insoluble  
162 polymer that tightly interacts with the nuclear periphery. <sup>[78]</sup> This property complicates its  
163 separation from the highly abundant nuclear lamina, a 10–30 nm thick meshwork of  
164 intermediate filaments. <sup>[79]</sup> Further, chromatin is not uniformly distributed throughout the  
165 nucleus but rather displays different densities and physical resistances. For instance,  
166 moving from the periphery to the center of the nucleus of human epithelial cells, the  
167 chromatin concentration comprises 50% and 20% of the local subnuclear volume,  
168 respectively. <sup>[78]</sup> Moreover, in contrast to euchromatin, the dense peripheral constitutive  
169 heterochromatin offers resistance to mechanical, enzymatic, and ion-based extraction.  
170 <sup>[80,81,82]</sup> Hence, while chromatin extractions in mild conditions might lead to an incomplete  
171 representation of the nuclear heterochromatin, labile euchromatin fragments or weakly  
172 bound proteins can be lost during isolation in harsh conditions.

173 Also, intense chromatin extraction methods from living cells can potentially introduce  
174 unpredicted artifacts in their proteomic composition. For instance, at constitutive  
175 heterochromatin, histone PTMs are labile upon mild physical perturbations in human  
176 epithelial cells. <sup>[83]</sup> Using low-amplitude stretches in these cells, for periods as short as 30  
177 min, causes a rapid and persistent chromatin loss of about 30% of H3K9me3 and a  
178 notable reduction in the elongating form of RNA polymerase II. <sup>[83]</sup> Thus, any experimental  
179

180 approach aiming to capture the chromatin-bound proteome in its native conditions must  
181 consider the rapid mechano-adaptation of the epigenome to external microenvironment-  
182 derived forces.

183 To date, several pioneering studies have developed very elegant biochemical strategies  
184 that, in combination with mass spectrometry, aim to investigate the chromatome.  
185 According to the broadness of the characterization, these methodologies can be classified  
186 as either target-specific or bulk chromatin proteomics. Target-specific methods aim to  
187 characterize: i) the proteomic composition of specific-loci, by isolating individual  
188 chromatin segments, <sup>[84]</sup> or ii) the protein-protein interactome within the chromatin, by  
189 capturing proteins of interest or specific histone PTMs. <sup>[2,85,86,87,88,89]</sup> On the other hand,  
190 the bulk chromatin proteomic methods aim to provide a global description of nuclear  
191 chromatin or large chromatin subtypes. These strategies have provided insight into the  
192 mechanisms governing chromatin regulation and organization, characterized the  
193 chromatome composition in different biological contexts, and identified *de novo*  
194 **chromatin-bound proteins**. Below, we discuss the biochemical principles and challenges  
195 of bulk chromatin proteomic methods and focus on providing a panoramic view.

## 196 **CHROMATIN ISOLATION FROM NATIVE NUCLEOUS**

197 Since the initial protocols described fifty years ago, <sup>[90]</sup> multiple methods for bulk chromatin  
198 isolation from living cells have been developed. These methods rely on limited  
199 biochemical principles to obtain a final soluble chromatin material outside of the nucleus  
200 for protein analysis (Figure 3). Physically, chromatin is a water-insoluble, stiff, and large  
201 polymer confined in the nucleus of eukaryotic cells. <sup>[79,90,91]</sup> Outside of the nucleus,  
202 chromatin self-associates in a condensed thick mass in low ionic strength buffer (<1 mM).  
203 <sup>[92]</sup> This property is used to collect large chromatin fragments upon nuclear breakdown  
204 followed by centrifugation. After chromatin precipitation, proteins can be solubilized with  
205 ionic detergents, <sup>[93,94,95]</sup> or by fragmenting DNA into small soluble fragments. <sup>[96]</sup>  
206 Alternatively, small chromatin fragments can be released directly from the nucleus and  
207 solubilized by digesting DNA with endonucleases in isotonic conditions (150 mM salt), <sup>[97]</sup>  
208 or by sequential digestion and subsequent salt-extraction. <sup>[98]</sup> Finally, the electrostatic  
209 interactions of proteins with chromatin can be disturbed by increasing the ionic strength  
210 of nuclear solutions, thus solubilizing the proteins outside of the nucleus (Figure 3). <sup>[82]</sup>

### **Chromatin isolation by nuclear breakdown**

In 2000, Mendez J and Stillman B. elaborated a fast and simple low ionic–based extraction method to purify insoluble material highly enriched in tightly bound chromatin proteins. <sup>[93]</sup> Very similar to a previous methodology, <sup>[91]</sup> Mendez & Stillman's method is based on a hypotonic swelling step, whereby the cells are lysed in the presence of a nonionic detergent, and the nuclei are collected by low centrifugation. A gentle nuclear breakdown is achieved in a low ionic strength buffer (< 1 mM) containing chelating agents (EDTA and EGTA) to further reduce residual divalent cations, and dithiothreitol to reduce disulfide bridges. Chromatin is subsequently collected by centrifugation for posterior analysis. Since its description, this chromatin enrichment strategy has become very popular and has been used both alone to analyze chromatin associations of particular proteins <sup>[99]</sup> as well as coupled with mass spectrometry-based proteomic studies. <sup>[94,95,100,101]</sup> Posteriorly, to increase the purity of chromatin preparation, variations in buffer composition and the addition of detergent were introduced to the original protocol to remove nuclear membrane components, as well as non-chromatin nucleoplasmic material. <sup>[102,103,104,105,106]</sup> Proteomic material from insoluble chromatin pellets was solubilized using ionic detergent–containing buffers (such as sodium dodecyl sulfate, SDS). <sup>[93,94,95]</sup>

### **Chromatin solubilization by nuclease digestion**

Alternatively, chromatin material can also be solubilized by enzymatic methods that fragment the large insoluble chromatin into small soluble fragments using nonspecific nucleases. Micrococcal nuclease (MNase) can create double-strand breaks within nucleosome linker regions, <sup>[107]</sup> while DNase I endonuclease preferentially cleaves GC-rich DNA unprotected by bound proteins, which are often located in active regulatory regions. <sup>[107]</sup> Importantly, MNase and DNase I display different digestion kinetics, according to the amount of enzyme used and the time of incubation; <sup>[107,108,109]</sup> these differences have been exploited to characterize the protein composition in different topological regions of the chromatin <sup>[96]</sup> as well as proteins with different interaction strengths with chromatin. <sup>[97]</sup> For instance, Dutta and collaborators treated insoluble chromatin pellets with endonucleases at different time points and characterized the temporal release of proteins associated with different chromatin types. <sup>[96]</sup> Proteins released early during treatment with both MNase and DNase I were enriched in factors associated with active GC-rich promoters or transcription start sites and loosely compacted euchromatin. On the other side, approximately half of non-histone proteins identified in this study belonged to the chromatin pellet, indicative of the large diversity of

250 protein composition in resistant heterochromatin. <sup>[96]</sup> A variation of this enzymatic  
251 approach was later adapted by the laboratory of E. Meshorer. <sup>[97]</sup> The technology (named  
252 differential chromatin-associated proteins, D-CAP) uses brief digestion with increasing  
253 concentrations of MNase in the presence of salt (150 mM); this leads to the immediate  
254 release of small fragments upon digestion. The dose-dependent enzymatic treatment in  
255 isolated nuclei simplified the experimental procedure and enabled the authors to  
256 standardize the same protocol in different biological conditions. By combining D-CAP with  
257 mass spectrometry, Alajem and collaborators explored the differential association of  
258 **chromatin-bound proteins** in pluripotent and differentiated cells. <sup>[97]</sup> They found that the  
259 SWI/SNF-type complex subunits SMARCC1 and SMARCD1 are more tightly associated  
260 with chromatin in differentiated cells with respect to pluripotent cells. As both proteins are  
261 expressed at similar levels in both cell types, these results point towards a  
262 posttranslational regulation of their chromatin association.

### 263 **Chromatome solubilization by salt extraction**

264 Protein–nucleic acid interactions are mostly mediated by electrostatic interactions. This  
265 property has long been used to differentiate loosely bound from tightly bound chromatin  
266 proteins. <sup>[110,111,112]</sup> Based on the differential physical properties of the chromatin proteins,  
267 Avgousti and colleagues recently elaborated a protocol to determine the changes in the  
268 chromatin composition of host cells in the presence of the adenoviral protein VII, which  
269 resembles cellular histones. <sup>[98,113]</sup> The protocol relies on the complete MNase digestion  
270 of nuclei, in this case in hypotonic conditions, thus preventing the release of chromatin  
271 fragments. Subsequent serial washes of the digested nuclei with increasing  
272 concentrations of salt (80-600 mM NaCl) in the presence of nonionic detergent (0.1%  
273 Triton X-100) enable the sequential release the chromatin material. In these conditions,  
274 the proteins weakly bound to chromatin are expected to be released in low-salt  
275 concentrations, while tightly **chromatin-bound** proteins would remain in the insoluble  
276 fraction. Using this protocol, the authors found that the viral protein VII causes changes  
277 in the chromatome composition of the host cell, with a remarkable increase in chromatin  
278 retention of high mobility group protein B family, a key protein involved in the activation of  
279 the immune response. <sup>[98]</sup>

281  
282 To increase proteomic sensitivity, chromatin enriching salt preparations have recently  
283 been coupled to data-independent acquisition (CHESS-DIA) mass spectrometry. <sup>[82]</sup> For  
284 this, isolated nuclei are directly subjected to a series of salt-based extraction of nuclear  
285 proteins. According to the ionic strength applied, proteins are classified as solubilized in

286 four different fractions: unbound nucleoplasmic proteins (15 mM NaCl), euchromatin  
287 proteins (250 mM), heterochromatin proteins (600 mM), and insoluble structural proteins.  
288 [82] CHESS-DIA offers a notable correlation between proteins classified as chromatin  
289 proteins using this protocol and their previous annotation as nuclear proteins in public  
290 imaging database (>85%). However, 55% of protein classified as nucleoplasmic were not  
291 observed in the nucleus by direct immunostaining, [82] thus alerting for the presence of  
292 contaminants in the nuclear fraction of CHESS, most likely derived from co-isolated  
293 organelles.

294  
295 In our view, some potential caveats must be taken into consideration when using one of  
296 these (now less technically challenging) methods to characterize the chromatin  
297 composition. First, insolubility in low ionic conditions is not an exclusive property of  
298 chromatin; hence, these isolation methods can eventually carry over impurities from other  
299 organelles (such as mitochondria and vesicles) that can co-precipitate with nuclei or  
300 chromatin preparations. [114] Second, the presence of ionic conditions and detergents can  
301 decrease retention of proteins to chromatin. [91,113,115,116] Thus, highly mobile nuclear  
302 proteins can potentially be lost during purification of chromatin. Third, as transient  
303 chromatin interactions are a common feature of chromatin-bound proteins, [117] proteins  
304 with a minor fraction bound to chromatin could escape the capture during native chromatin  
305 isolation. Fourth, the association of mechanical-sensitive chromatin-bound proteins and  
306 histone PTMs can be perturbed during extensive sample manipulation. [83] These  
307 perturbations are unpredictable and can be overlooked during sample preparation, thus  
308 compromising the interpretation of the results.

### 309 **CHROMATIN ISOLATION FROM CROSSLINKED NUCLEOUS**

310 Developed in the laboratory of Juri Rappsilber, the chromatin enrichment for proteomics  
311 (ChEP) protocol applies extremely stringent washing conditions to remove non-  
312 chromatin-bound proteins. [114,118] In this protocol, chromatin-bound proteins are  
313 covalently attached by *in vivo* crosslinking with formaldehyde either directly or indirectly  
314 to DNA. This chemical fixation method offers several benefits: it is cell-permeable and  
315 rapidly diffuses throughout the cell, thereby crosslinking DNA-protein and protein-protein  
316 complexes associated within a distance of less than 2 Å. Artefactual crosslinking is very  
317 unlikely, as experimentally proven by incubating DNA with high concentrations of BSA  
318 (50 mg/ml) in 1% of formaldehyde for several days. [119] Using ChEP, non-crosslinked  
319 contaminants are then washed away (using high denaturing extraction buffers containing  
320 4% SDS and 8 M urea, and intermediate RNase digestion reduces the purification of  
321

nascent RNA-associated proteins. Chromatin is then solubilized by sonication, and the soluble samples are reverse-crosslinked by heating before proteomic analysis. [114,118] Coupled to mass spectrometry, ChEP displays a notable enrichment in proteins associated with DNA- and chromatin-based processes, such as DNA replication, transcription, and repair. But in contrast to classical native chromatin enrichment, the presence of proteins involved in pre-rRNA processing and proteins with unrelated chromatin functions is reduced. [114,118] Thus, combining crosslinking with harsh washing conditions increases the capacity to discriminate true chromatin components from impurities.

Recently, Zaret and collaborators developed a method (Gradient-seq) to successfully discriminate between sonication-sensitive euchromatin from sonication-resistant heterochromatin in human fibroblasts. [80] By separating partially sonicated, crosslinked chromatin with linear sucrose gradients, the authors discriminate the dense chromatin (which sediments in the middle of the gradient) from sonication-sensitive chromatin (at the top of the gradient). Genomic characterization of the fractions indicated that the dense fractions correspond to constitutive heterochromatin dominated by the presence of H3K9me3 and lamin B1, marked by CpG methylation, and enriched in multiple repetitive elements. On the other hand, the sonication-sensitive chromatin encompasses the DNase-sensitive euchromatic domains and H3K27me3-marked facultative heterochromatin. In combination with mass spectrometry-based proteomics, Gradient-seq enabled 217 heterochromatin-specific proteins to be identified, nearly half of them being present in H3K9me3 domains. **However, the presence of soluble cellular proteins on the top gradient fraction hampered the determination of proteomic composition of the euchromatin.** Further functional analyses indicated that a notable proportion of heterochromatin proteins function as repressors of gene activation, and point towards heterochromatin stability as a barrier for cell lineage conversion. [80]

Schübeler and collaborators then adapted a strategy to separate crosslinked DNA-protein complexes with buoyant, density-based fractionation in a cesium chloride (CsCl) gradient (DEMAC, for density-based enrichment for mass spectrometry analysis of chromatin). [3] In this protocol, nuclear fractions are first purified after hypotonic lysis, and the isolated nucleus is crosslinked with formaldehyde and then sonicated, giving fragments ranging in size from 0.1–12 kb. These fragments are recovered using a stable isopycnic density gradient of 1.39 g/cm<sup>3</sup>, after 48 h of centrifugation. Using this protocol, the complete chromatin can be recovered without any topological biases. In comparison to the cellular and nuclear proteome, the chromatin samples have reduced levels of ribosome and

358 spliceosome proteins, which are RNA-bound proteins abundantly found in the nucleus,  
359 as the result of adding RNase A before centrifugation. However, RNA depletion can also  
360 result in the loss of chromatin retention of relevant proteins attached to chromatin in an  
361 RNA-dependent manner.

362 At the beginning of the 2000s, Sharpless and collaborators developed the concept and  
363 methodology of “click chemistry”.<sup>[120]</sup> Click chemistry encompasses a group of simple and  
364 highly efficient chemical reactions that enable a set of molecules (“building blocks”) to be  
365 assembled to synthesize new compounds. Since its development, click chemistry has been  
366 applied to a wide range of research areas, including chemistry, material science, and  
367 biological sciences.<sup>[121]</sup> In 2011, two different laboratories elaborated in parallel a very  
368 similar method to capture nascent DNA during replication from cells in a very efficient  
369 manner, by covalently linking the emergent DNA to biotin moieties using click chemistry.  
370<sup>[122,123]</sup> The methods of isolation of proteins on nascent DNA (iPOND) and the DNA-  
371 mediated chromatin pulldown (Dm-ChP) rely on an efficient incorporation of the thymidine  
372 analog 5-ethynyl-2'-deoxyuridine (EdU) during DNA replication, the addition of a biotin  
373 moiety to the incorporated EdU using mild conditions, and streptavidin–biotin affinity to  
374 capture sheared EdU-labelled chromatin.<sup>[122,123]</sup> Inspired by these technologies, we  
375 recently elaborated a simple, robust, and straightforward experimental strategy that  
376 combines a biochemical method to capture DNA with high-resolution mass spectrometry  
377 analysis and a subsequent statistical assessment, for identification of *bona fide*  
378 chromatin-bound proteins.<sup>[124,125]</sup> We based our strategy on i) whole-genome metabolic  
379 labeling with the thymidine analog 5-ethynyl-2'-deoxyuridine (EdU) during several rounds  
380 of cell division, in a non-cytotoxic manner; ii) a chemical crosslinking step, which also  
381 preserves weak but specific interactions; iii) addition of a biotin moiety to the incorporated  
382 EdU, using the click reaction; iv) fragmentation of chromatin; v) streptavidin–biotin affinity  
383 purification, to capture chromatin; vi) mass spectrometry analysis; and, vii) Significance  
384 Analysis of INTeractome (SAINT), to identify *bona fide* chromatin-bound proteins. The  
385 biochemical procedure stands out for its simplicity, robustness, and usability in a wide range  
386 of cells and flexibility for combining with techniques (such as conventional affinity  
387 purification and ChIP). The complete procedure enables the *identification of Proteins on*  
388 *Total DNA* (named iPOTD, based on its biochemical and phonetical similarity with iPOND).  
389<sup>[125]</sup> Using iPOTD, we have recently provided a broad and comprehensive characterization  
390 of the chromatome of murine pluripotent embryonic stem cells. Importantly, we proved the  
391 power of this novel strategy by discovering and characterizing the unexpected chromatin  
392 association of a major one-carbon pathway metabolic enzyme, namely  
393 adenosylhomocysteinase (AHCY), which is involved in the methionine cycle.<sup>[124,125]</sup>

## CONCLUSIONS AND OUTLOOK

Chromatin-bound proteins organize the three-dimensional structure of chromatin, regulate gene expression, replicate DNA, and transmit epigenetic information to cellular progeny. [18,19,126,127,128] Remarkably, human diseases are highly influenced by alterations in the chromatin-bound protein composition. [129] Considering that only 40% of the protein level variability can be attributed to differences in mRNA levels in mammalian cells, [12] the application of chromatome profiling methods is key to fully understanding the functionality of cells, as well as to unveiling disease-driven molecular mechanism.

Chromatin has a highly heterogenic composition and comprises diverse structural features, such that no single isolation method can be used to study all the different aspects of nuclear chromatin. Therefore, the method selected for chromatin analysis should depend on the particular problem to be investigated. However, in our view, an optimal approach to characterize the chromatin composition must: i) be as simple as possible, to increase the yield of isolation and to reduce technical variability in and between laboratories; ii) preserve weak and transient molecular interactions; iii) be robust enough to minimize the presence of impurities from other subcellular organelles; and iv) be as direct as possible, to unequivocally identify uncharacterized chromatin-bound factors.

As there is currently no absolute criterion of purity for chromatin, the *de novo* identification of chromatin binding proteins requires additional experimental validations, including chromatin immunoprecipitation combined with massive parallel sequencing. In particular, recent studies have characterized the unexpected association of metabolic enzymes to chromatin. [124,130,131,132,133] Chromatin recruitment of metabolic enzymes is considered to be an adaptive cell solution for the highly compartmentalized metabolic and subcellular local demands of metabolites. These strategies can also exploit solutions found by cancer cells that, similar to pluripotent cells, have an elevated proliferation rate. [124,133] Considered as cellular vulnerability points, pharmacological targeting of these enzymes compromises cellular fitness, [124,133] thus indicating that the *de novo* identification of chromatin-bound proteins can open as of yet unexplored therapeutic avenues against human diseases.

**Chromatin fractionation strategies can be instrumental to clarify the protein composition of subnuclear compartments.** These membrane-less compartments (e.g. nucleolus,

430 enhancer clusters, or Polycomb bodies) are thought to self-organize by two distinct  
431 mechanisms: polymer-polymer phase-separation, by which chromatin binders function as  
432 a bridge among different chromatin segments, or ii) liquid–liquid phase separation,  
433 through multivalent interactions among proteins and other molecules that bind the  
434 chromatin. <sup>[134]</sup> The mechanism by which the subnuclear compartments self-assemble is  
435 predicted to impact their physical and functional properties, such as the size and  
436 spreading of the subnuclear compartment across multiple genomic loci. **Thus, the**  
437 **proteomic characterization of the subnuclear compartments could contribute to gain**  
438 **insights into the fundamental principles governing chromatin compartmentalization by**  
439 **phase separation.**

## 441 **ACKNOWLEDGMENTS**

442 We thank all the members of Di Croce laboratory for helpful discussions, and V. A. Raker  
443 for scientific editing. I.E. is supported by La Caixa INPhINIT program. L.D.C is supported  
444 by grants from the Spanish of Economy, Industry and Competitiveness (MEIC)  
445 (BFU2016-75008-P), “Fundación Vencer El Cancer” (VEC), the European Regional  
446 Development Fund (FEDER), Fundació “La Marató de TV3”, and from AGAUR. S.A. is  
447 funded by Ramón y Cajal Program MICIU-FSE (RYC2018-025002-I) and ISCIII-FEDER  
448 (PI19/01814). We acknowledge support of the Spanish Ministry Science and Innovation  
449 to the EMBL partnership, the Centro de Excelencia Severo Ochoa, and the CERCA  
450 Programme / Generalitat de Catalunya.

451 The authors declare no conflict of interest.

- 457 [1] Imhof A, Bonaldi T. (2005). "Chromatomics" the analysis of the chromatome. *Mol Biosyst*, 1(2), 112-  
458 6.
- 459 [2] Noberini R, Sigismondo G, Bonaldi T. (2016). The contribution of mass spectrometry-based  
460 proteomics to understanding epigenetics. *Epigenomics*, 8(3), 429-45.
- 461 [3] Ginno PA, Burger L, Seebacher J, Iesmantavicius V, Schubeler D. (2018). Cell cycle-resolved  
462 chromatin proteomics reveals the extent of mitotic preservation of the genomic regulatory landscape.  
463 *Nat Commun*, 9(1), 4048.
- 464 [4] Aebersold R, Agar JN, Amster IJ, Baker MS, Bertozzi CR, Boja ES, . . . Zhang B. (2018). How many  
465 human proteoforms are there? *Nat Chem Biol*, 14(3), 206-14.
- 466 [5] Arrowsmith CH, Schapira M. (2019). Targeting non-bromodomain chromatin readers. *Nat Struct Mol  
467 Biol*, 26(10), 863-9.
- 468 [6] Bonnet J, Lindeboom RGH, Pokrovsky D, Stricker G, Celik MH, Rupp RAW, . . . Muller J. (2019).  
469 Quantification of Proteins and Histone Marks in *Drosophila* Embryos Reveals Stoichiometric  
470 Relationships Impacting Chromatin Regulation. *Dev Cell*, 51(5), 632-44 e6.
- 471 [7] Poorey K, Viswanathan R, Carver MN, Karpova TS, Cirimotich SM, McNally JG, . . . Auble DT. (2013).  
472 Measuring chromatin interaction dynamics on the second time scale at single-copy genes. *Science*,  
473 342(6156), 369-72.
- 474 [8] Wierer M, Mann M. (2016). Proteomics to study DNA-bound and chromatin-associated gene  
475 regulatory complexes. *Hum Mol Genet*, 25(R2), R106-R14.
- 476 [9] Dawson MA, Kouzarides T. (2012). Cancer epigenetics: from mechanism to therapy. *Cell*, 150(1), 12-  
477 27.
- 478 [10] Eubanks CG, Dayebgadah G, Liu X, Washburn MP. (2017). Unravelling the biology of chromatin in  
479 health and cancer using proteomic approaches. *Expert Rev Proteomics*, 14(10), 905-15.
- 480 [11] Marchione DM, Garcia BA, Wojcik J. (2019). Proteomic approaches for cancer epigenetics research.  
481 *Expert Rev Proteomics*, 16(1), 33-47.
- 482 [12] Schwanhausser B, Busse D, Li N, Dittmar G, Schuchhardt J, Wolf J, . . . Selbach M. (2011). Global  
483 quantification of mammalian gene expression control. *Nature*, 473(7347), 337-42.
- 484 [13] de Sousa Abreu R, Penalva LO, Marcotte EM, Vogel C. (2009). Global signatures of protein and  
485 mRNA expression levels. *Mol Biosyst*, 5(12), 1512-26.
- 486 [14] Maier T, Guell M, Serrano L. (2009). Correlation of mRNA and protein in complex biological samples.  
487 *FEBS Lett*, 583(24), 3966-73.
- 488 [15] Vogel C, Abreu Rde S, Ko D, Le SY, Shapiro BA, Burns SC, . . . Penalva LO. (2010). Sequence  
489 signatures and mRNA concentration can explain two-thirds of protein abundance variation in a human  
490 cell line. *Mol Syst Biol*, 6, 400.
- 491 [16] Wang J, Ma Z, Carr SA, Mertins P, Zhang H, Zhang Z, . . . Zhang B. (2017). Proteome Profiling  
492 Outperforms Transcriptome Profiling for Coexpression Based Gene Function Prediction. *Mol Cell  
493 Proteomics*, 16(1), 121-34.
- 494 [17] Kustatscher G, Grabowski P, Schrader TA, Passmore JB, Schrader M, Rappsilber J. (2019). Co-  
495 regulation map of the human proteome enables identification of protein functions. *Nat Biotechnol*,  
496 37(11), 1361-71.

- 497 [18] Aranda S, Mas G, Di Croce L. (2015). Regulation of gene transcription by Polycomb proteins. *Sci*  
498 *Adv*, 1(11), e1500737.
- 499 [19] Cramer P. (2014). A tale of chromatin and transcription in 100 structures. *Cell*, 159(5), 985-94.
- 500 [20] Fyodorov DV, Zhou BR, Skoultchi AI, Bai Y. (2018). Emerging roles of linker histones in regulating  
501 chromatin structure and function. *Nat Rev Mol Cell Biol*, 19(3), 192-206.
- 502 [21] Klemm SL, Shipony Z, Greenleaf WJ. (2019). Chromatin accessibility and the regulatory epigenome.  
503 *Nat Rev Genet*, 20(4), 207-20.
- 504 [22] Allshire RC, Madhani HD. (2018). Ten principles of heterochromatin formation and function. *Nat Rev*  
505 *Mol Cell Biol*, 19(4), 229-44.
- 506 [23] Saksouk N, Simboeck E, Dejardin J. (2015). Constitutive heterochromatin formation and transcription  
507 in mammals. *Epigenetics Chromatin*, 8, 3.
- 508 [24] Stewart-Morgan KR, Reveron-Gomez N, Groth A. (2019). Transcription Restart Establishes  
509 Chromatin Accessibility after DNA Replication. *Mol Cell*, 75(2), 284-97 e6.
- 510 [25] Thurman RE, Rynes E, Humbert R, Vierstra J, Maurano MT, Haugen E, . . . Stamatoyannopoulos JA.  
511 (2012). The accessible chromatin landscape of the human genome. *Nature*, 489(7414), 75-82.
- 512 [26] Hnisz D, Abraham BJ, Lee TI, Lau A, Saint-Andre V, Sigova AA, . . . Young RA. (2013). Super-  
513 enhancers in the control of cell identity and disease. *Cell*, 155(4), 934-47.
- 514 [27] Lambert SA, Jolma A, Campitelli LF, Das PK, Yin Y, Albu M, . . . Weirauch MT. (2018). The Human  
515 Transcription Factors. *Cell*, 172(4), 650-65.
- 516 [28] Lee TI, Young RA. (2013). Transcriptional regulation and its misregulation in disease. *Cell*, 152(6),  
517 1237-51.
- 518 [29] Bradner JE, Hnisz D, Young RA. (2017). Transcriptional Addiction in Cancer. *Cell*, 168(4), 629-43.
- 519 [30] Young RA. (2011). Control of the embryonic stem cell state. *Cell*, 144(6), 940-54.
- 520 [31] Iwafuchi-Doi M, Donahue G, Kakumanu A, Watts JA, Mahony S, Pugh BF, . . . Zaret KS. (2016). The  
521 Pioneer Transcription Factor FoxA Maintains an Accessible Nucleosome Configuration at Enhancers  
522 for Tissue-Specific Gene Activation. *Mol Cell*, 62(1), 79-91.
- 523 [32] Brahma S, Henikoff S. (2020). Epigenome Regulation by Dynamic Nucleosome Unwrapping. *Trends*  
524 *Biochem Sci*, 45(1), 13-26.
- 525 [33] Hota SK, Bruneau BG. (2016). ATP-dependent chromatin remodeling during mammalian  
526 development. *Development*, 143(16), 2882-97.
- 527 [34] Clapier CR, Iwasa J, Cairns BR, Peterson CL. (2017). Mechanisms of action and regulation of ATP-  
528 dependent chromatin-remodelling complexes. *Nat Rev Mol Cell Biol*, 18(7), 407-22.
- 529 [35] Narlikar GJ, Sundaramoorthy R, Owen-Hughes T. (2013). Mechanisms and functions of ATP-  
530 dependent chromatin-remodeling enzymes. *Cell*, 154(3), 490-503.
- 531 [36] Sokpor G, Castro-Hernandez R, Rosenbusch J, Staiger JF, Tuoc T. (2018). ATP-Dependent  
532 Chromatin Remodeling During Cortical Neurogenesis. *Front Neurosci*, 12, 226.
- 533 [37] Talbert PB, Henikoff S. (2017). Histone variants on the move: substrates for chromatin dynamics. *Nat*  
534 *Rev Mol Cell Biol*, 18(2), 115-26.

- 535 [38] Strahl BD, Allis CD. (2000). The language of covalent histone modifications. *Nature*, 403(6765), 41-  
536 5.
- 537 [39] Zaware N, Zhou MM. (2019). Bromodomain biology and drug discovery. *Nat Struct Mol Biol*, 26(10),  
538 870-9.
- 539 [40] Janssen KA, Sidoli S, Garcia BA. (2017). Recent Achievements in Characterizing the Histone Code  
540 and Approaches to Integrating Epigenomics and Systems Biology. *Methods Enzymol*, 586, 359-78.
- 541 [41] Khare SP, Habib F, Sharma R, Gadewal N, Gupta S, Galande S. (2012). Histome--a relational  
542 knowledgebase of human histone proteins and histone modifying enzymes. *Nucleic Acids Res*,  
543 40(Database issue), D337-42.
- 544 [42] Huang H, Sabari BR, Garcia BA, Allis CD, Zhao Y. (2014). SnapShot: histone modifications. *Cell*,  
545 159(2), 458- e1.
- 546 [43] Zhao Y, Garcia BA. (2015). Comprehensive Catalog of Currently Documented Histone Modifications.  
547 *Cold Spring Harbor Perspectives in Biology*, 7(9).
- 548 [44] Sidoli S, Lopes M, Lund PJ, Goldman N, Fasolino M, Coradin M, . . . Garcia BA. (2019). A mass  
549 spectrometry-based assay using metabolic labeling to rapidly monitor chromatin accessibility of  
550 modified histone proteins. *Sci Rep*, 9(1), 13613.
- 551 [45] Simithy J, Sidoli S, Garcia BA. (2018). Integrating Proteomics and Targeted Metabolomics to  
552 Understand Global Changes in Histone Modifications. *Proteomics*, 18(18), e1700309.
- 553 [46] Ji X, Dadon DB, Abraham BJ, Lee TI, Jaenisch R, Bradner JE, Young RA. (2015). Chromatin  
554 proteomic profiling reveals novel proteins associated with histone-marked genomic regions. *Proc Natl  
555 Acad Sci U S A*, 112(12), 3841-6.
- 556 [47] Fujisawa T, Filippakopoulos P. (2017). Functions of bromodomain-containing proteins and their roles  
557 in homeostasis and cancer. *Nat Rev Mol Cell Biol*, 18(4), 246-62.
- 558 [48] Mahmood N, Rabbani SA. (2019). DNA Methylation Readers and Cancer: Mechanistic and  
559 Therapeutic Applications. *Front Oncol*, 9, 489.
- 560 [49] Jones PA. (2012). Functions of DNA methylation: islands, start sites, gene bodies and beyond. *Nat  
561 Rev Genet*, 13(7), 484-92.
- 562 [50] Zhu H, Wang G, Qian J. (2016). Transcription factors as readers and effectors of DNA methylation.  
563 *Nat Rev Genet*, 17(9), 551-65.
- 564 [51] Zheng H, Xie W. (2019). The role of 3D genome organization in development and cell differentiation.  
565 *Nat Rev Mol Cell Biol*, 20(9), 535-50.
- 566 [52] Hnisz D, Day DS, Young RA. (2016). Insulated Neighborhoods: Structural and Functional Units of  
567 Mammalian Gene Control. *Cell*, 167(5), 1188-200.
- 568 [53] Lek M, Karczewski KJ, Minikel EV, Samocha KE, Banks E, Fennell T, . . . Exome Aggregation C.  
569 (2016). Analysis of protein-coding genetic variation in 60,706 humans. *Nature*, 536(7616), 285-91.
- 570 [54] Tsurusaki Y, Okamoto N, Ohashi H, Kosho T, Imai Y, Hibi-Ko Y, . . . Matsumoto N. (2012). Mutations  
571 affecting components of the SWI/SNF complex cause Coffin-Siris syndrome. *Nat Genet*, 44(4), 376-  
572 8.
- 573 [55] Maurano MT, Humbert R, Rynes E, Thurman RE, Haugen E, Wang H, . . . Stamatoyannopoulos JA.  
574 (2012). Systematic localization of common disease-associated variation in regulatory DNA. *Science*,  
575 337(6099), 1190-5.

- 576 [56] Fadason T, Schierding W, Lumley T, O'Sullivan JM. (2018). Chromatin interactions and expression  
577 quantitative trait loci reveal genetic drivers of multimorbidities. *Nat Commun*, 9(1), 5198.
- 578 [57] Gloss BS, Dinger ME. (2018). Realizing the significance of noncoding functionality in clinical  
579 genomics. *Exp Mol Med*, 50(8), 97.
- 580 [58] Chabot B, Shkreta L. (2016). Defective control of pre-messenger RNA splicing in human disease. *J*  
581 *Cell Biol*, 212(1), 13-27.
- 582 [59] Lupianez DG, Kraft K, Heinrich V, Krawitz P, Brancati F, Klopocki E, . . . Mundlos S. (2015).  
583 Disruptions of topological chromatin domains cause pathogenic rewiring of gene-enhancer  
584 interactions. *Cell*, 161(5), 1012-25.
- 585 [60] Anna A, Monika G. (2018). Splicing mutations in human genetic disorders: examples, detection, and  
586 confirmation. *J Appl Genet*, 59(3), 253-68.
- 587 [61] Soldner F, Stelzer Y, Shivalila CS, Abraham BJ, Latourelle JC, Barrasa MI, . . . Jaenisch R. (2016).  
588 Parkinson-associated risk variant in distal enhancer of alpha-synuclein modulates target gene  
589 expression. *Nature*, 533(7601), 95-9.
- 590 [62] Valencia AM, Kadoch C. (2019). Chromatin regulatory mechanisms and therapeutic opportunities in  
591 cancer. *Nat Cell Biol*, 21(2), 152-61.
- 592 [63] Bailey MH, Tokheim C, Porta-Pardo E, Sengupta S, Bertrand D, Weerasinghe A, . . . Ding L. (2018).  
593 Comprehensive Characterization of Cancer Driver Genes and Mutations. *Cell*, 174(4), 1034-5.
- 594 [64] Lawrence MS, Stojanov P, Mermel CH, Robinson JT, Garraway LA, Golub TR, . . . Getz G. (2014).  
595 Discovery and saturation analysis of cancer genes across 21 tumour types. *Nature*, 505(7484), 495-  
596 501.
- 597 [65] Martincorena I, Raine KM, Gerstung M, Dawson KJ, Haase K, Van Loo P, . . . Campbell PJ. (2017).  
598 Universal Patterns of Selection in Cancer and Somatic Tissues. *Cell*, 171(5), 1029-41 e21.
- 599 [66] Dietlein F, Weghorn D, Taylor-Weiner A, Richters A, Reardon B, Liu D, . . . Sunyaev SR. (2020).  
600 Identification of cancer driver genes based on nucleotide context. *Nat Genet*, 52(2), 208-18.
- 601 [67] Kandoth C, McLellan MD, Vandin F, Ye K, Niu B, Lu C, . . . Ding L. (2013). Mutational landscape and  
602 significance across 12 major cancer types. *Nature*, 502(7471), 333-9.
- 603 [68] Lund K, Adams PD, Copland M. (2014). EZH2 in normal and malignant hematopoiesis. *Leukemia*,  
604 28(1), 44-9.
- 605 [69] Schwartzenuber J, Korshunov A, Liu XY, Jones DT, Pfaff E, Jacob K, . . . Jabado N. (2012). Driver  
606 mutations in histone H3.3 and chromatin remodelling genes in paediatric glioblastoma. *Nature*,  
607 482(7384), 226-31.
- 608 [70] Wu G, Broniscer A, McEachron TA, Lu C, Paugh BS, Becksfors J, . . . St. Jude Children's Research  
609 Hospital-Washington University Pediatric Cancer Genome P. (2012). Somatic histone H3 alterations  
610 in pediatric diffuse intrinsic pontine gliomas and non-brainstem glioblastomas. *Nat Genet*, 44(3), 251-  
611 3.
- 612 [71] Bender S, Tang Y, Lindroth AM, Hovestadt V, Jones DT, Kool M, . . . Pfister SM. (2013). Reduced  
613 H3K27me3 and DNA hypomethylation are major drivers of gene expression in K27M mutant pediatric  
614 high-grade gliomas. *Cancer Cell*, 24(5), 660-72.
- 615 [72] Chan KM, Fang D, Gan H, Hashizume R, Yu C, Schroeder M, . . . Zhang Z. (2013). The histone  
616 H3.3K27M mutation in pediatric glioma reprograms H3K27 methylation and gene expression. *Genes*  
617 *Dev*, 27(9), 985-90.

- 618 [73] Lewis PW, Muller MM, Koletsky MS, Cordero F, Lin S, Banaszynski LA, . . . Allis CD. (2013). Inhibition  
619 of PRC2 activity by a gain-of-function H3 mutation found in pediatric glioblastoma. *Science*,  
620 340(6134), 857-61.
- 621 [74] Venneti S, Garimella MT, Sullivan LM, Martinez D, Huse JT, Heguy A, . . . Judkins AR. (2013).  
622 Evaluation of histone 3 lysine 27 trimethylation (H3K27me3) and enhancer of Zest 2 (EZH2) in  
623 pediatric glial and glioneuronal tumors shows decreased H3K27me3 in H3F3A K27M mutant  
624 glioblastomas. *Brain Pathol*, 23(5), 558-64.
- 625 [75] Larson JD, Kasper LH, Paugh BS, Jin H, Wu G, Kwon CH, . . . Baker SJ. (2019). Histone H3.3 K27M  
626 Accelerates Spontaneous Brainstem Glioma and Drives Restricted Changes in Bivalent Gene  
627 Expression. *Cancer Cell*, 35(1), 140-55 e7.
- 628 [76] Piunti A, Hashizume R, Morgan MA, Bartom ET, Horbinski CM, Marshall SA, . . . Shilatifard A. (2017).  
629 Therapeutic targeting of polycomb and BET bromodomain proteins in diffuse intrinsic pontine gliomas.  
630 *Nat Med*, 23(4), 493-500.
- 631 [77] Mohammad F, Weissmann S, Leblanc B, Pandey DP, Hojfeldt JW, Comet I, . . . Helin K. (2017). EZH2  
632 is a potential therapeutic target for H3K27M-mutant pediatric gliomas. *Nat Med*, 23(4), 483-92.
- 633 [78] Ou HD, Phan S, Deerinck TJ, Thor A, Ellisman MH, O'Shea CC. (2017). ChromEMT: Visualizing 3D  
634 chromatin structure and compaction in interphase and mitotic cells. *Science*, 357(6349).
- 635 [79] Stephens AD, Banigan EJ, Marko JF. (2019). Chromatin's physical properties shape the nucleus and  
636 its functions. *Curr Opin Cell Biol*, 58, 76-84.
- 637 [80] Becker JS, McCarthy RL, Sidoli S, Donahue G, Kaeding KE, He Z, . . . Zaret KS. (2017). Genomic  
638 and Proteomic Resolution of Heterochromatin and Its Restriction of Alternate Fate Genes. *Mol Cell*,  
639 68(6), 1023-37 e15.
- 640 [81] Teves SS, Henikoff S. (2012). Salt fractionation of nucleosomes for genome-wide profiling. *Methods*  
641 *Mol Biol*, 833, 421-32.
- 642 [82] Federation AJ, Nandakumar V, Searle BC, Stergachis A, Wang H, Pino LK, . . . Stamatoyannopoulos  
643 JA. (2020). Highly Parallel Quantification and Compartment Localization of Transcription Factors and  
644 Nuclear Proteins. *Cell Rep*, 30(8), 2463-71 e5.
- 645 [83] Nava MM, Miroshnikova YA, Biggs LC, Whitefield DB, Metge F, Boucas J, . . . Wickstrom SA. (2020).  
646 Heterochromatin-Driven Nuclear Softening Protects the Genome against Mechanical Stress-Induced  
647 Damage. *Cell*, 181(4), 800-17 e22.
- 648 [84] Gauchier M, van Mierlo G, Vermeulen M, Dejardin J. (2020). Purification and enrichment of specific  
649 chromatin loci. *Nat Methods*, 17(4), 380-9.
- 650 [85] Ummethum H, Hamperl S. (2020). Proximity Labeling Techniques to Study Chromatin. *Front Genet*,  
651 11, 450.
- 652 [86] Rafiee MR, Girardot C, Sigismondo G, Krijgsveld J. (2016). Expanding the Circuitry of Pluripotency  
653 by Selective Isolation of Chromatin-Associated Proteins. *Mol Cell*, 64(3), 624-35.
- 654 [87] Kleiner RE, Hang LE, Molloy KR, Chait BT, Kapoor TM. (2018). A Chemical Proteomics Approach to  
655 Reveal Direct Protein-Protein Interactions in Living Cells. *Cell Chem Biol*, 25(1), 110-20 e3.
- 656 [88] Villasenor R, Pfaendler R, Ambrosi C, Butz S, Giuliani S, Bryan E, . . . Baubec T. (2020). ChromID  
657 identifies the protein interactome at chromatin marks. *Nat Biotechnol*, 38(6), 728-36.
- 658 [89] Burton AJ, Haugbro M, Gates LA, Bagert JD, Allis CD, Muir TW. (2020). In situ chromatin  
659 interactomics using a chemical bait and trap approach. *Nature Chemistry*, 12(6), 520-7.

- 660 [90] Garrard WT, Hancock R. (1978). Preparation of chromatin from animal tissues and cultured cells.  
661 *Methods Cell Biol*, 17, 27-50.
- 662 [91] Hancock R, Faber AJ, Fakan S. (1977). Isolation of interphase chromatin structures from cultured  
663 cells. *Methods Cell Biol*, 15, 127-47.
- 664 [92] Cai S, Song Y, Chen C, Shi J, Gan L. (2018). Natural chromatin is heterogeneous and self-associates  
665 in vitro. *Mol Biol Cell*, 29(13), 1652-63.
- 666 [93] Mendez J, Stillman B. (2000). Chromatin association of human origin recognition complex, cdc6, and  
667 minichromosome maintenance proteins during the cell cycle: assembly of prereplication complexes  
668 in late mitosis. *Mol Cell Biol*, 20(22), 8602-12.
- 669 [94] Shiio Y, Eisenman RN, Yi EC, Donohoe S, Goodlett DR, Aebersold R. (2003). Quantitative proteomic  
670 analysis of chromatin-associated factors. *J Am Soc Mass Spectrom*, 14(7), 696-703.
- 671 [95] Torrente MP, Zee BM, Young NL, Baliban RC, LeRoy G, Floudas CA, . . . Garcia BA. (2011).  
672 Proteomic interrogation of human chromatin. *PLoS One*, 6(9), e24747.
- 673 [96] Dutta B, Adav SS, Koh CG, Lim SK, Meshorer E, Sze SK. (2012). Elucidating the temporal dynamics  
674 of chromatin-associated protein release upon DNA digestion by quantitative proteomic approach. *J*  
675 *Proteomics*, 75(17), 5493-506.
- 676 [97] Alajem A, Biran A, Harikumar A, Sailaja BS, Aaronson Y, Livyatan I, . . . Meshorer E. (2015).  
677 Differential association of chromatin proteins identifies BAF60a/SMARCD1 as a regulator of  
678 embryonic stem cell differentiation. *Cell Rep*, 10(12), 2019-31.
- 679 [98] Avgousti DC, Herrmann C, Kulej K, Pancholi NJ, Sekulic N, Petrescu J, . . . Weitzman MD. (2016). A  
680 core viral protein binds host nucleosomes to sequester immune danger signals. *Nature*, 535(7610),  
681 173-7.
- 682 [99] Wysocka J, Reilly PT, Herr W. (2001). Loss of HCF-1-chromatin association precedes temperature-  
683 induced growth arrest of tsBN67 cells. *Mol Cell Biol*, 21(11), 3820-9.
- 684 [100] Mulvey CM, Breckels LM, Geladaki A, Britovsek NK, Nightingale DJH, Christoforou A, . . . Lilley KS.  
685 (2017). Using hyperLOPIT to perform high-resolution mapping of the spatial proteome. *Nat Protoc*,  
686 12(6), 1110-35.
- 687 [101] Geladaki A, Kocevar Britovsek N, Breckels LM, Smith TS, Vennard OL, Mulvey CM, . . . Lilley KS.  
688 (2019). Combining LOPIT with differential ultracentrifugation for high-resolution spatial proteomics.  
689 *Nat Commun*, 10(1), 331.
- 690 [102] Monte E, Mouillesseaux K, Chen H, Kimball T, Ren S, Wang Y, . . . Franklin S. (2013). Systems  
691 proteomics of cardiac chromatin identifies nucleolin as a regulator of growth and cellular plasticity in  
692 cardiomyocytes. *Am J Physiol Heart Circ Physiol*, 305(11), H1624-38.
- 693 [103] Franklin S, Zhang MJ, Chen H, Paulsson AK, Mitchell-Jordan SA, Li Y, . . . Vondriska TM. (2011).  
694 Specialized compartments of cardiac nuclei exhibit distinct proteomic anatomy. *Mol Cell Proteomics*,  
695 10(1), M110 000703.
- 696 [104] Franklin S, Chen H, Mitchell-Jordan S, Ren S, Wang Y, Vondriska TM. (2012). Quantitative analysis  
697 of the chromatin proteome in disease reveals remodeling principles and identifies high mobility group  
698 protein B2 as a regulator of hypertrophic growth. *Mol Cell Proteomics*, 11(6), M111 014258.
- 699 [105] Wang X, Andreassen PR, D'Andrea AD. (2004). Functional interaction of monoubiquitinated FANCD2  
700 and BRCA2/FANCD1 in chromatin. *Mol Cell Biol*, 24(13), 5850-62.
- 701 [106] Chou DM, Adamson B, Dephoure NE, Tan X, Nottke AC, Hurov KE, . . . Elledge SJ. (2010). A  
702 chromatin localization screen reveals poly (ADP ribose)-regulated recruitment of the repressive

- 703 polycomb and NuRD complexes to sites of DNA damage. *Proc Natl Acad Sci U S A*, 107(43), 18475-  
704 80.
- 705 [107] Klein DC, Hainer SJ. (2020). Genomic methods in profiling DNA accessibility and factor localization.  
706 *Chromosome Res*, 28(1), 69-85.
- 707 [108] Mieczkowski J, Cook A, Bowman SK, Mueller B, Alver BH, Kundu S, . . . Tolstorukov MY. (2016).  
708 MNase titration reveals differences between nucleosome occupancy and chromatin accessibility. *Nat*  
709 *Commun*, 7, 11485.
- 710 [109] Zaret K. (2005). Micrococcal nuclease analysis of chromatin structure. *Curr Protoc Mol Biol*, Chapter  
711 21, Unit 21 1.
- 712 [110] Sanders MM. (1978). Fractionation of nucleosomes by salt elution from micrococcal nuclease-  
713 digested nuclei. *J Cell Biol*, 79(1), 97-109.
- 714 [111] Bloom KS, Anderson JN. (1978). Fractionation of hen oviduct chromatin into transcriptionally active  
715 and inactive regions after selective micrococcal nuclease digestion. *Cell*, 15(1), 141-50.
- 716 [112] Rocha E, Davie JR, van Holde KE, Weintraub H. (1984). Differential salt fractionation of active and  
717 inactive genomic domains in chicken erythrocyte. *J Biol Chem*, 259(13), 8558-63.
- 718 [113] Herrmann C, Avgousti DC, Weitzman MD. (2017). Differential Salt Fractionation of Nuclei to Analyze  
719 Chromatin-associated Proteins from Cultured Mammalian Cells. *Bio Protoc*, 7(6).
- 720 [114] Kustatscher G, Hegarat N, Wills KL, Furlan C, Bukowski-Wills JC, Hochegger H, Rappsilber J. (2014).  
721 Proteomics of a fuzzy organelle: interphase chromatin. *EMBO J*, 33(6), 648-64.
- 722 [115] Montagna RA, Wang TY. (1976). A comparison of the loosely bound and tightly bound nonhistone  
723 proteins from Ehrlich ascites tumor chromatin. *Cancer Res*, 36(9 pt.1), 3138-42.
- 724 [116] Kostraba NC, Montagna RA, Wang TY. (1975). Study of the loosely bound non-histone chromatin  
725 proteins. Stimulation of deoxyribonucleic acid-templated ribonucleic acid synthesis by a specific  
726 deoxyribonucleic acid-binding phosphoprotein fraction. *J Biol Chem*, 250(4), 1548-55.
- 727 [117] Phair RD, Scaffidi P, Elbi C, Vecerova J, Dey A, Ozato K, . . . Misteli T. (2004). Global nature of  
728 dynamic protein-chromatin interactions in vivo: three-dimensional genome scanning and dynamic  
729 interaction networks of chromatin proteins. *Mol Cell Biol*, 24(14), 6393-402.
- 730 [118] Kustatscher G, Wills KL, Furlan C, Rappsilber J. (2014). Chromatin enrichment for proteomics. *Nat*  
731 *Protoc*, 9(9), 2090-9.
- 732 [119] Solomon MJ, Varshavsky A. (1985). Formaldehyde-mediated DNA-protein crosslinking: a probe for  
733 in vivo chromatin structures. *Proc Natl Acad Sci U S A*, 82(19), 6470-4.
- 734 [120] Kolb HC, Finn MG, Sharpless KB. (2001). Click Chemistry: Diverse Chemical Function from a Few  
735 Good Reactions. *Angew Chem Int Ed Engl*, 40(11), 2004-21.
- 736 [121] Mamidyala SK, Finn MG. (2010). In situ click chemistry: probing the binding landscapes of biological  
737 molecules. *Chem Soc Rev*, 39(4), 1252-61.
- 738 [122] Sirbu BM, Couch FB, Feigerle JT, Bhaskara S, Hiebert SW, Cortez D. (2011). Analysis of protein  
739 dynamics at active, stalled, and collapsed replication forks. *Genes Dev*, 25(12), 1320-7.
- 740 [123] Kliszczak AE, Rainey MD, Harhen B, Boisvert FM, Santocanale C. (2011). DNA mediated chromatin  
741 pull-down for the study of chromatin replication. *Sci Rep*, 1, 95.
- 742 [124] Aranda S, Alcaine-Colet A, Blanco E, Borrás E, Caillot C, Sabido E, Di Croce L. (2019). Chromatin  
743 capture links the metabolic enzyme AHCY to stem cell proliferation. *Sci Adv*, 5(3), eaav2448.

- 744 [125] Aranda S, Borràs E, Sabidó E, Di Croce L. (2020). Chromatin-Bound Proteome Profiling by Genome  
745 Capture. STAR Protocols, 100014.
- 746 [126] Bonev B, Cavalli G. (2016). Organization and function of the 3D genome. Nat Rev Genet, 17(11),  
747 661-78.
- 748 [127] Almouzni G, Cedar H. (2016). Maintenance of Epigenetic Information. Cold Spring Harb Perspect  
749 Biol, 8(5).
- 750 [128] Gilbert DM, Takebayashi SI, Ryba T, Lu J, Pope BD, Wilson KA, Hiratani I. (2010). Space and time  
751 in the nucleus: developmental control of replication timing and chromosome architecture. Cold Spring  
752 Harb Symp Quant Biol, 75, 143-53.
- 753 [129] Mirabella AC, Foster BM, Bartke T. (2016). Chromatin deregulation in disease. Chromosoma, 125(1),  
754 75-93.
- 755 [130] Li X, Yu W, Qian X, Xia Y, Zheng Y, Lee JH, . . . Lu Z. (2017). Nucleus-Translocated ACSS2 Promotes  
756 Gene Transcription for Lysosomal Biogenesis and Autophagy. Mol Cell, 66(5), 684-97 e9.
- 757 [131] Mews P, Donahue G, Drake AM, Luczak V, Abel T, Berger SL. (2017). Acetyl-CoA synthetase  
758 regulates histone acetylation and hippocampal memory. Nature, 546(7658), 381-6.
- 759 [132] Li X, Egervari G, Wang Y, Berger SL, Lu Z. (2018). Regulation of chromatin and gene expression by  
760 metabolic enzymes and metabolites. Nat Rev Mol Cell Biol, 19(9), 563-78.
- 761 [133] Sdelci S, Rendeiro AF, Rathert P, You W, Lin JG, Ringler A, . . . Kubicek S. (2019). MTHFD1  
762 interaction with BRD4 links folate metabolism to transcriptional regulation. Nat Genet, 51(6), 990-8.
- 763 [134] Erdel F, Rippe K. (2018). Formation of Chromatin Subcompartments by Phase Separation. Biophys  
764 J, 114(10), 2262-70.  
765  
766

767 **FIGURE LEGENDS**

768 **Figure 1. Principal chromatin-bound proteins that mediate chromatin topology and**  
769 **function.** CR, chromatin remodeling; TF, transcription factor.

770  
771 **Figure 2. Influence of chromatin-bound proteins in human genetic disease.** (a) A list  
772 of chromatin-bound proteins was established based on public protein databases and  
773 bibliographic research. Using the “chromatin” associated category, a list of potential  
774 chromatin-bound proteins of 2311 proteins from at least two different protein databases.  
775 Additionally, 2308 proteins were obtained from an extensive manual bibliographic search  
776 of previously published lists of chromatin regulators and well-established chromatin  
777 interactors (including TFs, histone writers and erasers, and ATP-remodelers). Merging of  
778 both gave a final list of 3097 known and potential chromatin-bound proteins. (b) The  
779 resultant percentage and absolute number of the 3097 identified chromatin-bound  
780 proteins (a) that were also in a list of: i) human proteins with a high intolerance to suffer  
781 loss-of-function mutations (Lek et al. 2016), ii) commonly identified cancer driver genes  
782 (Bailey et al. 2018, Lawrence, 2014, Martincorena, 2017, Dietlein, 2020), and iii) the  
783 most commonly mutated genes in the PanCancer cohort (Kandoth et al 2013).  
784

785 **Figure 3. Methods for global chromatin isolation from cells.** Methods are classified  
786 as native chromatin isolation methods when the nucleus is obtained from living cells in  
787 native conditions, and as crosslinked chromatin isolation methods when the components  
788 of the nucleus have been chemically crosslinked. Dig., digestion.  
789  
790  
791  
792  
793  
794  
795  
796  
797  
798  
799

800

FIGURE 1

### HETEROCHROMATIN

### EUCHROMATIN

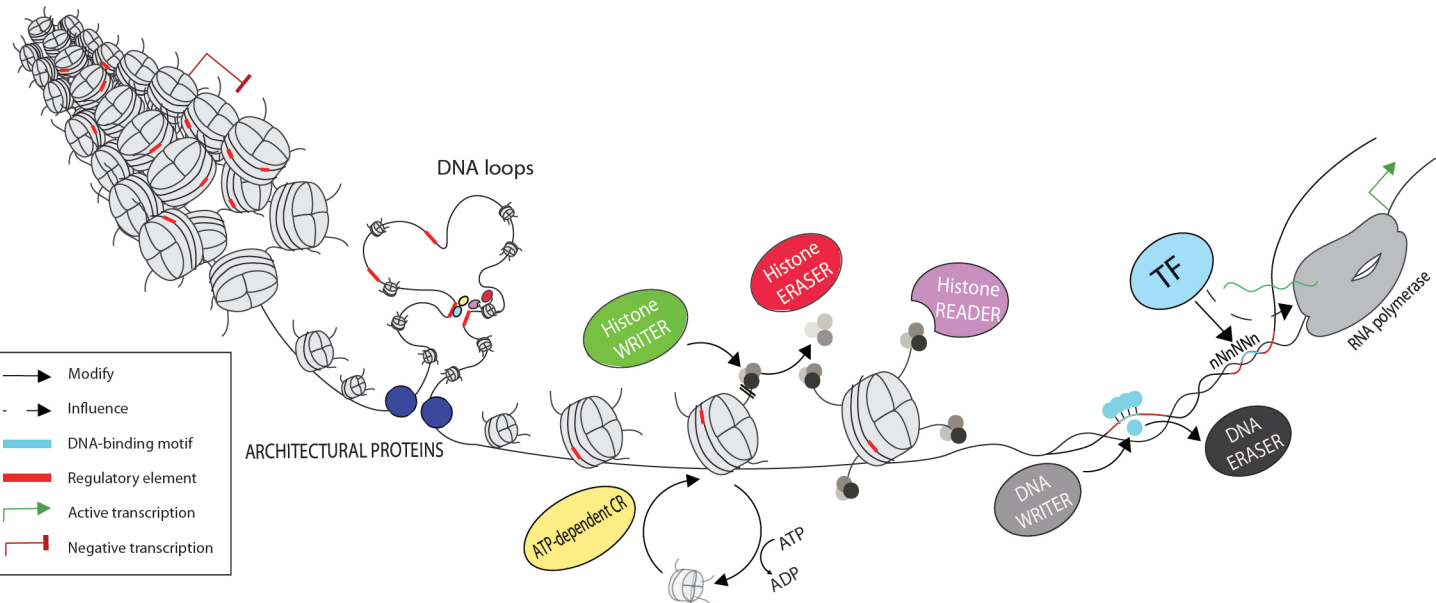


FIGURE 2

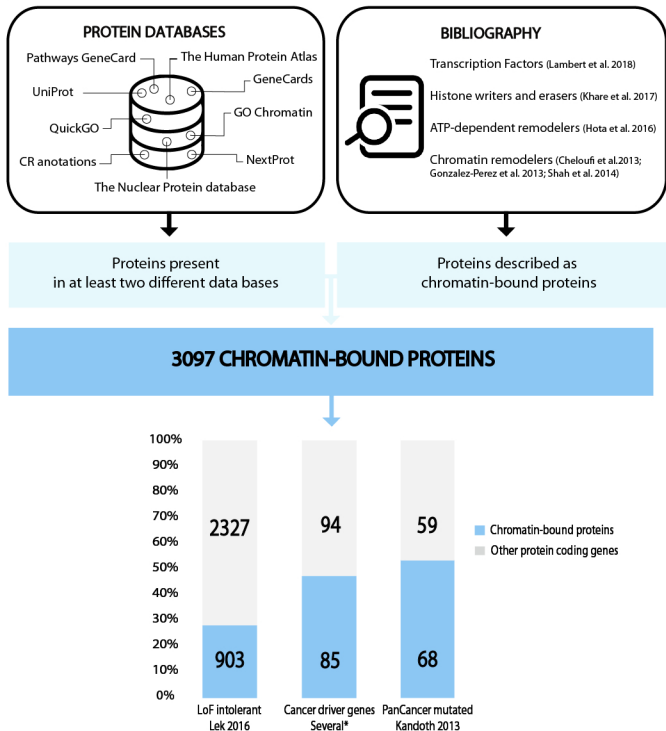
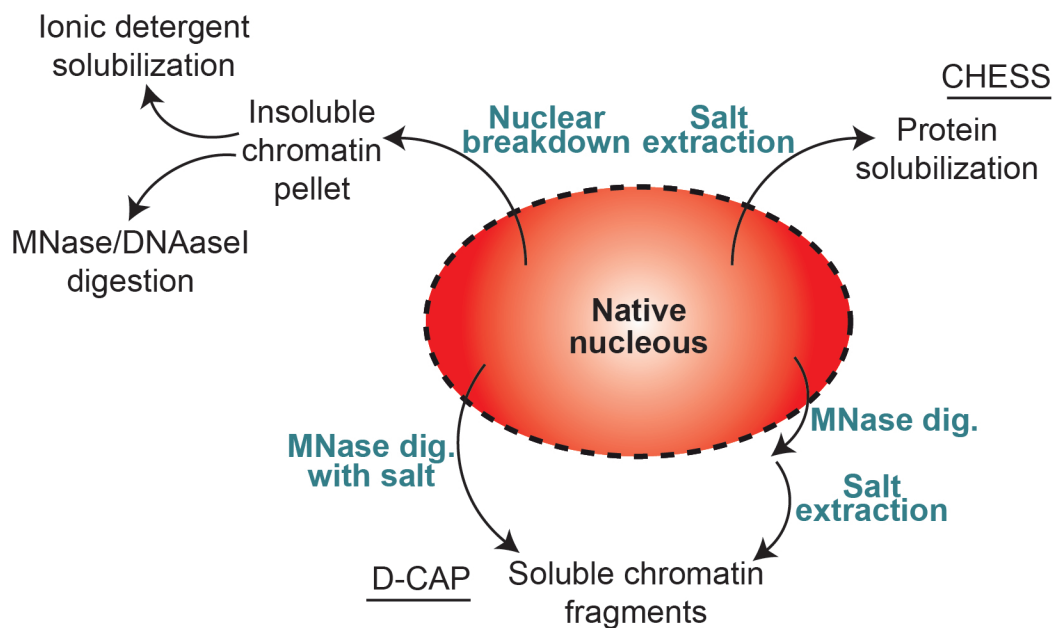
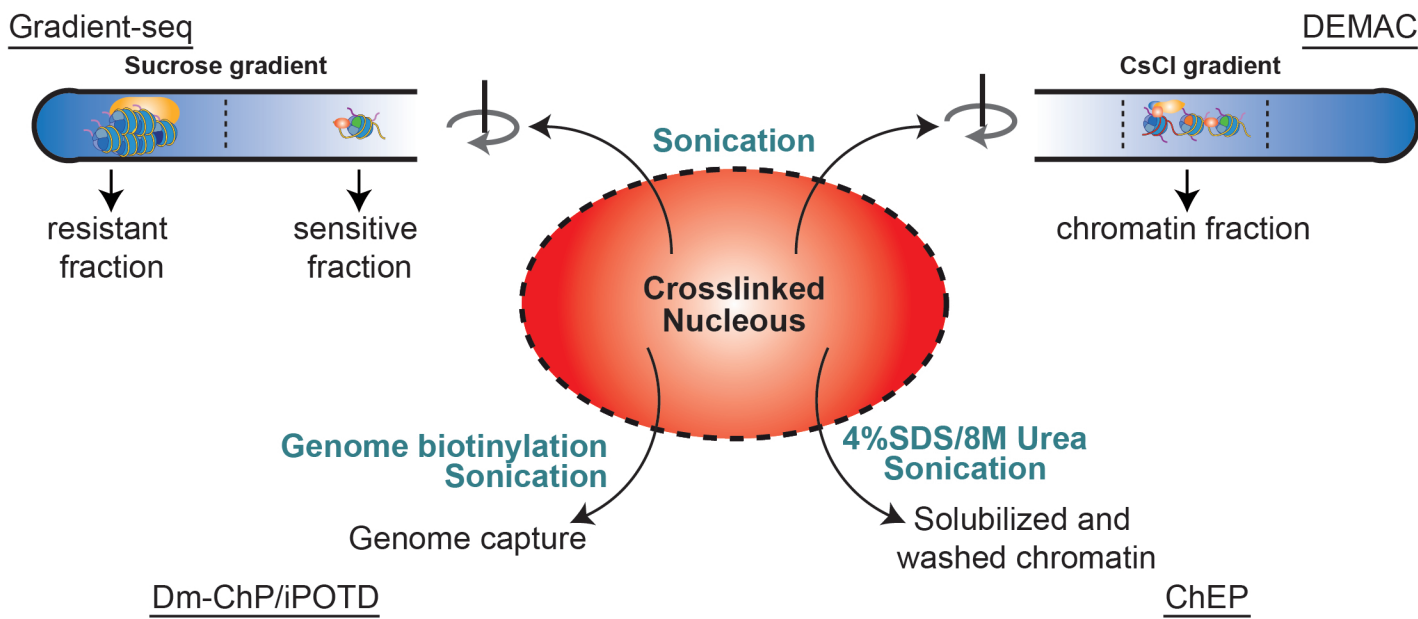


FIGURE 3

### Native chromatin isolation methods



### Crosslinked chromatin isolation methods



List of 3098 chromatin genes

Present in at least two categories of all the different consulted datasets\*

1600027N09RIK  
2410016O06RIK  
2410018M08RIK  
2900092E17RIK  
4931414P19RIK  
ABCF2  
ABRAXAS1  
AC008770.3  
AC023509.3  
AC092835.1  
AC138696.1  
ACIN1  
ACTA1  
ACTB  
ACTL6A  
ACTL6B  
ACTN4  
ACTR5  
ACTR6  
ACTR8  
ACTRT1  
ADA  
ADAR  
ADNP  
ADNP2  
ADPRH  
ADPRHL2  
AEBP1  
AEBP2  
AFF4  
AHCY  
AHCTF1  
AHDC1  
AHR  
AHRR  
AICDA  
AIFM1  
AIRE  
AJUBA  
AKAP1  
AKAP8  
AKAP8L  
AKNA  
ALKBH1  
ALKBH2  
ALKBH3  
ALX1  
ALX3  
ALX4

\*Consulted datasets

Histone remodeleres (Khare et al. 017)  
Lambert et al. 2018  
Remodelers paper (Gonzalez-Perez et al. 2013; Cheloufi  
ATP-dependent chromatin remodelers paper (Hota et al  
UniProt  
QuickGO (Chromatin&others)  
QuickGO GONAME (Chromatin&others)  
GO\_Chromatin  
The human protein atlas  
NextProt (Chromatin-associated proteins)  
GeneCards (Chromatin)  
Pathways Genecards  
CR anotations  
The Nuclear protein database

ANHX  
ANKRD11  
ANKRD17  
ANKRD2  
ANKRD31  
ANKZF1  
ANP32E  
ANXA1  
APBB1  
APEX1  
APLF  
APOBEC1  
APOBEC2  
APOBEC3  
APOBEC3B  
APOBEC4  
APTX  
AR  
ARGFX  
ARHGAP35  
ARID1A  
ARID1B  
ARID2  
ARID3A  
ARID3B  
ARID3C  
ARID4A  
ARID4B  
ARID5A  
ARID5B  
ARIH2  
ARNT  
ARNT2  
ARNTL  
ARNTL2  
ARRB1  
ART1  
ARX  
ASAP1  
ASCL1  
ASCL2  
ASCL3  
ASCL4  
ASCL5  
ASF1A  
ASF1B  
ASH1L  
ASH2L  
ASXL1  
ASXL2  
ASXL3

ATAD2  
ATAD2B  
ATAT1  
ATF1  
ATF2  
ATF3  
ATF4  
ATF5  
ATF6  
ATF6B  
ATF7  
ATF7IP  
ATF7IP2  
ATM  
ATMIN  
ATOH1  
ATOH7  
ATOH8  
ATR  
ATRX  
ATXN3  
ATXN7  
ATXN7L3  
AURKA  
AURKB  
AUTS2  
BABAM1  
BABAM2  
BACH1  
BACH2  
BAG6  
BAHCC1  
BAHD1  
BANF1  
BANP  
BAP1  
BAP18  
BARHL1  
BARHL2  
BARX1  
BARX2  
BATF  
BATF2  
BATF3  
BAZ1A  
BAZ1B  
BAZ2A  
BAZ2B  
BBX  
BCAS3  
BCL11A

BCL11B  
BCL6  
BCL6B  
BCOR  
BCORL1  
BDP1  
BEND3  
BEND6  
BHLHA15  
BHLHA9  
BHLHE22  
BHLHE23  
BHLHE40  
BHLHE41  
BICRA  
BICRAL  
BLM  
BMI1  
BNC1  
BNC2  
BOP1  
BORCS8-MEF2B  
BPTF  
BRCA1  
BRCA2  
BRCC3  
BRD1  
BRD2  
BRD3  
BRD4  
BRD7  
BRD8  
BRD9  
BRDT  
BRE  
BRF2  
BRIP1  
BRMS1  
BRMS1L  
BRPF1  
BRPF3  
BRWD1  
BRWD3  
BSX  
BTAF1  
BUB3  
BUD23  
BUD31  
C11orf95  
C14orf169  
C14orf93

C17orf49  
C17orf96  
CABIN1  
CALCOCO1  
CAMK4  
CAMKMT  
CAMTA1  
CAMTA2  
CAND1  
CAPN2  
CARF  
CARM1  
CASZ1  
CBFA2T2  
CBFA2T3  
CBX1  
CBX2  
CBX3  
CBX4  
CBX5  
CBX6  
CBX7  
CBX8  
CC2D1A  
CCAR2  
CCDC101  
CCDC169-SOHLH2  
CCDC17  
CCNA1  
CCND2  
CCNT1  
CCNT2  
CDA  
CDAN1  
CDC45  
CDC5L  
CDC6  
CDC73  
CDCA2  
CDCA5  
CDCA7L  
CDCA8  
CDK1  
CDK12  
CDK13  
CDK2AP1  
CDK4  
CDK5  
CDK9  
CDKN2A  
CDT1

CDX1  
CDX2  
CDX4  
CDY1  
CDY1B  
CDY2A  
CDY2B  
CDYL  
CDYL2  
CEBPA  
CEBPB  
CEBPD  
CEBPE  
CEBPG  
CEBPZ  
CECR2  
CENPA  
CENPB  
CENPBD1  
CENPC  
CENPF  
CENPH  
CENPI  
CENPK  
CENPL  
CENPM  
CENPN  
CENPO  
CENPP  
CENPQ  
CENPS  
CENPT  
CENPU  
CENPV  
CENPW  
CENPX  
CEP164  
CGAS  
CGGBP1  
CHAF1A  
CHAF1B  
CHAMP1  
CHCHD3  
CHD1  
CHD1L  
CHD2  
CHD3  
CHD4  
CHD5  
CHD6  
CHD7

CHD8  
CHD9  
CHEK1  
CHEK2  
CHMP1A  
CHMP1B  
CHMP2A  
CHMP2B  
CHMP4A  
CHMP4B  
CHMP4C  
CHMP5  
CHMP6  
CHMP7  
CHRA1  
CHTF18  
CHTF8  
CHTOP  
CHUK  
CIC  
CINP  
CITED1  
CITED2  
CKS2  
CLOCK  
COPRS  
COPS3  
COPS4  
COPS5  
COPS6  
COPS9  
COQ7  
CPEB1  
CPHL  
CPSF6  
CPXCR1  
CRAMP1  
CREB1  
CREB3  
CREB3L1  
CREB3L2  
CREB3L3  
CREB3L4  
CREB5  
CREBBP  
CREBL2  
CREBZF  
CREM  
CRTC2  
CRX  
CSNK2A1

CSNK2A2  
CSNK2B  
CSNKA2IP  
CSRNP1  
CSRNP2  
CSRNP3  
CTBP1  
CTBP2  
CTCF  
CTCFL  
CTDSPL2  
CTNNB1  
CTR9  
CTSL  
CUL1  
CUL4B  
CUX1  
CUX2  
CXXC1  
CXXC4  
CXXC5  
D14ERTD668E  
DACH1  
DACH2  
DAPK3  
DAXX  
DBF4B  
DBP  
DBX1  
DBX2  
DCAF1  
DDB1  
DDB2  
DDIT3  
DDX1  
DDX11  
DDX17  
DDX21  
DDX23  
DDX3X  
DDX41  
DDX5  
DDX6  
DEAF1  
DEK  
DFFA  
DFFB  
DGCR8  
DHX29  
DHX30  
DHX36

DHX9  
DIDO1  
DKC1  
DLD  
DLST  
DLX1  
DLX2  
DLX3  
DLX4  
DLX5  
DLX6  
DMAP1  
DMBX1  
DMRT1  
DMRT2  
DMRT3  
DMRTA1  
DMRTA2  
DMRTB1  
DMRTC1  
DMRTC1B  
DMRTC2  
DMTF1  
DNAJC2  
DNASE1L3  
DNMT1  
DNMT3A  
DNMT3B  
DNMT3L  
DNTT  
DNTTIP1  
DNTTIP2  
DOT1L  
DPF1  
DPF2  
DPF3  
DPPA2  
DPPA3  
DPPA4  
DPRX  
DPY30  
DR1  
DRAP1  
DRGX  
DSCC1  
DTD1  
DTX3L  
DUB2A  
DUX1  
DUX3  
DUX4

DUXA  
DVL3  
DZIP1  
DZIP3  
E130308A19RIK  
E2F1  
E2F2  
E2F3  
E2F4  
E2F5  
E2F6  
E2F7  
E2F8  
E4F1  
EBF1  
EBF2  
EBF3  
EBF4  
EDF1  
EEA1  
EED  
EG330129  
EG546387  
EGFR  
EGR1  
EGR2  
EGR3  
EGR4  
EHF  
EHMT1  
EHMT2  
EID1  
EIF3E  
EIF4A3  
ELF1  
ELF2  
ELF3  
ELF4  
ELF5  
ELK1  
ELK3  
ELK4  
ELL  
ELOB  
ELOF1  
ELP1  
ELP2  
ELP3  
ELP4  
EMD  
EME1

EME2  
EMG1  
EMSY  
EMX1  
EMX2  
EN1  
EN2  
ENC1  
ENY2  
EOMES  
EP300  
EP400  
EPAS1  
EPC1  
EPC2  
EPOP  
ERCC1  
ERCC3  
ERCC4  
ERCC5  
ERCC6  
ERCC6L  
ERF  
ERG  
ESCO1  
ESCO2  
ESR1  
ESR2  
ESRRA  
ESRRB  
ESRRG  
ESX1  
ETS1  
ETS2  
ETV1  
ETV2  
ETV3  
ETV3L  
ETV4  
ETV5  
ETV6  
ETV7  
EVX1  
EVX2  
EWSR1  
EXD2  
EXO1  
EXOSC10  
EXOSC3  
EXOSC4  
EXOSC5

EXOSC9  
EYA1  
EYA2  
EYA3  
EYA4  
EZH1  
EZH2  
FAAP24  
FABP1  
FACT  
FAF1  
FAM111A  
FAM170A  
FAM175A  
FAM175B  
FAM200B  
FANCM  
FANK1  
FBH1  
FBL  
FBXL19  
FBXO17  
FBXO44  
FBXW9  
FEM1B  
FER  
FERD3L  
FEV  
FEZF1  
FEZF2  
FIGLA  
FIZ1  
FKBP1A  
FKBP2  
FKBP5  
FLI1  
FLNA  
FLYWCH1  
FMR1  
FNBP4  
FOS  
FOSB  
FOSL1  
FOSL2  
FOXA1  
FOXA2  
FOXA3  
FOXB1  
FOXB2  
FOXC1  
FOXC2

FOXD1  
FOXD2  
FOXD3  
FOXD4  
FOXD4L1  
FOXD4L3  
FOXD4L4  
FOXD4L5  
FOXD4L6  
FOXE1  
FOXE3  
FOXF1  
FOXF2  
FOXG1  
FOXH1  
FOXI1  
FOXI2  
FOXI3  
FOXJ1  
FOXJ2  
FOXJ3  
FOXK1  
FOXK2  
FOXL1  
FOXL2  
FOXM1  
FOXN1  
FOXN2  
FOXN3  
FOXN4  
FOXO1  
FOXO3  
FOXO4  
FOXO6  
FOXP1  
FOXP2  
FOXP3  
FOXP4  
FOXQ1  
FOXR1  
FOXR2  
FOXS1  
FSHR  
FTSJ3  
FUBP3  
FUS  
FXR1  
FXR2  
G2E3  
GABPA  
GADD45A

GADD45B  
GATA1  
GATA2  
GATA3  
GATA4  
GATA5  
GATA6  
GATAD1  
GATAD2A  
GATAD2B  
GBX1  
GBX2  
GCM1  
GCM2  
GF1  
GF1B  
GLI1  
GLI2  
GLI3  
GLI4  
GLIS1  
GLIS2  
GLIS3  
GLMP  
GLYR1  
GM4349  
GMEB1  
GMEB2  
GMNC  
GMNN  
GPBP1  
GPBP1L1  
GPER1  
GPS2  
GPX4  
GRHL1  
GRHL2  
GRHL3  
GRWD1  
GSC  
GSC2  
GSG2  
GSX1  
GSX2  
GTF2B  
GTF2F1  
GTF2H1  
GTF2I  
GTF2IRD1  
GTF2IRD2  
GTF2IRD2B

GTF3A  
GTF3C1  
GTF3C4  
GTF3C5  
GZF1  
H1-0  
H1-1  
H1-10  
H1-2  
H1-3  
H1-4  
H1-5  
H1-6  
H1-7  
H1-8  
H1F0  
H1FNT  
H1FOO  
H1FX  
H2AB1  
H2AB2  
H2AB3  
H2AC1  
H2AC11  
H2AC12  
H2AC13  
H2AC14  
H2AC15  
H2AC16  
H2AC17  
H2AC18  
H2AC19  
H2AC20  
H2AC21  
H2AC4  
H2AC6  
H2AC7  
H2AC8  
H2AFB1  
H2AFB2  
H2AFB3  
H2AFJ  
H2AFV  
H2AFX  
H2AFY  
H2AFY2  
H2AFZ  
H2AJ  
H2AP  
H2AW  
H2AX

H2AZ1  
H2AZ2  
H2BC1  
H2BC10  
H2BC11  
H2BC12  
H2BC13  
H2BC14  
H2BC15  
H2BC17  
H2BC18  
H2BC21  
H2BC3  
H2BC4  
H2BC5  
H2BC6  
H2BC7  
H2BC8  
H2BC9  
H2BFM  
H2BFS  
H2BFWT  
H2BU1  
H2BW2  
H3-3A  
H3-3B  
H3-5  
H3C1  
H3C10  
H3C11  
H3C12  
H3C13  
H3C14  
H3C15  
H3C2  
H3C3  
H3C4  
H3C6  
H3C7  
H3C8  
H3F3A  
H3F3B  
H3F3C  
H4-16  
H4C1  
H4C11  
H4C12  
H4C13  
H4C14  
H4C15  
H4C2

H4C3  
H4C4  
H4C5  
H4C6  
H4C8  
H4C9  
HAND1  
HAND2  
HASPIN  
HAT1  
HBP1  
HCFC1  
HCFC2  
HDAC1  
HDAC10  
HDAC11  
HDAC2  
HDAC3  
HDAC4  
HDAC5  
HDAC6  
HDAC7  
HDAC8  
HDAC9  
HDGF  
HDGFL1  
HDGFL2  
HDGFRP2  
HDGFRP3  
HDLBP  
HDX  
HEATR1  
HELB  
HELLS  
HELT  
HES1  
HES2  
HES3  
HES4  
HES5  
HES6  
HES7  
HESX1  
HEY1  
HEY2  
HEYL  
HHEX  
HIC1  
HIC2  
HIF1A  
HIF3A

HILS1  
HINFP  
HIPK1  
HIRA  
HIRIP3  
HIST1H1A  
HIST1H1B  
HIST1H1C  
HIST1H1D  
HIST1H1E  
HIST1H1T  
HIST1H2AA  
HIST1H2AB  
HIST1H2AC  
HIST1H2AD  
HIST1H2AE  
HIST1H2AG  
HIST1H2AH  
HIST1H2AI  
HIST1H2AJ  
HIST1H2AK  
HIST1H2AL  
HIST1H2AM  
HIST1H2BA  
HIST1H2BB  
HIST1H2BC  
HIST1H2BD  
HIST1H2BE  
HIST1H2BF  
HIST1H2BG  
HIST1H2BH  
HIST1H2BI  
HIST1H2BJ  
HIST1H2BK  
HIST1H2BL  
HIST1H2BM  
HIST1H2BN  
HIST1H2BO  
HIST1H3A  
HIST1H3B  
HIST1H3C  
HIST1H3D  
HIST1H3E  
HIST1H3F  
HIST1H3G  
HIST1H3H  
HIST1H3I  
HIST1H3J  
HIST1H4A  
HIST1H4B  
HIST1H4C

HIST1H4D  
HIST1H4E  
HIST1H4F  
HIST1H4G  
HIST1H4H  
HIST1H4I  
HIST1H4J  
HIST1H4K  
HIST1H4L  
HIST2H2AA3  
HIST2H2AB  
HIST2H2AC  
HIST2H2BC  
HIST2H2BE  
HIST2H2BF  
HIST2H3C  
HIST3H2A  
HIST3H2BB  
HIST3H3  
HIST4H4  
HIVEP1  
HIVEP2  
HIVEP3  
HJURP  
HKR1  
HLCS  
HLF  
HLTF  
HLX  
HMBOX1  
HMCES  
HMG20A  
HMG20B  
HMGA1  
HMGA2  
HMGB1  
HMGB1P1  
HMGB2  
HMGB3  
HMGB4  
HMGN1  
HMGN2  
HMGN3  
HMGN4  
HMGN5  
HMGXB4  
HMX1  
HMX2  
HMX3  
HNF1A  
HNF1B

HNF4A  
HNF4G  
HNRNPA0  
HNRNPA1  
HNRNPA2B1  
HNRNPC  
HNRNPD  
HNRNPF  
HNRNPK  
HNRNPL  
HNRNPM  
HNRNPR  
HNRNPU  
HNRNPUL1  
HOMEZ  
HOPX  
HORMAD1  
HOXA1  
HOXA10  
HOXA11  
HOXA13  
HOXA2  
HOXA3  
HOXA4  
HOXA5  
HOXA6  
HOXA7  
HOXA9  
HOXB1  
HOXB13  
HOXB2  
HOXB3  
HOXB4  
HOXB5  
HOXB6  
HOXB7  
HOXB8  
HOXB9  
HOXC10  
HOXC11  
HOXC12  
HOXC13  
HOXC4  
HOXC5  
HOXC6  
HOXC8  
HOXC9  
HOXD1  
HOXD10  
HOXD11  
HOXD12

HOXD13  
HOXD3  
HOXD4  
HOXD8  
HOXD9  
HP1BP3  
HPRT  
HR  
HSF1  
HSF2  
HSF4  
HSF5  
HSFX1  
HSFX2  
HSFX3  
HSFY1  
HSFY2  
HTRA2  
HUWE1  
HYPM  
ICE1  
ICE2  
IFI16  
IFT74  
IGF2BP3  
IKBKAP  
IKZF1  
IKZF2  
IKZF3  
IKZF4  
IKZF5  
IL33  
ILF2  
ILF3  
INCENP  
ING1  
ING2  
ING3  
ING4  
ING5  
INO80  
INO80B  
INO80C  
INO80D  
INO80E  
INSM1  
INSM2  
INTS12  
IPO4  
IRF1  
IRF2

IRF3  
IRF4  
IRF5  
IRF6  
IRF7  
IRF8  
IRF9  
IRX1  
IRX2  
IRX3  
IRX4  
IRX5  
IRX6  
ISL1  
ISL2  
IST1  
ISX  
ITGB3BP  
IWS1  
JADE1  
JADE2  
JADE3  
JAK2  
JARID2  
JAZF1  
JDP2  
JHDM1D  
JMJD1C  
JMJD4  
JMJD5  
JMJD6  
JMJD8  
JRK  
JRKL  
JUN  
JUNB  
JUND  
KANSL1  
KANSL2  
KANSL3  
KAT2A  
KAT2B  
KAT5  
KAT6A  
KAT6B  
KAT7  
KAT8  
KCMF1  
KCNIP3  
KDM1A  
KDM1B

KDM2A  
KDM2B  
KDM3A  
KDM3B  
KDM4A  
KDM4B  
KDM4C  
KDM4D  
KDM4DL  
KDM4E  
KDM5A  
KDM5B  
KDM5C  
KDM5D  
KDM6A  
KDM6B  
KDM7A  
KDM8  
KHDRBS1  
KIAA1045  
KIAA1958  
KIAA2026  
KIF22  
KIN  
KLF1  
KLF10  
KLF11  
KLF12  
KLF13  
KLF14  
KLF15  
KLF16  
KLF17  
KLF2  
KLF3  
KLF4  
KLF5  
KLF6  
KLF7  
KLF8  
KLF9  
KLHDC3  
KMT2A  
KMT2B  
KMT2C  
KMT2D  
KMT2E  
KMT5A  
KMT5B  
KMT5C  
KNL1

L3MBTL  
L3MBTL1  
L3MBTL2  
L3MBTL3  
L3MBTL4  
LAS1L  
LBR  
LBX1  
LBX2  
LCOR  
LCORL  
LDB1  
LEF1  
LEMD2  
LEUTX  
LHX1  
LHX2  
LHX3  
LHX4  
LHX5  
LHX6  
LHX8  
LHX9  
LIG4  
LIN28A  
LIN28B  
LIN54  
LIN9  
LMNA  
LMNB1  
LMNB2  
LMX1A  
LMX1B  
LNX1  
LOC100040412  
LOC100044324  
LOC100048887  
LOC100129278  
LOC664892  
LOXL2  
LRWD1  
LTF  
LYL1  
M1AP  
MACROH2A1  
MACROH2A2  
MAEA  
MAEL  
MAF  
MAFA  
MAFB

MAFF  
MAFG  
MAFK  
MAGED1  
MAML1  
MAP1S  
MAP3K12  
MAPK1  
MAPK15  
MAPKAPK3  
MATR3  
MAU2  
MAX  
MAZ  
MBD1  
MBD2  
MBD3  
MBD3L1  
MBD3L2  
MBD3L3  
MBD3L4  
MBD3L5  
MBD4  
MBD5  
MBD6  
MBIP  
MBNL2  
MBTD1  
MCM10  
MCM2  
MCM3  
MCM3AP  
MCM4  
MCM5  
MCM6  
MCM7  
MCM8  
MCM9  
MCMBP  
MCRS1  
MDC1  
MEAF6  
MECOM  
MECP2  
MED1  
MED12  
MED25  
MED26  
MED6  
MEF2A  
MEF2B

MEF2C  
MEF2D  
MEIOB  
MEIS1  
MEIS2  
MEIS3  
MEN1  
MEOX1  
MEOX2  
MEPCE  
MESP1  
MESP2  
METTL21D  
METTL8  
MGA  
MGEA5  
MGMT  
MIER1  
MINA  
MIS12  
MIS18A  
MIS18BP1  
MITF  
MIXL1  
MIZF  
MKI67  
MKX  
MLH1  
MLH3  
MLL  
MLL1  
MLL2  
MLL3  
MLL4  
MLL5  
MLLT1  
MLLT10  
MLLT3  
MLLT6  
MLX  
MLXIP  
MLXIPL  
MNDA  
MNT  
MNX1  
MORC2  
MORF4L1  
MORF4L2  
MOS  
MPG  
MPHOSPH8

MPO  
MRE11  
MRGBP  
MRNIP  
MSANTD1  
MSANTD3  
MSANTD4  
MSC  
MSGN1  
MSH2  
MSH6  
MSL1  
MSL2  
MSL3  
MSL3L1  
MSX1  
MSX2  
MTA1  
MTA2  
MTA3  
MTBP  
MTERF  
MTERF1  
MTERF2  
MTERF3  
MTERF4  
MTF1  
MTF2  
MTHFR  
MTHFD1  
MTR  
MTREX  
MUC1  
MUM1  
MUM1L1  
MXD1  
MXD3  
MXD4  
MXI1  
MXRA8  
MYB  
MYBBP1A  
MYBL1  
MYBL2  
MYC  
MYCL  
MYCN  
MYEF2  
MYF5  
MYF6  
MYNN

MYO1C  
MYOCD  
MYOD1  
MYOG  
MYPOP  
MYRF  
MYRFL  
MYSM1  
MYST1  
MYST2  
MYST3  
MYST4  
MYT1  
MYT1L  
MZF1  
N28178  
NAA10  
NAA15  
NAA60  
NACC1  
NACC2  
NAIF1  
NANOG  
NANOGB  
NANOGP8  
NAP1L1  
NAP1L2  
NAP1L3  
NAP1L4  
NASP  
NAT10  
NAT6  
NBN  
NCAPD2  
NCAPD3  
NCAPG  
NCAPH  
NCAPH2  
NCL  
NCOA1  
NCOA2  
NCOA3  
NCOA5  
NCOA6  
NCOR1  
NCOR1P1  
NCOR2  
NEDD4  
NEDD4L  
NEIL1  
NEK6



NKX3-1  
NKX3-2  
NKX6-1  
NKX6-2  
NKX6-3  
NME2  
NO66  
NOBOX  
NOC2L  
NOC3L  
NOLC1  
NONO  
NOP53  
NOP56  
NOP58  
NOTCH1  
NOTO  
NPAS1  
NPAS2  
NPAS3  
NPAS4  
NPM1  
NPM2  
NPM3  
NR0B1  
NR0B2  
NR1D1  
NR1D2  
NR1H2  
NR1H3  
NR1H4  
NR1I2  
NR1I3  
NR2C1  
NR2C2  
NR2E1  
NR2E3  
NR2F1  
NR2F2  
NR2F6  
NR3C1  
NR3C2  
NR4A1  
NR4A2  
NR4A3  
NR5A1  
NR5A2  
NR6A1  
NRDE2  
NRF1  
NRIP1

NRL  
NSD1  
NSD2  
NSD3  
NSMF  
NUCKS1  
NUDT16L1  
NUDT21  
NUDT5  
NUFIP1  
NUP107  
NUP133  
NUP155  
NUP160  
NUP205  
NUP62  
NUP85  
NUP98  
NUPR1  
NUSAP1  
OBI1  
OGT  
OIP5  
OLIG1  
OLIG2  
OLIG3  
ONECUT1  
ONECUT2  
ONECUT3  
ORC1  
ORC2  
ORC3  
ORC4  
ORC5  
OSR1  
OSR2  
OTP  
OTX1  
OTX2  
OVOL1  
OVOL2  
OVOL3  
p53  
PA2G4  
PABPC1L  
PADI1  
PADI2  
PADI3  
PADI4  
PADI6  
PAF1

PAG1  
PAGR1  
PAK1  
PALB2  
PARG  
PARK7  
PARP1  
PARP10  
PARP11  
PARP12  
PARP14  
PARP16  
PARP2  
PARP3  
PARP4  
PARP6  
PARP8  
PARP9  
PARPBP  
PATZ1  
PAWR  
PAX1  
PAX2  
PAX3  
PAX4  
PAX5  
PAX6  
PAX7  
PAX8  
PAX9  
PAXBP1  
PAXIP1  
PBRM1  
PBX1  
PBX2  
PBX3  
PBX4  
PCGF1  
PCGF2  
PCGF6  
PCID2  
PCLAF  
PCMT1  
PCNA  
PDS5A  
PDS5B  
PDX1  
PEG3  
PELP1  
PER1  
PGR

PHB  
PHC1  
PHC2  
PHC3  
PHF1  
PHF10  
PHF11  
PHF12  
PHF13  
PHF14  
PHF15  
PHF16  
PHF17  
PHF19  
PHF2  
PHF20  
PHF20L1  
PHF21A  
PHF21B  
PHF23  
PHF3  
PHF5A  
PHF6  
PHF7  
PHF8  
PHIP  
PHOX2A  
PHOX2B  
PHRF1  
PIAS1  
PIH1D1  
PIN1  
PINK1  
PITX1  
PITX2  
PITX3  
PIWIL1  
PKN1  
PKNOX1  
PKNOX2  
PLAC8  
PLAG1  
PLAGL1  
PLAGL2  
PLCB1  
PLK1  
PLK2  
PLSCR1  
PML  
POGK  
POGZ

POLA1  
POLD1  
POLE  
POLE3  
POLG  
POLH  
POLQ  
POLR1A  
POLR2A  
POLR2B  
POLR2E  
POLR3A  
POLR3D  
POLR3G  
POLR3GL  
POU1F1  
POU2AF1  
POU2F1  
POU2F2  
POU2F3  
POU3F1  
POU3F2  
POU3F3  
POU3F4  
POU4F1  
POU4F2  
POU4F3  
POU5F1  
POU5F1B  
POU5F2  
POU6F1  
POU6F2  
PPARA  
PPARD  
PPARG  
PPARGC1A  
PPHLN1  
PPIB  
PPM1D  
PPP1CA  
PPP1CB  
PPP1CC  
PPP1R10  
PPP3CA  
PPP4C  
PRDM1  
PRDM10  
PRDM11  
PRDM12  
PRDM13  
PRDM14

PRDM15  
PRDM16  
PRDM2  
PRDM4  
PRDM5  
PRDM6  
PRDM7  
PRDM8  
PRDM9  
PREB  
PRIMPOL  
PRKAA1  
PRKAA2  
PRKCB  
PRKCD  
PRKDC  
PRM1  
PRM2  
PRM3  
PRMT1  
PRMT2  
PRMT3  
PRMT5  
PRMT6  
PRMT7  
PRMT8  
PROP1  
PROX1  
PROX2  
PRPF19  
PRPF3  
PRPF4  
PRR12  
PRR14  
PRRC2B  
PRRX1  
PRRX2  
PSD3  
PSIP1  
PSMA2  
PSMA4  
PSMA5  
PSMA6  
PSMA7  
PSMB1  
PSMB3  
PSMB4  
PSMB5  
PSMB6  
PSMC1  
PSMC2

PSMC3  
PSMC4  
PSMC5  
PSMC6  
PSMD1  
PSMD11  
PSMD12  
PSMD13  
PSMD14  
PSMD2  
PSMD3  
PSMD4  
PSMD6  
PSMD7  
PSMD8  
PSME4  
PTF1A  
PTMA  
PTPN2  
PURA  
PURB  
PURG  
PWP1  
PWWP2A  
PWWP2B  
PWWP3A  
PYGO1  
PYGO2  
Q6ZW69  
RAD17  
RAD18  
RAD21  
RAD21L1  
RAD23B  
RAD50  
RAD51  
RAD51AP1  
RAD54L  
RAE1  
RAG1  
RAG2  
RAI1  
RAN  
RANBP1  
RANBP2  
RANGAP1  
RARA  
RARB  
RARG  
RAX  
RAX2

RB1  
RBAK  
RBBP4  
RBBP5  
RBBP7  
RBBP8  
RBCK1  
RBL1  
RBL2  
RBM10  
RBMX  
RBPJ  
RBPJL  
RBSN  
RC3H1  
RCBTB1  
RCC1  
RCCD1  
RCOR1  
REC8  
REL  
RELA  
RELB  
Remodeleres  
REPIN1  
RERE papers (Nuria's+St papers)  
RESF1  
REST  
REV3L  
REXO4  
RFC1  
RFC2  
RFC3  
RFWD2  
RFX1  
RFX2  
RFX3  
RFX4  
RFX5  
RFX6  
RFX7  
RFX8  
RFXANK  
RFXAP  
RHOXF1  
RHOXF2  
RHOXF2B  
RIF1  
RING1  
RIOX1  
RIOX2

RIT2  
RLF  
RNF168  
RNF169  
RNF17  
RNF2  
RNF20  
RNF217  
RNF40  
RNF8  
RORA  
RORB  
RORC  
RPA1  
RPA2  
RPA3  
RPL26  
RPL3  
RPS19BP1  
RPS2  
RPS6KA3  
RPS6KA4  
RPS6KA5  
RREB1  
RRP1B  
RRP8  
RSBN1  
RSF1  
RTF1  
RUNX1  
RUNX1T1  
RUNX2  
RUNX3  
RUVBL1  
RUVBL2  
RXRA  
RXRB  
RXRG  
RYBP  
SAFB  
SAFB2  
SALL1  
SALL2  
SALL3  
SALL4  
SAP130  
SAP18  
SAP30  
SAP30L  
SART1  
SATB1

SATB2  
SBNO1  
SCMH1  
SCML2  
SCML4  
SCRT1  
SCRT2  
SCX  
SDR16C5  
SEBOX  
SEH1L  
SENP2  
SENP3  
SERBP1  
SET  
SETBP1  
SETD1A  
SETD1B  
SETD2  
SETD3  
SETD4  
SETD5  
SETD6  
SETD7  
SETD8  
SETD9  
SETDB1  
SETDB2  
SETMAR  
SETSIP  
SETX  
SF3A1  
SF3B1  
SF3B2  
SF3B3  
SFMBT1  
SFMBT2  
SFPQ  
SGF29  
SGSM2  
SHMT2  
SHOX  
SHOX2  
SHPRH  
SIAH2  
SIK1  
SIM1  
SIM2  
SIN3A  
SIN3B  
SINHCAF

SIRT1  
SIRT2  
SIRT3  
SIRT4  
SIRT5  
SIRT6  
SIRT7  
SIX1  
SIX2  
SIX3  
SIX4  
SIX5  
SIX6  
SKI  
SKIL  
SKOR1  
SKOR2  
SKP1  
SKP2  
SLC2A4RG  
SLC30A9  
SLF1  
SLF2  
SLK  
SLX4  
SMAD1  
SMAD2  
SMAD3  
SMAD4  
SMAD5  
SMAD6  
SMAD7  
SMAD9  
SMARCA1  
SMARCA2  
SMARCA4  
SMARCA5  
SMARCAD1  
SMARCAL1  
SMARCB1  
SMARCC1  
SMARCC2  
SMARCD1  
SMARCD2  
SMARCD3  
SMARCE1  
SMC1A  
SMC1B  
SMC2  
SMC3  
SMC4

SMC5  
SMC6  
SMCHD1  
SMCR8  
SMN1  
SMN2  
SMNDC1  
SMYD1  
SMYD2  
SMYD3  
SMYD4  
SMYD5  
SNAI1  
SNAI2  
SNAI3  
SNAPC2  
SNAPC4  
SNAPC5  
SND1  
SNRPD2  
SNW1  
SOHLH1  
SOHLH2  
SON  
SOS1  
SOS2  
SOX1  
SOX10  
SOX11  
SOX12  
SOX13  
SOX14  
SOX15  
SOX17  
SOX18  
SOX2  
SOX21  
SOX3  
SOX30  
SOX4  
SOX5  
SOX6  
SOX7  
SOX8  
SOX9  
SP1  
SP100  
SP110  
SP140  
SP140L  
SP2

SP3  
SP4  
SP5  
SP6  
SP7  
SP8  
SP9  
SPATA24  
SPDEF  
SPEN  
SPHK2  
SPI1  
SPIB  
SPIC  
SPIN1  
SPINDOC  
SPTY2D1  
SPZ1  
SRBD1  
SRCAP  
SREBF1  
SREBF2  
SRF  
SRPK1  
SRSF2  
SRY  
SS18  
SS18L1  
SSBP1  
SSRP1  
SSU72  
ST18  
STAG1  
STAG2  
STAG3  
STAG3L1  
STAG3L2  
STAG3L3  
STAG3L4  
STAT1  
STAT2  
STAT3  
STAT4  
STAT5A  
STAT5B  
STAT6  
STIP1  
STK3  
STK31  
STK4  
STPG4

SUB1  
SUDS3  
SUMO1  
SUMO2  
SUMO3  
SUPT16H  
SUPT3H  
SUPT4H1  
SUPT5H  
SUPT6H  
SUPT7L  
SUPV3L1  
SUV39H1  
SUV39H2  
SUV420H1  
SUV420H2  
SUZ12  
SVEP1  
SYCE1  
SYCE2  
SYCP1  
SYCP3  
SYNCRIP  
T  
TADA1  
TADA2A  
TADA2B  
TADA3  
TAF1  
TAF10  
TAF12  
TAF15  
TAF1L  
TAF2  
TAF3  
TAF4  
TAF5  
TAF5L  
TAF6L  
TAF9  
TAF9B  
TAL1  
TAL2  
TARDBP  
TASOR  
TBL1X  
TBL1XR1  
TBP  
TBPL1  
TBPL2  
TBR1

TBX1  
TBX10  
TBX15  
TBX18  
TBX19  
TBX2  
TBX20  
TBX21  
TBX22  
TBX3  
TBX4  
TBX5  
TBX6  
TBXT  
TCERG1  
TCF12  
TCF15  
TCF19  
TCF20  
TCF21  
TCF23  
TCF24  
TCF3  
TCF4  
TCF7  
TCF7L1  
TCF7L2  
TCFL5  
TCOF1  
TCP1  
TDG  
TDRD1  
TDRD10  
TDRD12  
TDRD3  
TDRD5  
TDRD6  
TDRD7  
TDRD9  
TDRKH  
TEAD1  
TEAD2  
TEAD3  
TEAD4  
TEF  
TERB1  
TERF1  
TERF2  
TERF2IP  
TET1  
TET2

TET3  
TEX10  
TFAM  
TFAP2A  
TFAP2B  
TFAP2C  
TFAP2D  
TFAP2E  
TFAP4  
TFCP2  
TFCP2L1  
TFDP1  
TFDP2  
TFDP3  
TFE3  
TFEB  
TFEC  
TFPT  
TGIF1  
TGIF2  
TGIF2LX  
TGIF2LY  
THAP1  
THAP10  
THAP11  
THAP12  
THAP2  
THAP3  
THAP4  
THAP5  
THAP6  
THAP7  
THAP8  
THAP9  
THRA  
THRAP3  
THRB  
THYN1  
TICRR  
TIGD1  
TIGD2  
TIGD3  
TIGD4  
TIGD5  
TIGD6  
TIGD7  
TIMELESS  
TIPARP  
TIPIN  
TLE1  
TLE4

TLK1  
TLK2  
TLX1  
TLX2  
TLX3  
TMF1  
TMPO  
TNKS1BP1  
TNP1  
TNP2  
TNRC18  
TOP1  
TOP2A  
TOP2B  
TOPORS  
TOX  
TOX3  
TOX4  
TP53  
TP53BP1  
TP63  
TP73  
TPR  
TPRX1  
TPX2  
TRAFD1  
TRDMT1  
TRERF1  
TRIM24  
TRIM28  
TRIM33  
TRIM37  
TRIM5  
TRIM66  
TRIP12  
TRNP1  
TRP53BP1  
TRPS1  
TRRAP  
TSC22D1  
TSHZ1  
TSHZ2  
TSHZ3  
TSPYL2  
TSSK6  
TTC21B  
TTC37  
TTC5  
TTF1  
TTF2  
TUBA1A

TUBA1B  
TWIST1  
TWIST2  
UBA1  
UBA52  
UBA7  
UBB  
UBE2A  
UBE2B  
UBE2C  
UBE2E1  
UBE2E3  
UBE2I  
UBE2M  
UBE2N  
UBE2O  
UBE2Q2  
UBE2T  
UBE2U  
UBE3A  
UBE4A  
UBN1  
UBP1  
UBR1  
UBR2  
UBR3  
UBR4  
UBR5  
UBR7  
UBTF  
UCHL5  
UHRF1  
UHRF2  
UIMC1  
UNCX  
UPF1  
URI1  
USF1  
USF2  
USF3  
USP11  
USP12  
USP13  
USP16  
USP21  
USP22  
USP27X  
USP3  
USP34  
USP35  
USP46

USP49  
USP51  
USP7  
UTF1  
UTP15  
UTP3  
UTP4  
UTY  
UXT  
VAX1  
VAX2  
VCP  
VCX  
VDR  
VENTX  
VEZF1  
VIRMA  
VPS72  
VRK1  
VRK2  
VSX1  
VSX2  
WAC  
WAPL  
WBP2  
WBP2NL  
WBP7  
WDHD1  
WDR13  
WDR18  
WDR43  
WDR5  
WDR61  
WDR77  
WDR82  
WHSC1  
WHSC1L1  
WIZ  
WNT5A  
WRN  
WT1  
WTAP  
XBP1  
XPA  
XPC  
XPO1  
XRCC1  
XRCC5  
XRCC6  
YAF2  
YAP1

YBX1  
YBX2  
YBX3  
YEATS2  
YEATS4  
YTHDC1  
YWHAQ  
YY1  
YY1AP1  
YY2  
ZBED1  
ZBED2  
ZBED3  
ZBED4  
ZBED5  
ZBED6  
ZBED9  
ZBTB1  
ZBTB10  
ZBTB11  
ZBTB12  
ZBTB14  
ZBTB16  
ZBTB17  
ZBTB18  
ZBTB2  
ZBTB20  
ZBTB21  
ZBTB22  
ZBTB24  
ZBTB25  
ZBTB26  
ZBTB3  
ZBTB32  
ZBTB33  
ZBTB34  
ZBTB37  
ZBTB38  
ZBTB39  
ZBTB4  
ZBTB40  
ZBTB41  
ZBTB42  
ZBTB43  
ZBTB44  
ZBTB45  
ZBTB46  
ZBTB47  
ZBTB48  
ZBTB49  
ZBTB5

ZBTB6  
ZBTB7A  
ZBTB7B  
ZBTB7C  
ZBTB8A  
ZBTB8B  
ZBTB9  
ZC3H12A  
ZC3H4  
ZC3H6  
ZC3H8  
ZCWPW1  
ZCWPW2  
ZEB1  
ZEB2  
ZFAT  
ZFHX2  
ZFHX3  
ZFHX4  
ZFP1  
ZFP14  
ZFP2  
ZFP28  
ZFP295  
ZFP3  
ZFP30  
ZFP37  
ZFP41  
ZFP42  
ZFP57  
ZFP62  
ZFP64  
ZFP69  
ZFP69B  
ZFP740  
ZFP787  
ZFP82  
ZFP90  
ZFP91  
ZFP92  
ZFPM1  
ZFPM2  
ZFX  
ZFY  
ZGLP1  
ZGPAT  
ZHX1  
ZHX2  
ZHX3  
ZIC1  
ZIC2

ZIC3  
ZIC4  
ZIC5  
ZIK1  
ZIM2  
ZIM3  
ZKSCAN1  
ZKSCAN2  
ZKSCAN3  
ZKSCAN4  
ZKSCAN5  
ZKSCAN7  
ZKSCAN8  
ZMAT1  
ZMAT4  
ZMYM2  
ZMYM3  
ZMYM4  
ZMYND11  
ZMYND8  
ZNF10  
ZNF100  
ZNF101  
ZNF107  
ZNF112  
ZNF114  
ZNF117  
ZNF12  
ZNF121  
ZNF124  
ZNF131  
ZNF132  
ZNF133  
ZNF134  
ZNF135  
ZNF136  
ZNF138  
ZNF14  
ZNF140  
ZNF141  
ZNF142  
ZNF143  
ZNF146  
ZNF148  
ZNF154  
ZNF155  
ZNF157  
ZNF16  
ZNF160  
ZNF165  
ZNF169

ZNF17  
ZNF174  
ZNF175  
ZNF177  
ZNF18  
ZNF180  
ZNF181  
ZNF182  
ZNF184  
ZNF189  
ZNF19  
ZNF195  
ZNF197  
ZNF2  
ZNF20  
ZNF200  
ZNF202  
ZNF205  
ZNF207  
ZNF208  
ZNF211  
ZNF212  
ZNF213  
ZNF214  
ZNF215  
ZNF217  
ZNF219  
ZNF22  
ZNF221  
ZNF222  
ZNF223  
ZNF224  
ZNF225  
ZNF226  
ZNF227  
ZNF229  
ZNF23  
ZNF230  
ZNF232  
ZNF233  
ZNF234  
ZNF235  
ZNF236  
ZNF239  
ZNF24  
ZNF248  
ZNF25  
ZNF250  
ZNF251  
ZNF253  
ZNF254

ZNF256  
ZNF257  
ZNF26  
ZNF260  
ZNF263  
ZNF264  
ZNF266  
ZNF267  
ZNF268  
ZNF273  
ZNF274  
ZNF275  
ZNF276  
ZNF277  
ZNF28  
ZNF280A  
ZNF280B  
ZNF280C  
ZNF280D  
ZNF281  
ZNF282  
ZNF283  
ZNF284  
ZNF285  
ZNF286A  
ZNF286B  
ZNF287  
ZNF292  
ZNF296  
ZNF3  
ZNF30  
ZNF300  
ZNF302  
ZNF304  
ZNF311  
ZNF316  
ZNF317  
ZNF318  
ZNF319  
ZNF32  
ZNF320  
ZNF322  
ZNF324  
ZNF324B  
ZNF326  
ZNF329  
ZNF331  
ZNF333  
ZNF334  
ZNF335  
ZNF337

ZNF33A  
ZNF33B  
ZNF34  
ZNF341  
ZNF343  
ZNF345  
ZNF346  
ZNF347  
ZNF35  
ZNF350  
ZNF354A  
ZNF354B  
ZNF354C  
ZNF358  
ZNF362  
ZNF365  
ZNF366  
ZNF367  
ZNF37A  
ZNF382  
ZNF383  
ZNF384  
ZNF385A  
ZNF385B  
ZNF385C  
ZNF385D  
ZNF391  
ZNF394  
ZNF395  
ZNF396  
ZNF397  
ZNF398  
ZNF404  
ZNF407  
ZNF408  
ZNF41  
ZNF410  
ZNF414  
ZNF415  
ZNF416  
ZNF417  
ZNF418  
ZNF419  
ZNF420  
ZNF423  
ZNF425  
ZNF426  
ZNF428  
ZNF429  
ZNF43  
ZNF430

ZNF431  
ZNF432  
ZNF433  
ZNF436  
ZNF438  
ZNF439  
ZNF44  
ZNF440  
ZNF441  
ZNF442  
ZNF443  
ZNF444  
ZNF445  
ZNF446  
ZNF449  
ZNF45  
ZNF451  
ZNF454  
ZNF460  
ZNF461  
ZNF462  
ZNF467  
ZNF468  
ZNF469  
ZNF470  
ZNF471  
ZNF473  
ZNF474  
ZNF479  
ZNF48  
ZNF480  
ZNF483  
ZNF484  
ZNF485  
ZNF486  
ZNF487  
ZNF488  
ZNF490  
ZNF491  
ZNF492  
ZNF493  
ZNF496  
ZNF497  
ZNF500  
ZNF501  
ZNF502  
ZNF503  
ZNF506  
ZNF507  
ZNF510  
ZNF511

ZNF512  
ZNF512B  
ZNF513  
ZNF514  
ZNF516  
ZNF517  
ZNF518A  
ZNF518B  
ZNF519  
ZNF521  
ZNF524  
ZNF525  
ZNF526  
ZNF527  
ZNF528  
ZNF529  
ZNF530  
ZNF532  
ZNF534  
ZNF536  
ZNF540  
ZNF541  
ZNF543  
ZNF544  
ZNF546  
ZNF547  
ZNF548  
ZNF549  
ZNF550  
ZNF551  
ZNF552  
ZNF554  
ZNF555  
ZNF556  
ZNF557  
ZNF558  
ZNF559  
ZNF560  
ZNF561  
ZNF562  
ZNF563  
ZNF564  
ZNF565  
ZNF566  
ZNF567  
ZNF568  
ZNF569  
ZNF57  
ZNF570  
ZNF571  
ZNF572

ZNF573  
ZNF574  
ZNF575  
ZNF576  
ZNF577  
ZNF578  
ZNF579  
ZNF580  
ZNF581  
ZNF582  
ZNF583  
ZNF584  
ZNF585A  
ZNF585B  
ZNF586  
ZNF587  
ZNF587B  
ZNF589  
ZNF592  
ZNF594  
ZNF595  
ZNF596  
ZNF597  
ZNF598  
ZNF599  
ZNF600  
ZNF605  
ZNF606  
ZNF607  
ZNF608  
ZNF609  
ZNF610  
ZNF611  
ZNF613  
ZNF614  
ZNF615  
ZNF616  
ZNF618  
ZNF619  
ZNF620  
ZNF621  
ZNF623  
ZNF624  
ZNF625  
ZNF626  
ZNF627  
ZNF628  
ZNF629  
ZNF630  
ZNF638  
ZNF639

ZNF641  
ZNF644  
ZNF645  
ZNF646  
ZNF648  
ZNF649  
ZNF652  
ZNF653  
ZNF654  
ZNF655  
ZNF658  
ZNF66  
ZNF660  
ZNF662  
ZNF664  
ZNF665  
ZNF667  
ZNF668  
ZNF669  
ZNF670  
ZNF671  
ZNF672  
ZNF674  
ZNF675  
ZNF676  
ZNF677  
ZNF678  
ZNF679  
ZNF680  
ZNF681  
ZNF682  
ZNF683  
ZNF684  
ZNF687  
ZNF688  
ZNF689  
ZNF69  
ZNF691  
ZNF692  
ZNF695  
ZNF696  
ZNF697  
ZNF699  
ZNF7  
ZNF70  
ZNF700  
ZNF701  
ZNF703  
ZNF704  
ZNF705A  
ZNF705B

ZNF705D  
ZNF705E  
ZNF705G  
ZNF706  
ZNF707  
ZNF708  
ZNF709  
ZNF71  
ZNF710  
ZNF711  
ZNF713  
ZNF714  
ZNF716  
ZNF717  
ZNF718  
ZNF721  
ZNF724  
ZNF726  
ZNF727  
ZNF728  
ZNF729  
ZNF730  
ZNF732  
ZNF735  
ZNF736  
ZNF737  
ZNF74  
ZNF740  
ZNF746  
ZNF747  
ZNF749  
ZNF750  
ZNF75A  
ZNF75D  
ZNF76  
ZNF761  
ZNF763  
ZNF764  
ZNF765  
ZNF766  
ZNF768  
ZNF77  
ZNF770  
ZNF771  
ZNF772  
ZNF773  
ZNF774  
ZNF775  
ZNF776  
ZNF777  
ZNF778

ZNF780A  
ZNF780B  
ZNF781  
ZNF782  
ZNF783  
ZNF784  
ZNF785  
ZNF786  
ZNF787  
ZNF788  
ZNF789  
ZNF79  
ZNF790  
ZNF791  
ZNF792  
ZNF793  
ZNF799  
ZNF8  
ZNF80  
ZNF800  
ZNF804A  
ZNF804B  
ZNF805  
ZNF808  
ZNF81  
ZNF813  
ZNF814  
ZNF816  
ZNF821  
ZNF823  
ZNF827  
ZNF829  
ZNF83  
ZNF830  
ZNF831  
ZNF835  
ZNF836  
ZNF837  
ZNF84  
ZNF841  
ZNF843  
ZNF844  
ZNF845  
ZNF846  
ZNF85  
ZNF850  
ZNF852  
ZNF853  
ZNF860  
ZNF865  
ZNF878

ZNF879  
ZNF880  
ZNF883  
ZNF888  
ZNF891  
ZNF90  
ZNF91  
ZNF92  
ZNF93  
ZNF98  
ZNF99  
ZNFX1  
ZNHIT1  
ZSCAN1  
ZSCAN10  
ZSCAN12  
ZSCAN16  
ZSCAN18  
ZSCAN2  
ZSCAN20  
ZSCAN21  
ZSCAN22  
ZSCAN23  
ZSCAN25  
ZSCAN26  
ZSCAN29  
ZSCAN30  
ZSCAN31  
ZSCAN32  
ZSCAN4  
ZSCAN5A  
ZSCAN5B  
ZSCAN5C  
ZSCAN9  
ZUFSP  
ZXDA  
ZXDB  
ZXDC  
ZZZ3  
BCL7A  
BCL7B  
BCL7C

| 460 cancer driver genes (Dietlin et al 2020) | 299 cancer driver genes (Bailey et al 2018) | 369 cancer driver genes (Martincorena et al. 2017) | 260 cancer driver genes (Lawrence et al. 2014) | Loss of function mutations intolerant genes (Lek et al. 2016) | 127 most commonly mutated genes in Cancer (Kandoth 2013) |
|--|---|--|--|---|--|
| TP53   | ABL1  | ABL1   | ACO1   | SKI   | MIR142   |
| KRAS   | ACVR1                                       | ACO1   | ACVR1B   | GNB1  | B4GALT3  |
| TP53   | ACVR1B                                      | ACVR1  | ACVR2B   | GABRD   | EGR3   |
| APC  | ACVR2A                                      | ACVR1B   | ADNP   | RER1  | CRIPAK   |
| TP53   | AJUBA                                       | ACVR2A   | AJUBA  | PRDM16  | PRX  |
| TP53   | AKT1  | ACVR2B   | AKT1   | TP73  | LIFR   |
| BRAF   | ALB   | ADNP   | ALK  | PANK4   | AR   |
| PTEN   | ALK   | AJUBA  | ALKBH6   | ICMT  | EPPK1  |
| TP53   | AMER1                                       | AKT1   | ALPK2  | AJAP1   | HGF  |
| TP53   | APC   | ALB  | ANK3   | CHD5  | NPM1   |
| PIK3CA                                       | APOB  | ALK  | APC  | PHF13   | USP9X  |
| VHL  | AR  | ALPK2  | APOL2  | DNAJC11   | NCOR1  |
| TP53   | ARAF  | AMER1  | ARHGAP35                                       | PIK3CD  | POLQ   |
| BRAF   | ARHGAP35                                    | APC  | ARID1A   | CAMTA1  | ARHGAP35   |
| GNA11  | ARID1A                                      | APOL2  | ARID2  | PARK7   | MALAT1   |
| TP53   | ARID2                                       | ARHGAP35   | ARID5B   | RERE  | LRRK2  |
| KRAS   | ARID5B                                      | ARHGAP5  | ASXL1  | TARDBP  | NOTCH1   |
| TP53   | ASXL1                                       | ARID1A   | ASXL2  | PGD   | NAV3   |
| IDH1   | ASXL2                                       | ARID1B   | ATM  | CASZ1   | STK11  |
| TP53   | ATF7IP                                      | ARID2  | ATP5B  | KIF1B   | MTOR   |
| GTF2I  | ATM   | ARID5B   | AXIN2  | UBE4B   | RPL5   |
| TP53   | ATR   | ASXL1  | AZGP1  | MFN2  | RPL22  |
| TP53   | ATRX  | ATM  | B2M  | MTOR  | PTPN11   |
| PIK3CA                                       | ATXN3                                       | ATP1A1   | BAP1   | VPS13D  | PPP2R1A  |
| ARID1A                                       | AXIN1                                       | ATP1B1   | BCLAF1   | PRDM2   | NFE2L3   |
| PBRM1  | AXIN2                                       | ATP2B3   | BCOR   | SPEN  | NFE2L2   |
| KRAS   | B2M   | ATRX   | BHMT2  | ZBTB17  | IDH2   |
| PIK3R1                                       | BAP1  | AXIN1  | BRAF   | DDI2  | IDH1   |
| CTNNB1                                       | BCL2  | AXIN2  | BRCA1  | FBXO42  | TET2   |
| BAP1   | BCL2L11                                     | AZGP1  | BRE  | UBR4  | DNMT3A   |
| PIK3CA                                       | BCOR  | B2M  | C3orf70  | EIF4G3  | AJUBA  |
| TP53   | BRAF  | BAP1   | CAP2   | ECE1  | CDH1   |
| NRAS   | BRCA1                                       | BCLAF1   | CARD11   | HP1BP3  | PCBP1  |
| ATRX   | BRCA2                                       | BCOR   | CASP8  | RAP1GAP   | U2AF1  |
| CTNNB1                                       | BRD7  | BHMT2  | CBFB   | EPHB2   | SF3B1  |
| BAP1   | BTG2  | BIRC3  | CCDC120  | USP48   | SPOP   |
| KDM6A  | CACNA1A                                     | BMPR2  | CCDC6  | KDM1A   | KEAP1  |
| SF3B1  | CARD11                                      | BRAF   | CCND1  | HNRNPR  | FBXW7  |
| PIK3CA                                       | CASP8                                       | BRCA1  | CD1D   | TCEB3   | HIST1H2BD  |
| ARID1A                                       | CBFB  | BRCA2  | CD70   | LYPLA2  | H3F3C  |
| TP53   | CBWD3                                       | BRD7   | CD79B  | E2F2  | HIST1H1C   |
| NF2  | CCND1                                       | C3orf70  | CDC27  | TMEM57  | SOX17  |
| FBXW7  | CD70  | CACNA1D  | CDH1   | GRHL3   | TBL1XR1  |
| KRAS   | CD79B                                       | CALR   | CDK12  | SRRM1   | AXIN2  |
| FAT1   | CDH1  | CARD11   | CDK4   | WDTC1   | CTNNB1   |
| SMAD4  | CDK12                                       | CASP8  | CDKN1A   | ARID1A  | APC  |
| KMT2C  | CDK4  | CBFB   | CDKN1B   | SLC9A1  | ACVR2A   |
| TP53   | CDKN1A                                      | CBL  | CDKN2A   | EYA3  | SMAD2  |
| ARID1A                                       | CDKN1B                                      | CBLB   | CEBPA  | PPP1R8  | ACVR1B   |
| PIK3CA                                       | CDKN2A                                      | CCDC120  | CEP76  | AHDC1   | TGFBR2   |
| NOTCH1                                       | CDKN2C                                      | CCDC6  | CHD4   | WASF2   | SMAD4  |
| CDKN2A                                       | CEBPA                                       | CCND1  | CHD8   | SRSF4   | AKT1   |
| NF1  | CHD3  | CD1D   | CNBD1  | PUM1  | PIK3CG   |
| FLG  | CHD4  | CD58   | CNKSRI   | PTPRU   | TLR4   |
| RB1  | CHD8  | CD70   | COL5A1   | GMEB1   | PIK3R1   |
| KMT2D  | CHEK2                                       | CD79A  | COL5A3   | YTHDF2  | PTEN   |
| PIM1   | CIC   | CD79B  | CREBBP   | BAI2  | PIK3CA   |
| KMT2D  | CNBD1                                       | CDC27  | CTCF   | KPNA6   | MAPK8IP1   |
| PIK3CA                                       | COL5A1                                      | CDC73  | CTNNB1   | TXLNA   | MAP2K4   |
| CTCF   | CREB3L3                                     | CDH1   | CUL4B  | KHDRBS1   | NRAS   |
| EGFR   | CREBBP                                      | CDH10  | CUX1   | ZBTB80S   | BRAF   |
| STK11  | CSDE1                                       | CDK12  | DDX3X  | HDAC1   | MAP3K1   |
| KEAP1  | CTCF  | CDK4   | DDX5   | RBBP4   | NF1  |

|         |          |         |          |          |        |
|---------|----------|---------|----------|----------|--------|
| CARD11  | CTNNB1   | CDKN1A  | DIAPH1   | LCK      | KRAS   |
| TP53    | CTNND1   | CDKN1B  | DIS3     | S100PBP  | CDKN2C |
| ATRX    | CUL1     | CDKN2A  | DNAH12   | SFPQ     | CDKN1A |
| TP53    | CUL3     | CDKN2C  | DNER     | DLGAP3   | CCND1  |
| ERCC2   | CYLD     | CEBPA   | DNMT3A   | ZNF362   | CDKN1B |
| PTEN    | CYSLTR2  | CHD4    | EGFR     | ZMYM4    | CDK12  |
| PPP2R1A | DACH1    | CHD8    | EIF2S2   | AGO3     | RB1    |
| TP53    | DAZAP1   | CIB3    | ELF3     | AGO4     | CDKN2A |
| ARID2   | DDX3X    | CIC     | EP300    | MAP7D1   | FGFR3  |
| FGFR3   | DHX9     | CMTR2   | EPHA2    | CLSPN    | KIT    |
| EGFR    | DIAPH2   | CNBD1   | ERBB2    | PSMB2    | FGFR2  |
| PIK3CA  | DICER1   | CNOT3   | ERBB3    | AGO1     | EPHB6  |
| CDKN2A  | DMD      | COL2A1  | ERCC2    | NCDN     | PDGFRA |
| KIT     | DNMT3A   | COL5A1  | EZH1     | THRAP3   | ERBB4  |
| KRAS    | EEF1A1   | COL5A3  | EZH2     | STK40    | EPHA3  |
| POLE    | EEF2     | CREBBP  | EZR      | ZC3H12A  | FLT3   |
| BCL2    | EGFR     | CRLF2   | FAM166A  | MTF1     | EGFR   |
| MYD88   | EGR3     | CSDE1   | FAM46C   | SF3A3    | ERCC2  |
| CREBBP  | EIF1AX   | CSF1R   | FAT1     | SNIP1    | RAD21  |
| CDKN2A  | ELF3     | CSF3R   | FBXW7    | GRIK3    | CHEK2  |
| IGLL5   | EP300    | CTCF    | FGFBP1   | PPIE     | SMC3   |
| STAG2   | EPAS1    | CTNNA1  | FGFR2    | PABPC4   | SMC1A  |
| CDKN1A  | EPHA2    | CTNNB1  | FGFR3    | MACF1    | BRCA1  |
| FGFR2   | EPHA3    | CUL3    | FLG      | RLF      | BAP1   |
| RPL22   | ERBB2    | CUL4B   | FLT3     | CTPS1    | STAG2  |
| SETD2   | ERBB3    | CUX1    | FOXA1    | KCNQ4    | ATR    |
| TP53    | ERBB4    | CYLD    | FOXQ1    | MFSD2A   | BRCA2  |
| HRAS    | ERCC2    | DAXX    | FRMD7    | FOXJ3    | ATRX   |
| CDH1    | ESR1     | DDX3X   | GATA3    | SLC2A1   | ATM    |
| BRAF    | EZH2     | DDX5    | GNA13    | YBX1     | TP53   |
| RB1     | FAM46D   | DIAPH1  | GNB1     | PTPRF    | EZH2   |
| ZNF804B | FAT1     | DICER1  | GNPTAB   | ATP6V0B  | ASXL1  |
| ERBB4   | FBXW7    | DIS3    | GOT1     | KDM4A    | ARID5B |
| PIK3CA  | FGFR1    | DNM2    | GPS2     | IPO13    | MLL4   |
| GATA3   | FGFR2    | DNMT3A  | GUSB     | RNF220   | KDM6A  |
| IDH1    | FGFR3    | EEF1A1  | HIST1H1E | RPS8     | KDM5C  |
| NRAS    | FLNA     | EGFR    | HIST1H3B | LRRC41   | SETBP1 |
| CASP8   | FLT3     | EIF1AX  | HIST1H4E | DMBX1    | NSD1   |
| BAP1    | FOXA1    | EIF2S2  | HLA-A    | FAF1     | SETD2  |
| BRAF    | FOXA2    | ELF3    | HLA-B    | ZFYVE9   | PBRM1  |
| SPOP    | FOXQ1    | EML4    | HRAS     | OSBPL9   | ARID1A |
| PTEN    | FUBP1    | EP300   | HSP90AB1 | ELAVL4   | MLL2   |
| NRAS    | GABRA6   | EPAS1   | IDH1     | ZCCHC11  | MLL3   |
| ALB     | GATA3    | EPHA2   | IDH2     | NDC1     | FOXA2  |
| HRAS    | GNA11    | EPS8    | IL7R     | ZYG11B   | CEBPA  |
| NF1     | GNA13    | ERBB2   | ING1     | LRP8     | VEZF1  |
| CIC     | GNAQ     | ERBB3   | INPPL1   | PRPF38A  | ELF3   |
| KMT2C   | GNAS     | ERCC2   | INTS12   | SSBP3    | SOX9   |
| CDKN2A  | GPS2     | ERG     | IPO7     | DHCR24   | CBFB   |
| RNF43   | GRIN2D   | ESR1    | IRF4     | PPAP2B   | PHF6   |
| ARID1A  | GTF2I    | ETNK1   | IRF6     | DAB1     | FOXA1  |
| RXRA    | H3F3A    | EZH2    | ITGB7    | USP24    | EIF4A2 |
| CENPE   | H3F3C    | FAM104A | ITPKB    | NFIA     | WT1    |
| KDM6A   | HGF      | FAM166A | KDM5C    | ROR1     | SIN3A  |
| CREBBP  | HIST1H1C | FAM46C  | KDM6A    | USP1     | TBX3   |
| TP53    | HIST1H1E | FAT1    | KEAP1    | JAK1     | MECOM  |
| SF3B1   | HLA-A    | FBXO11  | KEL      | SGIP1    | RUNX1  |
| MAP3K1  | HLA-B    | FBXW7   | KIT      | MIER1    | TSHZ2  |
| AXIN1   | HRAS     | FGFR1   | KLHL8    | SERBP1   | TAF1   |
| APC     | HUWE1    | FGFR2   | KRAS     | LEPR     | CTCF   |
| ARID1A  | IDH1     | FGFR3   | LCTL     | DNAJC6   | EP300  |
| FOXA1   | IDH2     | FLG     | MAP2K1   | SRSF11   | TSHZ3  |
| SMARCA2 | IL6ST    | FLT3    | MAP2K4   | ZRANB2   | GATA3  |
| REV3L   | IL7R     | FOSL2   | MAP3K1   | NEGR1    | VHL    |
| NOTCH1  | INPPL1   | FOXA1   | MAP4K3   | LRRC7    |        |
| KRAS    | IRF2     | FOXA2   | MBD1     | ANKRD13C |        |
| DNMT3A  | IRF6     | FOXL2   | MED12    | FUBP1    |        |

|         |        |           |         |          |
|---------|--------|-----------|---------|----------|
| NRAS    | JAK1   | FOXQ1     | MED23   | ZZZ3     |
| FLT3    | JAK2   | FRMD7     | MET     | USP33    |
| NOTCH1  | JAK3   | FUBP1     | MGA     | LPHN2    |
| NPM1    | KANSL1 | GAGE12J   | MICALCL | PKN2     |
| KRAS    | KDM5C  | GATA1     | MLL     | ZNF326   |
| HRAS    | KDM6A  | GATA2     | MLL2    | ZNF644   |
| RB1     | KEAP1  | GATA3     | MLL3    | ABCD3    |
| PIK3CA  | KEL    | GNA11     | MLL4    | ARHGAP29 |
| RAC1    | KIF1A  | GNA13     | MORC4   | RPL5     |
| KIT     | KIT    | GNAQ      | MPO     | BCAR3    |
| SF3B1   | KLF5   | GNAS      | MTOR    | MTF2     |
| ATM     | KMT2A  | GNB1      | MUC17   | FNBP1L   |
| RB1     | KMT2B  | GNPTAB    | MXRA5   | HIAT1    |
| MAML2   | KMT2C  | GPS2      | MYB     | LPPR4    |
| IDH1    | KMT2D  | GTF2I     | MYCN    | LPPR5    |
| PBRM1   | KRAS   | GUSB      | MYD88   | PTBP2    |
| EZH2    | KRT222 | H3F3A     | MYOCD   | PRPF38B  |
| FUBP1   | LATS1  | H3F3B     | NBPF1   | COL11A1  |
| U2AF1   | LATS2  | HIST1H1C  | NCOR1   | WDR47    |
| GNAS    | LEMD2  | HIST1H1E  | NF1     | SORT1    |
| HRAS    | LZTR1  | HIST1H2BD | NFE2L2  | PSMA5    |
| MYD88   | MACF1  | HIST1H3B  | NOTCH1  | CELSR2   |
| IDH1    | MAP2K1 | HIST1H4E  | NPM1    | SARS     |
| IDH2    | MAP2K4 | HLA-A     | NRAS    | SLC6A17  |
| ERBB2   | MAP3K1 | HLA-B     | NSD1    | CSF1     |
| XPO1    | MAP3K4 | HLA-C     | NTN4    | RBM15    |
| TET2    | MAPK1  | HNF1A     | NUP210L | AHCYL1   |
| IDH2    | MAX    | HOXB3     | ODAM    | RAP1A    |
| SF3B1   | MECOM  | HRAS      | OMA1    | CEPT1    |
| AKT1    | MED12  | IDH1      | OR4A16  | HIPK1    |
| NEFH    | MEN1   | IDH2      | OR52N1  | CAPZA1   |
| PIK3CA  | MET    | IKBKB     | OTUD7A  | MOV10    |
| PBRM1   | MGA    | IKZF1     | PAPD5   | SYCP1    |
| HRAS    | MGMT   | IL6ST     | PBRM1   | NRAS     |
| PTEN    | MLH1   | IL7R      | PCBP1   | TRIM33   |
| CD79B   | MSH2   | ING1      | PDAP1   | CSDE1    |
| ARID2   | MSH3   | INTS12    | PDCD2L  | ATP1A1   |
| KMT2C   | MSH6   | IPO7      | PDSS2   | IGSF3    |
| CDH1    | MTOR   | IRF4      | PHF6    | MAN1A2   |
| CTNNB1  | MUC6   | ITGB7     | PIK3CA  | ANKRD34A |
| RBM10   | MYC    | ITPKB     | PIK3R1  | RBM8A    |
| BRAF    | MYCN   | JAK1      | PLCG2   | NOTCH2   |
| ERBB2   | MYD88  | JAK2      | POLE    | PIAS3    |
| NSD1    | MYH9   | JAK3      | POU2AF1 | FCGR1A   |
| MAP2K4  | NCOR1  | KANSL1    | POU2F2  | SF3B4    |
| ARID1A  | NF1    | KCNJ5     | PPM1D   | ANP32E   |
| ZNF479  | NF2    | KDM5C     | PPP2R1A | PRPF3    |
| PTEN    | NFE2L2 | KDM6A     | PPP6C   | PLEKHO1  |
| RB1     | NIPBL  | KDR       | PRDM1   | RPRD2    |
| CHEK2   | NOTCH1 | KEAP1     | PTEN    | MCL1     |
| U2AF1   | NOTCH2 | KEL       | PTPN11  | ARNT     |
| TGFBR2  | NPM1   | KIT       | QKI     | SETDB1   |
| BRAF    | NRAS   | KLF4      | RAB40A  | CERS2    |
| RPS6KA3 | NSD1   | KLF5      | RAC1    | PI4KB    |
| ERBB3   | NUP133 | KLHL8     | RAD21   | SNX27    |
| KMT2D   | NUP93  | KMT2A     | RASA1   | POGZ     |
| PIK3R1  | PAX5   | KMT2B     | RB1     | PSMD4    |
| CEBPA   | PBRM1  | KMT2C     | RBM10   | ZNF687   |
| SETD2   | PCBP1  | KMT2D     | RHEB    | RORC     |
| HLA-A   | PDGFRA | KRAS      | RHOA    | CHTOP    |
| EZH2    | PDS5B  | KRT5      | RIT1    | CRTC2    |
| PTEN    | PGR    | LATS2     | RPL5    | INTS3    |
| APC     | PHF6   | LCTL      | RPS15   | ILF2     |
| BACH1   | PIK3CA | LZTR1     | RPS2    | GATAD2B  |
| APC     | PIK3CB | MAP2K1    | RSBN1L  | DENND4B  |
| U2AF1   | PIK3CG | MAP2K2    | RUNX1   | UBAP2L   |
| BAP1    | PIK3R1 | MAP2K4    | RXRA    | ADAR     |

|           |         |         |           |              |
|-----------|---------|---------|-----------|--------------|
| MET       | PIK3R2  | MAP2K7  | SACS      | UBE2Q1       |
| CDK12     | PIM1    | MAP3K1  | SELP      | ATP8B2       |
| ESR1      | PLCB4   | MAX     |           | sep-12 PYGO2 |
| AMER1     | PLCG1   | MED12   | SERPINB13 | TRIM46       |
| KMT2C     | PLXNB2  | MED23   | SETD2     | ASH1L        |
| ACVR2A    | PMS1    | MEN1    | SETDB1    | GON4L        |
| IKZF3     | PMS2    | MET     | SF3B1     | KIAA0907     |
| ARHGAP35  | POLE    | MGA     | SFRS2     | CLK2         |
| CREBBP    | POLQ    | MLH1    | SGK1      | ARHGEF2      |
| KDM6A     | POLRMT  | MPL     | SIRT4     | UBQLN4       |
| TNFRSF11A | PPM1D   | MPO     | SLC1A3    | RUSC1        |
| TSC2      | PPP2R1A | MSH2    | SLC26A3   | LMNA         |
| LATS2     | PPP6C   | MSH6    | SLC44A3   | MEF2D        |
| BAP1      | PRKAR1A | MTOR    | SLC4A5    | CCT3         |
| CHD2      | PSIP1   | MUC17   | SMAD2     | SMG5         |
| SETD2     | PTCH1   | MUC6    | SMAD4     | ARHGEF11     |
| NFE2L2    | PTEN    | MXRA5   | SMARCA4   | PRCC         |
| KMT2D     | PTMA    | MYD88   | SMARCB1   | KIRREL       |
| KIT       | PTPDC1  | MYOCD   | SMC1A     | CADM3        |
| BRCA1     | PTPN11  | MYOD1   | SMC3      | DCAF8        |
| KMT2C     | PTPRC   | NBPF1   | SNX25     | COPA         |
| NF2       | PTPRD   | NCOR1   | SOS1      | NCSTN        |
| NOTCH1    | RAC1    | NF1     | SOX17     | VANGL2       |
| ARID2     | RAD21   | NF2     | SPEN      | ARHGAP30     |
| CCND1     | RAF1    | NFE2L2  | SPOP      | NDUFS2       |
| CTNNB1    | RARA    | NIPBL   | STAG2     | PBX1         |
| ASXL1     | RASA1   | NOTCH1  | STK11     | RXRG         |
| NF1       | RB1     | NOTCH2  | STK19     | UAP1         |
| CBFB      | RBM10   | NPM1    | STX2      | LMX1A        |
| HLA-B     | RET     | NRAS    | TAP1      | DDR2         |
| RNF43     | RFC1    | NSD1    | TBC1D12   | DCAF6        |
| POLR2A    | RHEB    | NT5C2   | TBL1XR1   | POGK         |
| KRAS      | RHOA    | NTN4    | TBX3      | UCK2         |
| KDM5C     | RHOB    | NTRK3   | TCEB1     | POU2F1       |
| NF1       | RIT1    | NUP210L | TCF7L2    | ATP1B1       |
| POU2F2    | RNF111  | OMA1    | TCP11L2   | PRRC2C       |
| MAP2K1    | RNF43   | OR4A16  | TDRD10    | VAMP4        |
| RET       | RPL22   | OR4N2   | TET2      | RFWD2        |
| TSC1      | RPL5    | OR52N1  | TGFBR2    | RC3H1        |
| NF1       | RPS6KA3 | OTUD7A  | TIMM17A   | CACYBP       |
| TCHH      | RQCD1   | PAPD5   | TNF       | SERPINC1     |
| HLA-B     | RRAS2   | PAX5    | TNFRSF14  | ASTN1        |
| NCOR1     | RUNX1   | PBRM1   | TP53      | BRINP2       |
| ARID1A    | RXRA    | PCBP1   | TP53BP1   | TNR          |
| EPAS1     | SCAF4   | PDAP1   | TPX2      | TDRD5        |
| FBXW7     | SETBP1  | PDGFRA  | TRAF3     | CEP350       |
| NUP93     | SETD2   | PDSS2   | TRIM23    | RALGPS2      |
| FAM157B   | SF1     | PDYN    | TSC1      | GLUL         |
| RUNX1     | SF3B1   | PHF6    | TTLL9     | CACNA1E      |
| EGR2      | SIN3A   | PHOX2B  | TXNDC8    | DHX9         |
| KRAS      | SMAD2   | PIK3CA  | U2AF1     | NMNAT2       |
| KMT2C     | SMAD4   | PIK3R1  | VHL       | LAMC1        |
| B2M       | SMARCA1 | PLCG1   | WASF3     | XPR1         |
| IDH2      | SMARCA4 | POLE    | WT1       | SMG7         |
| WT1       | SMARCB1 | POT1    | XIRP2     | RNF2         |
| RGPD3     | SMC1A   | POU2AF1 | XPO1      | IVNS1ABP     |
| KLHL6     | SMC3    | POU2F2  | ZFHX3     | TRMT1L       |
| PTEN      | SOS1    | PPM1D   | ZNF180    | TPR          |
| PTCH1     | SOX17   | PPP2R1A | ZNF471    | RGL1         |
| MAPK1     | SOX9    | PPP6C   | ZNF483    | CFH          |
| TBX3      | SPOP    | PRDM1   | ZNF620    | PTGS2        |
| EP300     | SPTA1   | PRKAR1A | ZNF750    | CDC73        |
| SF3B1     | SPTAN1  | PSG4    | ZRANB3    | KIF21B       |
| CDKN2A    | SRSF2   | PSIP1   |           | NR5A2        |
| EPHA2     | STAG2   | PTCH1   |           | CAMSAP2      |
| MAEA      | STK11   | PTEN    |           | ZNF281       |
| HS6ST1    | TAF1    | PTPN11  |           | LHX9         |

|          |         |         |          |
|----------|---------|---------|----------|
| ACPP     | TBL1XR1 | PTPRB   | PTPRC    |
| ARID1A   | TBX3    | QKI     | ELF3     |
| BCOR     | TCEB1   | RAC1    | IPO9     |
| CS       | TCF12   | RACGAP1 | NAV1     |
| RHPN2    | TCF7L2  | RAD21   | TMEM183A |
| ZNF280D  | TET2    | RASA1   | PIK3C2B  |
| FBXW7    | TGFBR2  | RB1     | ZC3H11A  |
| PIK3CA   | TGIF1   | RBM10   | MDM4     |
| SETD2    | THRAP3  | RET     | PLEKHA6  |
| RHOA     | TLR4    | RHEB    | RBBP5    |
| CNBD1    | TMSB4X  | RHOA    | SOX13    |
| NF1      | TNFAIP3 | RHOB    | NFASC    |
| KRAS     | TP53    | RIT1    | NUCKS1   |
| SOX9     | TRAF3   | RNF43   | MAPKAPK2 |
| BRD7     | TSC1    | RPL10   | SYT14    |
| KRAS     | TSC2    | RPL22   | IRF6     |
| PPP6C    | TXNIP   | RPL5    | PLXNA2   |
| ERBB2    | U2AF1   | RPS15   | SLC30A1  |
| ELF3     | UNCX    | RPS2    | PROX1    |
| KMT2D    | USP9X   | RPS6KA3 | LPGAT1   |
| GNAQ     | VHL     | RREB1   | PTPN14   |
| BIRC3    | WHSC1   | RUNX1   | TGFB2    |
| PTEN     | WT1     | RXRA    | MARK1    |
| AKT1     | XPO1    | SELP    | ESRRG    |
| ELF3     | ZBTB20  | SETBP1  | KCTD3    |
| NFE2L2   | ZBTB7B  | SETD2   | RAB3GAP2 |
| NFE2L2   | ZC3H12A | SF3B1   | SLC30A10 |
| APC      | ZCCHC12 | SGK1    | FBXO28   |
| BRCA2    | ZFHX3   | SH2B3   | WDR26    |
| IL6ST    | ZFP36L1 | SLC1A3  | ENAH     |
| PBRM1    | ZFP36L2 | SLC26A3 | LBR      |
| SMAD4    | ZMYM2   | SLC44A3 | ACBD3    |
| SMARCA4  | ZMYM3   | SLC4A5  | LIN9     |
| ATM      | ZNF133  | SMAD2   | ITPKB    |
| CLIP1    | ZNF750  | SMAD4   | CDC42BPA |
| RUNX1    |         | SMARCA4 | TAF5L    |
| RBM12    |         | SMARCB1 | TSNAX    |
| HNRNPM   |         | SMC1A   | EGLN1    |
| EMG1     |         | SMC3    | EXOC8    |
| ERC1     |         | SMO     | SPRTN    |
| PIK3CA   |         | SMTNL2  | SIPA1L2  |
| CDKN1B   |         | SNX25   | HEATR1   |
| BRCA2    |         | SOCS1   | RYR2     |
| B2M      |         | SOX17   | LYST     |
| TYRO3    |         | SOX9    | ARID4B   |
| FBXW7    |         | SPEN    | ACTN2    |
| MGA      |         | SPOP    | CHRM3    |
| STK19    |         | SPTAN1  | FMN2     |
| TMPRSS15 |         | SRC     | AKT3     |
| TCF12    |         | SRSF2   | ZBTB18   |
| TP53     |         | STAG2   | CNST     |
| CDKN2A   |         | STAT3   | DESI2    |
| PTEN     |         | STAT5B  | KIF26B   |
| CDC27    |         | STK11   | AHCTF1   |
| FOXA1    |         | STK19   | ZNF496   |
| KDM6A    |         | STX2    | HNRNPU   |
| GNA13    |         | SUFU    | MYT1L    |
| TMPRSS13 |         | TBC1D12 | RPS7     |
| CNOT9    |         | TBL1XR1 | ODC1     |
| AJUBA    |         | TBX3    | RRM2     |
| BRAF     |         | TCEB1   | ASAP2    |
| CHD4     |         | TCF12   | RNF144A  |
| ACVR1B   |         | TCF7L2  | ADAM17   |
| TPTE2    |         | TCP11L2 | GRHL1    |
| GPS2     |         | TDRD10  | MYCN     |
| LARP4B   |         | TERT    | DDX1     |
| RB1      |         | TET2    | TRIB2    |

|           |          |          |
|-----------|----------|----------|
| CLIP1     | TG       | ROCK2    |
| TRAF3     | TGFBR2   | PUM2     |
| ZNF430    | TGIF1    | NCOA1    |
| XYLT2     | TIMM17A  | ATAD2B   |
| CDKN1B    | TNF      | KIF3C    |
| SMAD4     | TNFAIP3  | DPYSL5   |
| MGA       | TNFRSF14 | ASXL2    |
| NRAS      | TOP2A    | RAB10    |
| EP300     | TP53     | ZNF513   |
| BCOR      | TRAF3    | CAD      |
| STAG2     | TRAF7    | GTF3C2   |
| ZFHX3     | TRIM23   | NRBP1    |
| CTNNB1    | TSC1     | ZNF512   |
| MBD6      | TSC2     | FOSL2    |
| NUMBL     | TSHR     | PPP1CB   |
| ARID1A    | TTL9     | PPM1G    |
| RB1       | TYRO3    | WDR43    |
| TET2      | U2AF1    | SPAST    |
| TNFRSF14  | UBR5     | CRIM1    |
| KMT2D     | UPF3A    | STRN     |
| IDH1      | VHL      | BIRC6    |
| SPEN      | WASF3    | SRSF7    |
| ZFP36L1   | WT1      | SLC8A1   |
| PIK3CA    | XIRP2    | ATL2     |
| SOX9      | XPO1     | SOS1     |
| ZNF292    | ZBTB20   | TMEM178A |
| FUBP1     | ZBTB7B   | EPAS1    |
| HMGCR     | ZFHX3    | PRKCE    |
| PEG3      | ZFP36L1  | FBXO11   |
| TSC1      | ZFP36L2  | PSME4    |
| USP28     | ZFX      | SPTBN1   |
| HRAS      | ZMYM3    | CCDC88A  |
| ERF       | ZNF471   | NRXN1    |
| ZC3H13    | ZNF620   | CCT4     |
| KDM6A     | ZNF750   | REL      |
| BTG2      | ZNF800   | PNPT1    |
| RB1       | ZNRF3    | XPO1     |
| NEFH      | ZRSR2    | PAPOLG   |
| LRRRC37A3 |          | USP34    |
| FAT1      |          | EFEMP1   |
| DLC1      |          | MEIS1    |
| CHIT1     |          | VPSS4    |
| POT1      |          | PELI1    |
| ZNF233    |          | ETAA1    |
| ARID1A    |          | EHBP1    |
| CDKN2A    |          | ACTR2    |
| PNPLA4    |          | MDH1     |
| ZFHX3     |          | AFTPH    |
| CDH1      |          | ANTXR1   |
| ERBB3     |          | GFPT1    |
| TMEM30A   |          | AAK1     |
| CIITA     |          | ADD2     |
| PABPC1    |          | FBXO41   |
| MAP2K1    |          | CCT7     |
| ERBB2     |          | ZNF638   |
| P2RY8     |          | CYP26B1  |
| FOXA2     |          | TET3     |
| RHPN2     |          | INO80B   |
| RHOA      |          | PCGF1    |
| SETD2     |          | CTNNA2   |
| LILRA3    |          | LRRTM1   |
| MSH3      |          | RMND5A   |
| MIA2      |          | POLR1A   |
| PBRM1     |          | KDM3A    |
| ERBB3     |          | REEP1    |
| EEF1A1    |          | KANSL3   |
| SGK1      |          | SNRNP200 |

MEF2B  
UBXN11  
HJURP  
KMT2D  
SF3B1  
NCOA6  
KMT2A  
PTEN  
KMT2D  
FGFRL1  
FAM104B  
RB1  
BAP1  
KCNT2  
ZMYM3  
SOX17  
FBXW7  
ZNF14  
FBXW7  
ERBB3  
FRMD4A  
CTNND1  
HLA-B  
TP53  
CDKN1A  
NRAS  
RBBP6  
STAG2  
MED12  
DOT1L  
EP300  
RAD21  
RBM10  
HLA-DRB1  
PAX5  
HLA-A  
RB1  
ATM  
PRSS48  
ARID2  
CCDC91  
ZFXH3  
MTOR  
NUP93  
HLA-A  
ZNF814  
HLA-A  
ERICH6B  
NUP210L  
USP9X  
UBE2A  
SPEN  
HLA-A  
WNK1  
ACVR2A  
KDM6A  
NF1  
TNFAIP3  
PBRM1  
C3orf70  
ZNF234  
SPOP  
CASP8  
TENT5D  
BCOR  
PTEN  
CTNNB1

ARID5A  
STARD7  
SEMA4C  
INPP4A  
TMEM131  
AFF3  
CNOT11  
REV1  
MAP4K4  
NPAS2  
RANBP2  
BCL2L11  
SH3RF3  
POLR1B  
ZC3H6  
IL1B  
TTL  
ACTR3  
CBWD2  
RABL2A  
DPP10  
PAX8  
MAP3K2  
PTPN4  
CLASP1  
TFCP2L1  
INHBB  
TSN  
GLI2  
HS6ST1  
WDR33  
AMMECR1L  
SAP130  
IWS1  
UBXN4  
MCM6  
MGAT5  
ACVR2A  
EPC2  
KIF5C  
ZEB2  
RND3  
LRP1B  
MBD5  
RIF1  
NR4A2  
ACVR1  
FMNL2  
KCNJ3  
PRPF40A  
MARCH7  
TBR1  
KCNH7  
BAZ2B  
RBMS1  
TANK  
SCN1A  
SCN3A  
STK39  
SCN2A  
PPIG  
TLK1  
LRP2  
UBR3  
RAPGEF4  
DLX1  
SP3

TP53BP1  
AKAP2  
PIK3R1  
NFE2L2  
SSC5D  
ZNF292  
VCX  
HNF1A  
ZNF750  
ATM  
ATM  
CTCF  
CTNNB1  
MB21D2  
CREBBP  
FAT3  
PIK3R1  
ARID1B  
ERRFI1  
DTX1  
HRNR  
STAT3  
TRAK1  
BAZ2A  
ZFP36L1  
SPEN  
CTNND2  
KMT2C  
CDK12  
POLQ  
FGFR2  
KMT2C  
NF1  
ZFX  
C10orf113  
AIM2  
NUDCD2  
ERBB4  
DDX3X  
RBM10  
RB1  
PCCA  
RASA1  
RGS7  
TTK  
KIF26B  
AKR1D1  
ZC3H13  
NF1  
HLA-B  
RASA1  
PIK3R1  
NRAS  
PTEN  
SETDB1  
CDK4  
ZKSCAN4  
DHX30  
AKAP9  
SMARCA4  
KMT2C  
NPFRR2  
FAM86B2  
ARID2  
NCOR1  
PABPC1  
RRP36

WIPF1  
HNRNPA3  
SESTD1  
OSBPL6  
AGPS  
CALCRL  
COL5A2  
ZC3H15  
NCKAP1  
COL3A1  
STAT4  
SLC40A1  
GLS  
STAT1  
SF3B1  
HSPD1  
SLC39A10  
HECW2  
ORC2  
FAM126B  
CFLAR  
SATB2  
SPATS2L  
BMPR2  
ADAM23  
KLF7  
INO80D  
RAPH1  
ABI2  
CREB1  
MAP2  
CCNYL1  
PIKFYVE  
ERBB4  
XRCC5  
IKZF2  
ARPC2  
USP37  
RQCD1  
CTDSP1  
TNS1  
EPHA4  
PAX3  
SPEG  
FARSB  
NYAP2  
CUL3  
AGFG1  
TRIP12  
PSMD1  
EIF4E2  
NCL  
DGKD  
GIGYF2  
NGEF  
ATG16L1  
AGAP1  
HDAC4  
ILKAP  
UBE2F  
PER2  
HDLBP  
SNED1  
KIF1A  
ATG4B  
GRM7  
BHLHE40

JMJD1C  
EYS  
FGFR4  
RIMS1  
SPATA31E1  
MAGI2  
TBC1D5  
DMWD  
NF1  
AKR1C3  
MAPK1  
PPM1F  
NFKBIA  
ACVR2A  
TP53  
BAX  
FRG1  
MYB  
KANK3  
MAP2K4  
IRF4  
CHORDC1  
ZBTB7A  
SPHKAP  
CDC27  
PRDM2  
CLIP1  
PIK3CA  
SCN9A  
SF3B1  
RB1  
ATP2B4  
ARID1A  
ATM  
MSH6  
CCNQ  
ZC3H12A  
NUP153  
ARID2  
PRSS50  
RNF152  
PSKH2  
PTPN11  
ELF3  
PCDH9  
BCL11B  
CIC  
C3orf70  
ARID5B  
SEMA4D  
DIS3  
IGHMBP2  
GNA13  
KDM6A  
HIST1H1C  
RPL21  
KEAP1  
TPTE  
SPEN  
RHOB  
ATM  
TEX13A  
CUX1  
HEPH  
NCOR2  
RASA1  
HOXC12

CNTN4  
ITPR1  
SRGAP3  
BRPF1  
ARPC4  
SETD5  
ATP2B2  
SLC6A1  
RAF1  
IQSEC1  
FGD5  
NR2C2  
SLC6A6  
ANKRD28  
DAZL  
PLCL2  
RARB  
UBE2E2  
THRB  
KAT2B  
TOP2B  
RPL15  
TRIM71  
STT3B  
CNOT10  
DYNC1LI1  
CLASP2  
UBP1  
SCN5A  
WDR48  
OXSR1  
ACVR2B  
CTNNB1  
ZBTB47  
RPL14  
NKTR  
ZNF445  
SNRK  
SETD2  
DHX30  
CDC25A  
SMARCC1  
KLHL18  
MAP4  
CELSR3  
IP6K2  
QRICH1  
ARIH2  
PRKAR2A  
DAG1  
RNF123  
USP19  
BSN  
RBM5  
CAMKV  
SEMA3F  
RBM6  
GRM2  
TEX264  
RBM15B  
DOCK3  
CACNA2D2  
RAD54L2  
ALAS1  
WDR82  
PBRM1  
WNT5A

IRF8  
KLF3  
ARL16  
MAP2K7  
PCNT  
ZNF479  
GNA11  
ANAPC1  
INMT  
BCOR  
ZIC4  
LILRB4  
DLGAP2  
RAD54B  
ARID1A  
RARS2  
PRB4  
MGA  
FAM8A1  
FAT4  
CDH11  
RECQL4  
MARK2  
PCDHA3  
ARID1A  
TEAD3  
ESR1  
ATM  
MDN1  
ARHGAP5  
ATM  
ZNF750  
THSD7B  
CCND1  
KDM6A  
DDX3X  
PJA2  
BOD1L1  
ARID1A  
RBM10  
SHROOM3  
ATM  
ZNF804B  
CCDC73  
CHEK2  
YLPM1  
PRDM1  
SF3B2  
NF1  
NCOR1  
ZC3H4  
NOTCH1  
CYLD  
STAT6  
RELN  
ZNF208  
SOX9  
TGFBR2  
PIK3CA  
MYB  
ZNF107  
RB1  
NOTCH2  
SELPLG  
PKHD1L1  
BDP1  
BRD7

CACNA1D  
ARHGEF3  
CACNA2D3  
SFMBT1  
ERC2  
DCP1A  
FAM208A  
TMEM110  
PRKCD  
ARF4  
P XK  
SLMAP  
MAG1  
PRICKLE2  
THOC7  
FEZF2  
PSMD6  
ATXN7  
PDZRN3  
MITF  
PPP4R2  
FOXP1  
UBA3  
EPHA6  
ROBO2  
ZNF654  
CADM2  
TOMM70A  
NFKBIZ  
SENP7  
BBX  
CBLB  
ALCAM  
ATG3  
LSAMP  
TMEM39A  
ZBTB20  
ARHGAP31  
ATP6V1A  
KIAA2018  
GSK3B  
STXBP5L  
FSTL1  
GTF2E1  
CD86  
KPNA1  
PTPLB  
ADCY5  
KALRN  
ZNF148  
PODXL2  
PLXNA1  
RUVBL1  
SEC61A1  
GATA2  
CNBP  
ISY1-RAB43  
RAB7A  
COPG1  
ISY1  
PLXND1  
DNAJC13  
ATP2C1  
EPHB1  
TOPBP1  
STAG1  
PPP2R3A

FRAS1  
STAG2  
FOXQ1  
RB1  
ARID1B  
AXIN1  
CACNA1B  
PPM1D  
ABCA12  
ATP11A  
CDH9  
BAP1  
KMT2A  
PTEN  
HLA-B  
SMAD3  
MCF2  
PDE3A  
AHNAK  
PTCH1  
BIRC6  
CCDC66  
ACVR2A  
FLT3LG  
RRAS2  
ROCK2  
SMTNL2  
PTPN14  
ARID2  
IRF4  
ATF7IP  
ZC3H13  
KMT2D  
PLXNA2  
ATF7IP  
SPTAN1  
NFKBIE  
PHRF1  
NOTCH2  
DNMT3A  
KNTC1  
CCDC66  
ZZEF1  
ZNF208  
ETV6  
ESRP1  
ASXL3  
CDKN1B  
PRKD2  
DICER1  
PLCB1  
KEAP1  
TBL1XR1  
FGFR3  
LRRTM4  
KLHL6  
TSC2  
MB21D2  
NLRP5  
CDKN1A  
DAZAP1  
FAT1  
BTG1  
RPL5  
TCF7L1  
APC  
EIF1AX

TMEM108  
COPB2  
PIK3CB  
ARMC8  
XRN1  
TFDP2  
ZBTB38  
U2SURP  
WWTR1  
MED12L  
MBNL1  
DHX36  
GMPS  
CCNL1  
TIPARP  
SCHIP1  
MECOM  
SERPINI1  
KPNA4  
PDCD10  
PHC3  
SEC62  
FNDC3B  
TNIK  
PIK3CA  
TBL1XR1  
ACTL6A  
FXR1  
DCUN1D1  
YEATS2  
ATP11B  
EIF2B5  
EPHB3  
DVL3  
AP2M1  
POLR2H  
EIF4G1  
PSMD2  
TRA2B  
IGF2BP2  
EIF4A2  
DNAJB11  
SENP2  
ETV5  
MAP3K13  
TP63  
BCL6  
ACAP2  
ATP13A3  
OPA1  
PAK2  
UBXN7  
SENP5  
RPL35A  
DLG1  
CTBP1  
GAK  
PCGF3  
WHSC1  
HTT  
FAM193A  
JAKMIP1  
TBC1D14  
KIAA0232  
CRMP1  
WDR1  
LDB2

LTBP3  
SON  
NLRC5  
GPRIN2  
EPS8  
NOTCH2  
SLIT1  
EVI5L  
TPTE  
ARFGEF2  
TMPRSS7  
DBR1  
CDK5RAP2  
NCOR1  
ZFH4  
PBRM1  
PFN1  
HLA-B  
ELF3  
DYRK1A  
TCF7L2  
RBM43  
IL6ST  
PREX2  
L3MBTL3  
CASZ1  
MED12  
EOMES  
CR1  
SRGAP3  
LILRB1  
ATP6V1B1  
SMARCB1  
STK11  
ARHGAP35  
EPHA2  
FAM135B  
FRAS1  
ITGA8  
A1CF  
TPTE  
TSC1  
NSD2  
SCN9A  
ERBB2  
ODF2L  
ADGRV1  
STAG3L2  
RECQL5  
FAT1  
USH2A  
FAT2  
ICE1  
MSH6  
LAMA2  
PTCH1  
PHF6  
U2AF1  
ZC3H18  
ADGRV1  
PTPRC  
ZNF750  
MET  
PREX1  
UBR5  
NOTCH1  
EBF1

BOD1L1  
FBXL5  
CPEB2  
PPARGC1A  
KCNIP4  
DHX15  
SLIT2  
LCORL  
GPR125  
RBPJ  
RBM47  
LIMCH1  
PDS5A  
UBE2K  
UCHL1  
RPL9  
GABRB1  
ATP8A1  
BEND4  
GABRA4  
GABRA2  
FRYL  
USP46  
CLOCK  
PPAT  
TMEM165  
KIT  
KDR  
PDGFRA  
YTHDC1  
LPHN3  
REST  
POLR2B  
UBA6  
SLC4A4  
RUFY3  
ALB  
ANKRD17  
USO1  
NUP54  
G3BP2  
CNOT6L  
COPS4  
HNRNPDL  
LIN54  
WDFY3  
HNRNPD  
PKD2  
BMPR1B  
GRID2  
SMARCAD1  
TSPAN5  
EIF4E  
DNAJB14  
PPP3CA  
NFKB1  
LEF1  
SEC24B  
ANK2  
ELOVL6  
CCNA2  
FAT4  
ANKRD50  
ADAD1  
ELF2  
RAB33B  
NAA15

EIF5B  
ZNF608  
RBMX  
TNFRSF10C  
BRAF  
MTMR1  
BRD8  
FBXW7  
NBEA  
CD70  
GNAS  
LAMA1  
USP9X  
CFAP58  
WBP1  
ITGA6  
STRIP2  
RBMX  
SETD1B  
TLE1  
NXF1  
HERC2  
ANKRD30A  
TAOK1  
NFE2L2  
FAM135B  
ETV6

PHF17  
OTUD4  
INPP4B  
HHIP  
IL15  
SMARCA5  
ABCE1  
FBXW7  
DCLK2  
ZNF827  
NR3C2  
EDNRA  
PLRG1  
KIAA0922  
RAPGEF2  
GRIA2  
NAF1  
FNIP2  
PDGFC  
CPE  
KLHL2  
CLCN3  
HMGB2  
MFAP3L  
GPM6A  
CDKN2AIP  
TENM3  
STOX2  
TRIP13  
SLC9A3  
PAPD7  
NSUN2  
KIAA0947  
ADCY2  
SLC6A3  
TRIO  
CTNND2  
CCT5  
MARCH6  
FAM105B  
MTMR12  
CDH6  
PDZD2  
CDH9  
ZFR  
DROSHA  
SKP2  
PRLR  
NADK2  
BRX1  
NUP155  
DAB2  
RICTOR  
NIPBL  
NNT  
ZNF131  
HMGCS1  
PAIP1  
HCN1  
FST  
MIER3  
PLK2  
GPBP1  
IL6ST  
DDX4  
MAP3K1  
KIF2A

PDE4D  
RGS7BP  
IPO11  
HTR1A  
SGTB  
PIK3R1  
ADAMTS6  
SREK1  
ERBB2IP  
MAP1B  
TNPO1  
UTP15  
FCHO2  
BTF3  
COL4A3BP  
HMGCR  
FAM169A  
AP3B1  
CRHBP  
PDE8B  
SSBP2  
HOMER1  
JMY  
RASGRF2  
VCAN  
ARRDC3  
RASA1  
ELL2  
LNPEP  
FBXL17  
FER  
CHD1  
APC  
YTHDC2  
SEMA6A  
DMXL1  
KCNN2  
LOX  
ZNF608  
LMNB1  
SNX2  
CSNK1G3  
MEGF10  
SLC12A2  
FBN2  
PDLIM4  
CTC-432M15.3  
FNIP1  
ADAMTS19  
RAPGEF6  
HSPA4  
KIF3A  
FSTL4  
AFF4

sep-08

PHF15  
DDX46  
PPP2CA  
VDAC1  
SMAD5  
KLHL3  
FAM13B  
HSPA9  
CDC23  
CTNNA1  
KDM3B  
MATR3

ETF1  
LRRTM2  
UBE2D2  
NRG2  
ANKHD1-EIF4EBP3  
ANKHD1  
ZMAT2  
PCDHAC2  
PCDHGC4  
HDAC3  
KCTD16  
ARHGAP26  
ARAP3  
YIPF5  
NDFIP1  
RBM27  
TCERG1  
DPYSL3  
JAKMIP2  
FBXO38  
PPP2R2B  
CAMK2A  
CSNK1A1  
CSF1R  
PPARGC1B  
PDGFRB  
SYNPO  
NDST1  
TNIP1  
RBM22  
DCTN4  
G3BP1  
LARP1  
GRIA1  
CYFIP2  
SOX30  
EBF1  
TENM2  
GABRA1  
GABRG2  
PWWP2A  
GABRB2  
DOCK2  
LCP2  
NPM1  
SLIT3  
FBXW11  
CPEB4  
CREBRF  
UNC5A  
FAF2  
PDLIM7  
FAM193B  
DBN1  
NSD1  
ADAMTS2  
HNRNPAB  
FLT4  
MAML1  
HNRNPH1  
TRIM41  
GNB2L1  
GMDS  
IRF4  
RREB1  
PRPF4B  
CDYL

DSP  
TFAP2A  
RANBP9  
HIVEP1  
JARID2  
KIF13A  
NUP153  
FAM65B  
C6orf62  
GABBR1  
TRIM39  
PPP1R10  
GNL1  
DDX39B  
BAG6  
CSNK2B  
ABHD16A  
PRRC2A  
AGPAT1  
BRD2  
COL11A2  
RXRB  
RING1  
RPS18  
SYNGAP1  
PHF1  
GRM4  
SCUBE3  
PPARD  
PACSIN1  
DEF6  
RPS10  
BRPF3  
MAPK14  
SRSF3  
MTCH1  
ZFAND3  
MDGA1  
RNF8  
CMTR1  
DAAM2  
CCND3  
TFEB  
TRERF1  
USP49  
UBR2  
GLTSCR1L  
PPP2R5D  
PTK7  
KLHDC3  
SRF  
TTBK1  
CUL9  
SLC29A1  
XPO5  
HSP90AB1  
TMEM63B  
GPR116  
RUNX2  
CDC5L  
OPN5  
TFAP2D  
ELOVL5  
TFAP2B  
GCM1  
TRAM2  
DST

KCNQ5  
SMAP1  
PHF3  
BAI3  
SENP6  
COL12A1  
PHIP  
EEF1A1  
IBTK  
SNAP91  
DOPEY1  
TBX18  
AKIRIN2  
SYNCRIP  
ZNF292  
MAP3K7  
EPHA7  
MDN1  
SIM1  
CCNC  
ATG5  
GRIK2  
PNISR  
PRDM1  
PREP  
NR2E1  
WASF1  
REV3L  
CDK19  
CDC40  
FYN  
AMD1  
HDAC2  
HSF2  
NCOA7  
EPB41L2  
PTPRK  
L3MBTL3  
SGK1  
PDE7B  
HBS1L  
KIAA1244  
MAP3K5  
REPS1  
MAP7  
TNFAIP3  
HIVEP2  
GRM1  
TAB2  
STXBP5  
LATS1  
FBXO30  
UST  
ESR1  
ZBTB2  
FBXO5  
SCAF8  
ZDHC14  
ARID1B  
TULP4  
IGF2R  
TAGAP  
TCP1  
EZR  
WTAP  
PDE10A  
QKI

MAP3K4  
DLL1  
MLLT4  
GET4  
CARD11  
FOKK1  
GNA12  
EIF3B  
TTYH3  
CCZ1  
USP42  
ACTB  
TNRC18  
ETV1  
THSD7A  
BZW2  
SNX13  
SP4  
HDAC9  
AHR  
ITGB8  
RAPGEF5  
MPP6  
HNRNPA2B1  
IGF2BP3  
HOXA3  
SKAP2  
JAZF1  
CREB5  
HERPUD2  
ANLN  
KBTBD2

sep-07

RALA  
PSMA2  
ELMO1  
GLI3  
HECW1  
OGDH  
ZMIZ2  
ADCY1  
TNS3  
COBL  
IKZF1  
EGFR  
CCT6A  
AUTS2  
STX1A  
BAZ1B  
LIMK1  
NCF1  
HIP1  
EIF4H  
GTF2IRD1  
GTF2I  
CLIP2  
PTPN12  
YWHAG  
SRRM3  
GNAI1  
DBF4  
SEMA3A  
GRM3  
DMTF1  
HGF  
CACNA2D1  
PCLO

ADAM22  
ANKIB1  
CDK6  
CCDC132  
COL1A2  
LMTK2  
TRRAP  
SMURF1  
GIGYF1  
MEPCE  
NYAP1  
GNB2  
ACTL6B  
SRRT  
EPHB4  
ACHE  
CUX1  
NAMPT  
SRPK2  
PSMC2  
RELN  
DNAJC2  
KMT2E  
PRKAR2B  
CBLL1  
DOCK4  
C7orf60  
MET  
CAPZA2  
FOXP2  
ST7  
ING3  
PTPRZ1  
KCND2  
CADPS2  
WASL  
ZNF800  
SND1  
FLNC  
KLHDC10  
UBE2H  
AHCYL2  
NRF1  
MEST  
MKLN1  
PLXNA4  
CALD1  
SLC13A4  
CNOT4  
NUP205  
TRIM24  
JHDM1D  
C7orf55-LUC7L2  
HIPK2  
KIAA1549  
UBN2  
DENND2A  
BRAF  
MKRN1  
FAM131B  
ZNF777  
EZH2  
ZNF398  
CUL1  
REPIN1  
KCNH2  
CDK5

ABCF2  
SLC4A2  
AGAP3  
RHEB  
PRKAG2  
KMT2C  
ACTR3B  
DPP6  
RBM33  
PAXIP1  
SHH  
NCAPG2  
DNAJB6  
UBE3C  
DLGAP2  
XKR6  
DLC1  
LONRF1  
CNOT7  
DMTN  
ATP6V1B2  
XPO7  
INTS10  
CHMP7  
CCAR2  
DPYSL2  
EBF2  
PPP2R2A  
HMBOX1  
PTK2B  
NRG1  
MAK16  
PURG  
LSM1  
ASH2L  
WHSC1L1  
FGFR1  
ANK1  
IKKBK  
FNTA  
PRKDC  
VDAC3  
KAT6A  
HOOK3  
ST18  
RB1CC1  
XKR4  
LYN  
CHD7  
YTHDF3  
RAB2A  
PRDM14  
MYBL1  
ARFGEF1  
VCIPI1  
NCOA2  
COPS5  
KCNB2  
STAU2  
RDH10  
UBE2W  
RPL7  
EYA1  
HEY1  
ZFX4  
ZNF704  
STMN2

MMP16  
OSGIN2  
WWP1  
INTS8  
RUNX1T1  
KIAA1429  
ESRP1  
GDF6  
GRHL2  
PABPC1  
UBR5  
ANKRD46  
ZFPM2  
ANGPT1  
LRP12  
AZIN1  
RIMS2  
RAD21  
CSMD3  
TRPS1  
EXT1  
HAS2  
SQLE  
ATAD2  
MTSS1  
FBXO32  
TRMT12  
FAM49B  
ASAP1  
KCNQ3  
PHF20L1  
FAM135B  
ARC  
BAI1  
PTK2  
AGO2  
ZC3H3  
SCRIB  
CYC1  
ADCK5  
RPL8  
CDC37L1  
SMARCA2  
RFX3  
RCL1  
UHRF2  
JAK2  
PTPRD  
PSIP1  
BNC2  
NFIB  
SH3GL2  
MLLT3  
KLHL9  
TEK  
ELAVL2  
SMU1  
NOL6  
TOPORS  
UBE2R2  
UBAP1  
CNTFR  
UBAP2  
RUSC2  
TESK1  
VCP  
CD72

TLN1  
NPR2  
PAX5  
DCAF10  
RNF38  
CLTA  
PGM5  
RORB  
ALDH1A1  
GDA  
ZFAND5  
ABHD17B  
SMC5  
TLE4  
TLE1  
GNAQ  
NAA35  
UBQLN1  
NTRK2  
ZCCHC6  
DAPK1  
HNRNPK  
SEMA4D  
NFIL3  
SYK  
SPIN1  
PHF2  
IPPK  
FAM120A  
PTCH1  
GABBR2  
NCBP1  
ANP32B  
TGFB1  
ERP44  
TEX10  
SMC2  
KLF4  
ZNF462  
SLC44A1  
RAD23B  
KIAA0368  
EPB41L4B  
UGCG  
PRPF4  
SNX30  
PTBP3  
ZNF618  
COL27A1  
PAPPA  
RAB14  
MEGF9  
PHF19  
DAB2IP  
ASTN2  
FBXW2  
BRINP1  
LHX6  
RC3H2  
RABGAP1  
LHX2  
DENND1A  
STRBP  
PSMB7  
SCAI  
NR6A1  
PPP6C

NR5A1  
RALGPS1  
MAPKAP1  
STXBP1  
GAPVD1  
CIZ1  
ENG  
DNM1  
SLC25A25  
SPTAN1  
ZER1  
SET  
GOLGA2  
NUP188  
PPP2R4  
LRRC8A  
NCS1  
ABL1  
PRRC2B  
RAPGEF1  
NUP214  
TSC1  
RPL7A  
COL5A1  
WDR5  
RXRA  
PPP1R26  
OLFM1  
NOTCH1  
RABL6  
ABCA2  
TRAF2  
FUT7  
EDF1  
GRIN1  
ANAPC2  
TUBB4B  
CACNA1B  
EHMT1  
WDR37  
GTPBP4  
DIP2C  
LARP4B  
ZMYND11  
KLF6  
FAM208B  
RBM17  
TAF3  
PRKCQ  
SFMBT2  
GDI2  
SEPHS1  
CAMK1D  
UPF2  
CELF2  
SEC61A2  
HSPA14  
FAM171A1  
SUV39H2  
FRMD4A  
VIM  
MLLT10  
STAM  
MRC1  
ARHGAP21  
SVIL  
MTPAP

WAC  
RAB18  
YME1L1  
PARD3  
ZEB1  
EPC1  
CUL2  
ITGB1  
NRP1  
RET  
RASGEF1A  
BMS1  
MAPK8  
PRKG1  
CDK1  
ANK3  
UBE2D1  
CCDC6  
HERC4  
JMJD1C  
SIRT1  
ARID5B  
HNRNPH3  
DDX21  
TET1  
H2AFY2  
CCAR1  
PSAP  
NODAL  
PPP3CB  
MCU  
KAT6B  
VCL  
SEC24C  
ZSWIM8  
CAMK2G  
ZMIZ1  
DLG5  
KCNMA1  
GRID1  
WAPAL  
PTEN  
HECTD2  
PCGF5  
SLC35G1  
CPEB3  
BTAF1  
LGI1  
KIF11  
CCNJ  
BLNK  
HELLS  
LCOR  
C10orf12  
PI4K2A  
PIK3AP1  
TM9SF3  
SLIT1  
CNNM1  
C10orf2  
CHUK  
ERLIN1  
PPRC1  
FGF8  
TRIM8  
SUFU  
ACTR1A

NFKB2  
CNNM2  
PSD  
WBP1L  
XPNPEP1  
TAF5  
SORCS1  
TCF7L2  
ADD3  
SMC3  
SHOC2  
TDRD1  
FAM160B1  
ABLIM1  
ATRNL1  
EMX2  
RAB11FIP2  
TIAL1  
EIF3A  
PDZD8  
SLC18A2  
GRK5  
HSPA12A  
MCMBP  
FGFR2  
ZRANB1  
EBF3  
INPP5A  
PSMD13  
PHRF1  
MUC5B  
AP2A2  
CD81  
NUP98  
STIM1  
NAP1L4  
RRM1  
ARFIP2  
TRIM3  
FAM160A2  
APBB1  
DCHS1  
ST5  
TMEM9B  
DENND5A  
USP47  
CTR9  
IPO7  
WEE1  
PSMA1  
COPB1  
ARNTL  
SOX6  
RPS13  
GTF2H1  
E2F8  
TSG101  
SPTY2D1  
NAV2  
KCNA4  
LGR4  
BDNF  
PAX6  
QSER1  
CSTF3  
FBXO3  
MPPED2

EIF3M  
CAPRIN1  
TRAF6  
SLC1A2  
EHF  
LRRC4C  
PRDM11  
API5  
TTC17  
MAPK8IP1  
DGKZ  
CHRM4  
CRY2  
PHF21A  
F2  
AMBRA1  
CKAP5  
ATG13  
CELF1  
PSMC3  
FNBP4  
CLP1  
SSRP1  
SERPING1  
ZDHHCS  
RTN4RL2  
ZFP91  
CTNND1  
OSBP  
PATL1  
DDB1  
PRPF19  
CPSF7  
MYRF  
SYT7  
FADS2  
DAGLA  
FTH1  
INCENP  
HNRNPUL2  
GANAB  
MTA2  
EEF1G  
INTS5  
SLC3A2  
NXF1  
CHRM1  
STIP1  
OTUB1  
MARK2  
NRXN2  
PLCB3  
RASGRP2  
RPS6KA4  
MEN1  
SF1  
PPP2R5B  
ATG2A  
SYVN1  
DPF2  
LTBP3  
RELA  
SF3B2  
SART1  
PACS1  
KLC2  
LRFN4

ANKRD13D  
RBM4  
RBM14  
KDM2A  
RBM14-RBM4  
SPTBN2  
ADRBK1  
PPP1CA  
LRP5  
SUV420H1  
CPT1A  
PPP6R3  
SHANK2  
ANO1  
PPFIA1  
PDE2A  
RNF121  
NUMA1  
FCHSD2  
ARHGEF17  
FAM168A  
PPME1  
POLD3  
C11orf30  
PRKRIR  
RPS3  
ARRB1  
RSF1  
EED  
PCF11  
RAB30  
PICALM  
GAB2  
TENM4  
FZD4  
GRM5  
FAT3  
CWC15  
MAML2  
YAP1  
SESN3  
DCUN1D5  
CUL5  
GRIA4  
SIK2  
ZC3H12C  
RDX  
C11orf57  
ZBTB16  
CADM1  
PAFAH1B2  
SIK3  
BACE1  
DSCAML1  
IL10RA  
ARCN1  
DDX6  
KMT2A  
BCL9L  
IFT46  
UBE4A  
HYOU1  
HMBS  
HINFP  
C2CD2L  
GRAMD1B  
HSPA8

ARHGEF12  
UBASH3B  
TBCEL  
SRPR  
PKNOX2  
STT3A  
EI24  
PRDM10  
ARHGAP32  
KIRREL3  
ZBTB44  
VPS26B  
IGSF9B  
IQSEC3  
WNK1  
CACNA1C  
FKBP4  
KDM5A  
CCND2  
KCNA6  
PRMT8  
TNFRSF1A  
CHD4  
USP5  
ZNF384  
MLF2  
ATN1  
PTPN6  
COPS7A  
CDCA3  
SLC2A14  
CLSTN3  
LPCAT3  
FOXJ2  
NANOG  
PHC1  
RIMKLB  
LRP6  
ETV6  
ATF7IP  
GRIN2B  
WBP11  
PLEKHA5  
EPS8  
AEBP2  
SOX5  
STK38L  
ASUN  
PTHLH  
FAM60A  
DENND5B  
FAR2  
IPO8  
SLC2A13  
CNTN1  
GXYLT1  
PRICKLE1  
SLC38A2  
SLC38A1  
ARID2  
SCAF11  
NELL2  
HDAC7  
SLC38A4  
CCNT1  
SENP1  
COL2A1

DDN  
DDX23  
RND1  
KMT2D  
PRPF40B  
SPATS2  
SMARCD1  
ASIC1  
KCNH3  
POU6F1  
LARP4  
CSRNP2  
DIP2B  
SLC4A8  
ACVR1B  
KRT6A  
NR4A1  
SCN8A  
GRASP  
KRT1  
EIF4B  
SPRYD3  
RARG  
ATF7  
MAP3K12  
SP1  
ESPL1  
PCBP2  
ITGA5  
NCKAP1L  
HNRNPA1  
HOXC6  
PDE1B  
SARNP  
DGKA  
CDK2  
IKZF4  
DNAJC14  
GDF11  
NABP2  
PA2G4  
SMARCC2  
CS  
PAN2  
ANKRD52  
ATP5B  
BAZ2A  
NAB2  
KIF5A  
DCTN2  
LRP1  
DTX3  
MBD6  
R3HDM2  
CDK4  
AGAP2  
LEMD3  
XPOT  
MON2  
USP15  
TBK1  
SRGAP1  
DYRK2  
GRIP1  
RAP1B  
MDM2  
CPSF6

CAND1  
CCT2  
FRS2  
PTPRB  
ZFC3H1  
CNOT2  
ZDHHC17  
PPP1R12A  
NAP1L1  
OSBPL8  
NAV3  
PPFIA2  
DUSP6  
ATP2B1  
PLXNC1  
NR2C1  
FGD6  
NTN4  
METAP2  
UHRF1BP1L  
ANKS1B  
SCYL2  
CDK17  
HSP90B1  
HCFC2  
RFX4  
SLC41A2  
CORO1C  
SART3  
RIC8B  
BTBD11  
SSH1  
ATP2A2  
ANAPC7  
ARPC3  
GIT2  
CUX2  
ATXN2  
VPS29  
PPP1CC  
NAA25  
HECTD4  
RPL6  
PTPN11  
MED13L  
NOS1  
FBXO21  
TAOK3  
TBX5  
KSR2  
TBX3  
RPLP0  
RAB35  
MSI1  
CIT  
GCN1L1  
CABP1  
KDM2B  
HNF1A  
SPPL3  
CLIP1  
MLXIP  
RSRC2  
PITPNM2  
SBNO1  
SETD8  
TMEM132D

NCOR2  
DHX37  
RAN  
ULK1  
EP400  
SFSWAP  
GOLGA3  
ZNF605  
PSPC1  
XPO4  
ZMYM2  
MPHOSPH8  
RNF17  
FGF9  
PAN3  
WASF3  
FLT1  
CDK8  
RPL21  
HSPH1  
FRY  
N4BP2L1  
KATNAL1  
PDS5B  
DCLK1  
TRPC4  
NBEA  
FOXO1  
KBTBD6  
TPT1  
COG3  
TSC22D1  
RB1  
ZC3H13  
FNDC3A  
LCP1  
LRCH1  
INTS6  
PCDH17  
SUGT1  
PCDH9  
KLF12  
DACH1  
RBM26  
MYCBP2  
SLITRK1  
SLAIN1  
SPRY2  
TM9SF2  
DNAJC3  
IPO5  
MBNL2  
DOCK9  
EFNB2  
TPP2  
ARGLU1  
TUBGCP3  
ATP11A  
ARHGEF7  
COL4A1  
TNFSF13B  
MYO16  
LAMP1  
TFDP1  
CHAMP1  
CDC16  
CUL4A

CHD8  
ZNF219  
SUPT16H  
HNRNPC  
MMP14  
PRMT5  
ACIN1  
RNF31  
CPNE6  
JPH4  
NFATC4  
SCFD1  
HECTD1  
NOVA1  
AKAP6  
NPAS3  
SRP54  
ARHGAP5  
PSMA6  
SNX6  
BAZ1A  
NFKBIA  
RALGAPA1  
MDGA2  
FBXO33  
PRPF39  
MGAT2  
SOS2  
MAP4K5  
ATL1  
NEMF  
TRIM9  
BMP4  
DDHD1  
STYX  
PSMC6  
FERMT2  
SAMD4A  
NAA30  
GCH1  
PELI2  
EXOC5  
ARID4A  
RTN1  
PSMA3  
DAAM1  
TRMT5  
PRKCH  
PPP2R5E  
SIX1  
PPM1A  
HIF1A  
GPHN  
MAX  
EIF2S1  
FUT8  
ZBTB1  
SPTB  
ACTN1  
DCAF5  
RBM25  
PSEN1  
SIPA1L1  
PCNX  
MAP3K9  
ZFYVE1  
ELMSAN1

FCF1  
YLPM1  
DLST  
TMEM63C  
TGFB3  
IRF2BPL  
GTF2A1  
NRXN3  
AHSA1  
SNW1  
RPS6KA5  
FOXN3  
TTC7B  
PSMC1  
ZC3H14  
ITPK1  
SMEK1  
FBLN5  
UNC79  
DICER1  
BCL11B  
PAPOLA  
WARS  
YY1  
EVL  
CCNK  
EML1  
DYNC1H1  
TECPR2  
WDR20  
TRAF3  
CDC42BPB  
RCOR1  
PPP2R5C  
PPP1R13B  
EIF5  
INF2  
JAG2  
MTA1  
AKT1  
PACS2  
MAGEL2  
CYFIP1  
GABRA5  
GABRB3  
HERC2  
GABRG3  
GOLGA8M  
UBE3A  
TJP1  
EMC7  
OTUD7A  
RYR3  
ACTC1  
EMC4  
AQR  
LPCAT4  
MEIS2  
SLC12A6  
THBS1  
BAHD1  
VPS18  
INO80  
DLL4  
RAD51  
MAPKBP1  
MGA

RTF1  
TTBK2  
MAP1A  
CDAN1  
TP53BP1  
FRMD5  
PDIA3  
MFAP1  
CTDSPL2  
MYEF2  
SLC30A4  
SEMA6D  
USP8  
AP4E1  
COPS2  
FBN1  
GABPB1  
MYO5A  
DMXL2  
LEO1  
RSL24D1  
FAM214A  
TCF12  
CCPG1  
RFX7  
PYGO1  
ADAM10  
RNF111  
TLN2  
RORA  
SLTM  
HERC1  
USP3  
CSNK1G1  
ZNF609  
CTD-2116N17.1  
SNX1  
DPP8  
MAP2K1  
RPL4  
RAB11A  
KIF23  
TLE3  
PIAS1  
ANP32A  
PARP6  
NEO1  
ARIH1  
PKM  
NPTN  
MYO9A  
ARID3B  
CLK3  
PML  
CSK  
SIN3A  
PTPN9  
C15orf39  
LINGO1  
HMG20A  
IREB2  
RASGRF1  
ARNT2  
AP3B2  
HDGFRP3  
CPEB1  
ZNF592

ACAN  
NTRK3  
ZNF710  
FURIN  
IQGAP1  
CRTC3  
CHD2  
NR2F2  
ASB7  
CHSY1  
ALDH1A3  
SNRPA1  
RAB11FIP3  
CAPN15  
FBXL16  
UBE2I  
TMEM204  
MAPK8IP3  
CLCN7  
CRAMP1L  
PKD1  
TSC2  
CASKIN1  
RNPS1  
PDPK1  
NAA60  
CREBBP  
GLIS2  
ADCY9  
TFAP4  
C16orf72  
GLYR1  
GRIN2A  
UBN1  
RBFOX1  
USP7  
GSPT1  
ZC3H7A  
MKL2  
KIAA0430  
SMG1  
MYH11  
XYLT1  
RBBP6  
TNRC6A  
CACNG3  
PRKCB  
PLK1  
ARHGAP17  
XPO6  
GTF3C1  
ATXN2L  
IL27  
SH2B1  
TAOK2  
MAZ  
CORO1A  
TBC1D10B  
ZNF629  
RNF40  
SRCAP  
FBRS  
FUS  
KAT8  
SETD1A  
STX1B  
FBXL19

VPS35  
SIAH1  
DNAJA2  
ZNF423  
PAPD5  
ITFG1  
NKD1  
BRD7  
RBL2  
CHD9  
CYLD  
TOX3  
SALL1  
GNAO1  
NUDT21  
RSPRY1  
FAM192A  
CX3CL1  
ZNF319  
CDH11  
CNOT1  
CDH8  
CSNK2A2  
CBFB  
ATP6V0D1  
CTCF  
RANBP10  
EDC4  
NFATC3  
WWP2  
VPS4A  
TERF2  
NFAT5  
AP1G1  
ST3GAL2  
SF3B3  
DDX19A  
GLG1  
ZFHX3  
BCAR1  
CMIP  
PLCG2  
KLHL36  
USP10  
FBXO31  
JPH3  
ZCCHC14  
FOXF1  
IRF8  
BANP  
ZC3H18  
ANKRD11  
RPL13  
TUBB3  
YWHAE  
PITPNA  
ABR  
SMG6  
MNT  
PRPF8  
METTL16  
PAFAH1B1  
CLUH  
RAP1GAP2  
ZZEF1  
ANKFY1  
PELP1

C17orf85  
CAMTA2  
MINK1  
PITPNM3  
RABEP1  
DERL2  
PHF23  
DLG4  
NEURL4  
YBX2  
NLGN2  
CTDNEP1  
EIF4A1  
TNFSF12  
SENP3  
POLR2A  
FXR2  
ZBTB4  
TNFSF12-TNFSF13  
TP53  
KDM6B  
CHD3  
MYH10  
RPL26  
NDEL1  
MAP2K4  
MYOCD  
ARHGAP44  
FLCN  
RAI1  
NCOR1  
COPS3  
LGALS9C  
SREBF1  
LLGL1  
GID4  
AKAP10  
WSB1  
USP22  
NLK  
SUPT6H  
FOXN1  
TAOK1  
PHF12  
GIT1  
NUFIP2  
MYO18A  
NF1  
CRLF3  
ATAD5  
SSH2  
ANKRD13B  
LRRC37B  
PSMD11  
RHOT1  
C17orf75  
SUZ12  
RAB11FIP4  
ASIC2  
AP2B1  
GGNBP2  
ACACA  
MLLT6  
HNF1B  
SRCIN1  
PIP4K2B  
SYNRG

SOCS7  
RPL23  
CACNB1  
RPL19  
FBXL20  
CDK12  
ERBB2  
MED1  
CASC3  
MSL1  
NR1D1  
RARA  
IKZF3  
PSMD3  
SMARCE1  
TOP2A  
KRT31  
ACLY  
KLHL10  
DNAJC7  
TUBG1  
ATP6V0A1  
STAT5B  
STAT3  
KCNH4  
STAT5A  
BECN1  
PSME3  
DHX8  
UBTF  
SLC4A1  
RUNDC3A  
LSM12  
C17orf104  
HDAC5  
GPATCH8  
ATXN7L3  
HEXIM1  
NMT1  
GJC1  
EFTUD2  
FMNL1  
NPEPPS  
KANSL1  
KPNB1  
WNT3  
NFE2L1  
SP2  
TBX21  
CBX1  
UBE2Z  
IGF2BP1  
ZNF652  
PPP1R9B  
KAT7  
COL1A1  
SPOP  
CA10  
SPAG9  
LUC7L3  
CACNA1G  
MBTD1  
MSI2  
SRSF1  
VEZF1  
MTMR4  
USP32

CLTC  
VMP1  
YPEL2  
PPM1E  
APPBP2  
DHX40  
RPS6KB1  
BCAS3  
MRC2  
MED13  
TANC2  
INTS2  
TLK2  
TBX2  
PSMC5  
DDX42  
ERN1  
CD79B  
SMARCD2  
MAP3K3  
PSMD12  
BPTF  
PITPNC1  
DDX5  
SMURF2  
HELZ  
PRKCA  
SOX9  
PRKAR1A  
MAP2K6  
NUP85  
CASKIN2  
UNK  
SLC25A19  
UBE2O  
TNRC6C  
CYTH1  
CBX8  
CBX2  
RPTOR  
EIF4A3  
NPLOC4  
RP11-1055B8.7  
FASN  
GPS1  
P4HB  
CSNK1D  
FOXK2  
COLEC12  
USP14  
SMCHD1  
TYMS  
DLGAP1  
PTPRM  
ANKRD12  
PPP4R1  
GNAL  
PTPN2  
ESCO1  
ROCK1  
C18orf8  
KCTD1  
SS18  
ZNF521  
ASXL3  
NOL4  
DSG1

TRAPPC8  
DTNA  
B4GALT6  
MAPRE2  
SETBP1  
ZNF24  
CELF4  
FHOD3  
ATP5A1  
RNF165  
PIAS2  
C18orf25  
CXXC1  
ZBTB7C  
SMAD7  
CTIF  
SMAD2  
MBD1  
TXNL1  
WDR7  
MBD2  
ONECUT2  
DCC  
MEX3C  
TCF4  
SMAD4  
ST8SIA3  
NEDD4L  
KIAA1468  
MALT1  
ZNF532  
CDH20  
PHLPP1  
ZNF407  
NETO1  
TSHZ1  
NFATC1  
CTDP1  
ZNF236  
MIER2  
PTBP1  
WDR18  
STK11  
MBD3  
DAZAP1  
APC2  
DOT1L  
CSNK1G2  
BTBD2  
LMNB2  
FZR1  
GNA11  
CELF5  
CACTIN  
EEF2  
PIAS4  
DPP9  
KDM4B  
SAFB2  
SAFB  
CHAF1A  
RANBP3  
MLLT1  
LONP1  
RFX2  
VAV1  
C3

KHSRP  
ARHGEF18  
CAMSAP3  
XAB2  
ELAVL1  
EVI5L  
MAP2K7  
HNRNPM  
ADAMTS10  
OLFM2  
EIF3G  
PDE4A  
CDC37  
DNMT1  
C19orf66  
RAVER1  
CARM1  
SMARCA4  
DNM2  
ILF3  
KANK2  
DKFZP761J1410  
MAST1  
TNPO2  
CALR  
CACNA1A  
NFIX  
NACC1  
RFX1  
LPHN1  
PRKACA  
DCAF15  
SLC1A6  
SYDE1  
BRD4  
WIZ  
AKAP8  
EPS15L1  
RAB8A  
SIN3B  
MYO9B  
CHERP  
MED26  
RPL18A  
FCHO1  
JAK3  
UNC13A  
ANO8  
ELL  
FKBP8  
PIK3R2  
MAST3  
SSBP4  
KCNN1  
LRRC25  
CRTC1  
UPF1  
SUGP2  
SUGP1  
ATP13A1  
MAU2  
GATAD2A  
ZNF536  
UBA2  
HPN  
USF2  
KMT2B

CLIP3  
SIPA1L3  
DPF1  
HNRNPL  
ACTN4  
MAP4K1  
SAMD4B  
SUPT5H  
DYRK1B  
AKT2  
FBL  
HNRNPUL1  
LTBP4  
RAB4B  
RPS19  
CD79A  
GRIK5  
MEGF8  
GSK3A  
CIC  
ZNF574  
POU2F2  
ARHGEF1  
ATP1A3  
CADM4  
TOMM40  
ZNF296  
RELB  
EXOC3L2  
CLASRP  
CLPTM1  
MARK4  
SYMPK  
IRF2BP1  
PPP5C  
PRKD2  
NPAS1  
SAE1  
ZC3H4  
ARHGAP35  
STRN4  
NAPA  
AP2S1  
GLTSCR1  
GRIN2D  
RASIP1  
CA11  
RUVBL2  
SNRNP70  
PPFIA3  
FLT3LG  
SLC17A7  
RPS11  
PRR12  
AP2A1  
PRMT1  
TSKS  
SCAF1  
MYH14  
SHANK1  
PRKCG  
TTYH1  
PRPF31  
CNOT3  
LENG8  
BRSK1  
PPP6R1

U2AF2  
ZNF628  
RPS5  
TRIM28  
CHMP2A  
CSNK2A1  
TBC1D20  
STK35  
PTPRA  
NOP56  
ATRN  
CENPB  
PLCB1  
BMP2  
PCNA  
SNAP25  
FLRT3  
TASP1  
PAK7  
JAG1  
ZNF133  
PCSK2  
SLC24A3  
NAPB  
TPX2  
C20orf112  
TM9SF4  
MAPRE1  
XKR7  
POFUT1  
DNMT3B  
E2F1  
CBFA2T2  
ITCH  
AHCY  
GDF5  
TRPC4AP  
GGT7  
NCOA6  
DLGAP4  
TGIF2-C20orf24  
SOGA1  
RBM39  
NDRG3  
PHF20  
PPP1R16B  
RALGAPB  
SRC  
PTPRT  
MYBL2  
CHD6  
TOP1  
SRSF6  
YWHAB  
PABPC1L  
RIMS4  
HNF4A  
NCOA5  
SLC12A5  
PCIF1  
ZNFX1  
CSE1L  
KCNB1  
ZMYND8  
STAU1  
ARFGEF2  
NCOA3

PREX1  
B4GALT5  
ATP9A  
ADNP  
NFATC2  
SALL4  
ZNF217  
TFAP2C  
CSTF1  
BMP7  
GNAS  
RAE1  
TAF4  
SYCP2  
CDH4  
PSMA7  
PHACTR3  
LSM14B  
TCFL5  
MRGBP  
LAMA5  
GID8  
YTHDF1  
DIDO1  
ADRM1  
KCNQ2  
EEF1A2  
GMEB2  
MYT1  
ZNF512B  
NRIP1  
USP25  
NCAM2  
CCT8  
GABPA  
TIAM1  
HUNK  
SCAF4  
SON  
PAXBP1  
ITSN1  
MORC3  
ETS2  
BRWD1  
DYRK1A  
ERG  
BACE2  
DSCAM  
ZBTB21  
SIK1  
U2AF1  
TRAPPC10  
PKNOX1  
AGPAT3  
PDXK  
COL6A1  
PCBP3  
MICAL3  
TBX1  
  
HIRA  
UFD1L  
DGCR8  
ZDHC8  
MED15  
HIC2  
MAPK1

sep-05

BCR  
SMARCB1  
SPECC1L  
SEZ6L  
SGSM1  
PITPNB  
NIPSNAP1  
AP1B1  
NF2  
ZNRF3  
EWSR1  
TBC1D10A  
MTMR3  
SF3A1  
EIF4ENIF1  
MORC2  
DRG1  
PRR14L  
DEPDC5  
PATZ1  
LARGE  
MYH9  
CACNG2  
EIF3D  
RBFOX2  
IL2RB  
GGA1  
CSNK1E  
EIF3L  
SOX10  
GTPBP1  
RPL3  
PDGFB  
CACNA1I  
RBX1  
TNRC6B  
EP300  
ZC3H7B  
SREBF2  
XRCC6  
TCF20  
SULT4A1  
SCUBE1  
PRR5  
SMC1B  
PHF21B  
CELSR1  
ZBED4  
GRAMD4  
BRD1  
TBC1D22A  
PLXNB2  
PIM3  
TRABD  
SHANK3  
MAPK8IP2  
KAL1  
WWC3  
NLGN4X  
TBL1X  
STS  
CLCN4  
PRPS2  
HCCS  
GLRA2  
OFD1  
ARHGAP6

GEMIN8  
FRMPD4  
MSL3  
TLR8  
PIGA  
RBBP7  
FANCB  
TXLNG  
ZRSR2  
ACE2  
MOSPD2  
CDKL5  
REPS2  
PDHA1  
GPR64  
SCML2  
NHS  
PPEF1  
CNKSR2  
SCML1  
SH3KBP1  
RPS6KA3  
PHKA2  
POLA1  
PTCHD1  
EIF2S3  
ZFX  
SMS  
MBTPS2  
PHEX  
PCYT1B  
KLHL15  
TAB3  
DMD  
IL1RAPL1  
GK  
TM4SF2  
RPGR  
BCOR  
OTC  
CYBB  
CXorf22  
CASK  
MED14  
MAOB  
DDX3X  
MAOA  
USP9X  
KDM6A  
SLC9A7  
EFHC2  
USP11  
UBA1  
PHF16  
CDK16  
RBM10  
CFP  
FTSJ1  
PORCN  
WAS  
WDR13  
SUV39H1  
SLC38A5  
GPKOW  
WDR45  
GRIPAP1  
TFE3

OTUD5  
HDAC6  
AF196779.12  
CCDC22  
FOXP3  
GSPT2  
AKAP4  
SHROOM4  
CLCN5  
MAGED1  
IQSEC2  
RIBC1  
HUWE1  
KDM5C  
SMC1A  
WNK3  
PHF8  
FGD1  
MAGED2  
USP51  
FAM120C  
ALAS2  
GNL3L  
MSN  
ARHGEF9  
ZC3H12B  
AMER1  
IGBP1  
EDA  
OPHN1  
AR  
CXorf65  
ZMYM3  
TAF1  
TEX11  
MED12  
KIF4A  
SLC7A3  
IL2RG  
NONO  
OGT  
ACRC  
DLG3  
HDAC8  
RLIM  
SLC16A2  
KIAA2022  
ABCB7  
ERCC6L  
ATRX  
TBX22  
ATP7A  
PGK1  
ZNF711  
PCDH11X  
BRWD3  
CHM  
DIAPH2  
PCDH19  
CENPI  
GLA  
SRPX2  
BTK  
PLP1  
FAM199X  
MORC4  
IL1RAPL2

FRMPD3  
AMMECR1  
MID2  
ACSL4  
COL4A6  
ATG4A  
COL4A5  
RGAG1  
AMOT  
ALG13  
LRCH2  
PAK3  
CAPN6  
SLC6A14  
TRPC5  
PLS3  
NKAP  
UPF3B  
CXorf56

sep-06

WDR44  
DOCK11  
NKRF  
IL13RA1  
LAMP2  
CUL4B  
TENM1  
XIAP  
THOC2  
OCRL  
SMARCA1  
STAG2  
GRIA3  
UTP14A  
BCORL1  
AIFM1  
ARHGAP36  
SLC25A14  
ZNF280C  
FRMD7  
IGSF1  
PHF6  
DDX26B  
GPC3  
HPRT1  
GPC4  
FHL1  
FGF13  
SLC9A6  
MCF2  
HTATSF1  
ARHGEF6  
F9  
RBMX  
ATP11C  
IDS  
MTM1  
AFF2  
MTMR1  
NSDHL  
BGN  
HAUS7  
SLC6A8  
ATP2B3  
IDH3G  
ABCD1  
IRAK1

PDZD4  
RENBP  
HCFC1  
OPN1LW  
ARHGAP4  
L1CAM  
FLNA  
G6PD  
RPL10  
TKTL1  
GDI1  
TAZ  
FAM50A  
PLXNA3  
MPP1  
GAB3  
DKC1  
F8